Title
Visibility

Authors
Duntley, Seibert Q
Gordon, Jacqueline I
Taylor, John H
et al.

Publication Date
1964-04-01

Visibility Laboratory
University of California
Scripps Institution of Oceanography
San Diego, California 92152

V I S I B I L I T Y

by

S. Q. Duntley, J. I. Gordon, J. H. Taylor, A. R. Boileau,
R. W. Austin, and J. L. Harris

April 1964

SIO Ref. 64-3

Bureau of Ships
Contract NObs-84075
Assignment No. 9

FOREWORD

Assignment 9 under Contract NObs-84075 provides funds to enable the Visibility Laboratory to analyze data which is presently in the Laboratory's files as a result of various experimental studies that have been conducted throughout the past 10 years. On the basis of these data, reports on atmospheric optics and related subjects are to be produced. The present report, the first to be produced under Assignment 9, is intended as a brief survey of the whole subject of visibility, specially prepared to illustrate by example the kinds of input data required for visibility calculations. The role of atmospheric data, as well as data on the pertinent optical properties of target surfaces, natural terrains, and man-made backgrounds is illustrated. Future reports planned for this series will present a wide variety of atmospheric, target, and background data.

Most of the subject matter of this report will appear as an article entitled "Visibility" in the May 1964 issue of the scientific journal, "Applied Optics," published by the Optical Society of America.

VISIBILITY

1. INTRODUCTION

by Seibert Q. Duntley

Man's ability to see objects through the atmosphere, underwater, or in space by naked eye or with the aid of magnifying and filtering devices is limited by the availability of light, its distribution on the object of regard and its background, the reflective properties of both, the image transmission characteristics of the intervening media, the properties of any magnifying and filtering optical devices employed, and the characteristics of the human visual system. For at least half a century answers have been sought to questions such as the following: Can some particular object of interest be seen? How far can it be seen? How dark may twilight become before the object will be lost to view? How rapidly can it move and yet be visible? What is the effect of object color? Will filters help? How much magnification is necessary to make the object visible at a given distance? What is the optimum procedure for visual search? What is the probability of success in sighting the object searched for? Under what circumstances can it be recognized? Is visual identification possible? How is visual performance affected by fatigue, discomfort, distraction, apprehension, motivation, and kindred factors?

Methods for generating answers to such questions have come into being, particularly during the last twenty years. Specialists in generating these answers refer to their subject as <u>visibility</u> and regard it as a professional specialty within optics. They are, however, not alone in the use of the word; meteorologists have long

used the term visibility as a meteorological parameter, highly restricted in its meaning and greatly limited in its applicability. The word visibility has also been used by designers of windows in aircraft, automobiles, and even buildings to denote the field of view which these apertures provide. Despite the universal wish of scientists and engineers for every word to have but a single technical meaning, it seems likely that the term visibility will continue to be ambiguous throughout the foreseeable future. Authors and readers must depend upon context to make clear the school of thought to which the word is applied in each instance. Throughout the remainder of this report, visibility will not be used in its meteorological or architectural connotations but only to denote the human capability to detect, recognize, and identify objects by means of the human visual mechanism used directly and with the aid of magnifying and filtering devices but without the aid of intervening sensor systems such as photography, television, image intensifiers, infrared devices, electronic displays, etc. Extension of the use of the term visibility to include the performance of the human visual system when aided by such sensors can be made but will not be attempted in this report.

The limiting performance of the human visual system to detect and recognize distant objects can be predicted by engineering-type calculations provided adequate input information is available. This form of optical engineering has been severely handicapped, however, by a greater lack of applicable data than has been generally appreciated. It is a purpose of this report to illustrate by example the types of information that are needed and to supply a more complete working sample than has heretofore appeared. Every effort has been

made to exclude from the report all previously published facts and concepts insofar as this can be done without sacrificing viewpoint and clarity. Concise summaries of certain vital concepts and principles are included throughout the account but the authors have depended heavily upon references and the willingness of the reader to use them. If, in a few instances, paragraphs which summarize known principles or facts seem to go somewhat beyond this criterion it is because of the belief that the need for such a summary exists.

The authors of this report have shared with many colleagues throughout the world in the development of visibility as a science and as an engineering procedure. The report is intended to provide an overview of some applied aspects of this subject. Sufficient input data has been included to enable certain sample visibility calculations to be carried out by those who wish to explore this branch of optical engineering, but a full professional treatment of the subject would require a book-length treatise. In order to achieve broad coverage and yet adequate technical depth in a compact report, it has been deemed best to call upon an integrated team of specialists to produce a unified presentation with each individual contributing in his specialty. Each major section of the present report, therefore, bears the name of the specialist who prepared it.

2. SUMMARY

Calculations of the limiting performance of the human visual system are based upon the separate properties of all of the physical components which, taken together, comprise a

system for the transfer of information from the object to the observer's consciousness by way of the visual pathway. Thus, light reflected or generated by the object forms a body of image-forming flux which, after transmission by the intervening media, forms a retinal image which, in turn, is transmitted to the brain and perceived by the observer. In like fashion, the background against which the object is seen generates flux from a different part of object space and this signal follows a corresponding path to the perceptual level of the observer. Discrimination of the object from its background depends upon the thresholds of the human visual system.

Prediction of the limiting human visual capability to detect any specific object begins, therefore, with the optical properties of that object and of its background. These in combination with the nature of the incident lighting define the inherent optical signal which is available in the direction of the observer. Assessment of the magnitude of this inherent optical signal is the first major step in any visibility calculation. It involves a considerable knowledge of the optical properties of both background and target as well as a detailed specification of their lighting.

2.1 Backgrounds

The nature of the background against which objects are seen most frequently depends upon whether the path of sight is inclined downward or upward. Some form of natural terrain may provide the background for objects viewed along downward-looking paths of sight whereas in upward-looking cases the background is usually the sky or a cloud.

The following discussion of backgrounds includes these and other cases.

Natural terrains are of wide variety but they can be grossly categorized as vegetated, barren, snowy, and watery. Vegetated terrains, because of shadow minimization and because of reflection from the vertical components of plant surfaces (leaves, stalks, etc.) exhibit a characteristic phenomenon often called back gloss (Duntley, 1946) or negative gloss (Judd, 1952, p. 303); this means that the directional reflectance of an unresolved vegetated surface is greatest when viewed by an observer with the sun at his back. Even bare soils, including sand, tend to exhibit back gloss, as is illustrated by Fig. 2.1. Snow covered terrains, nearly matte in their appearance when the snow is freshly fallen, develop gloss upon aging and particularly when they are rain-crusted (Middleton, 1952). Snowy terrains containing outcroppings of vegetation may exhibit a form of back gloss due to the shadows produced by this vegetation whenever these interruptions in the snow surface are unresolved.

Man-made surfaces, such as paints, pavements, or roofs vary widely in matteness but they seldom exhibit back gloss. Their gloss characteristics are usually of the "normal" form, illustrated by the data for a sample of matte brown paint in Fig. 2.1. Typically, therefore, man-made surfaces which match natural terrains when viewed vertically under medium or low-sun conditions appear brighter than the terrain when viewed toward the azimuth of the sun but darker than the terrain when the sun is behind the observer.

Spectral effects. The reflectance characteristics of many natural terrains vary markedly with wavelength. Interreflections between textural elements tend to intensify spectral reflectance effects; thus,

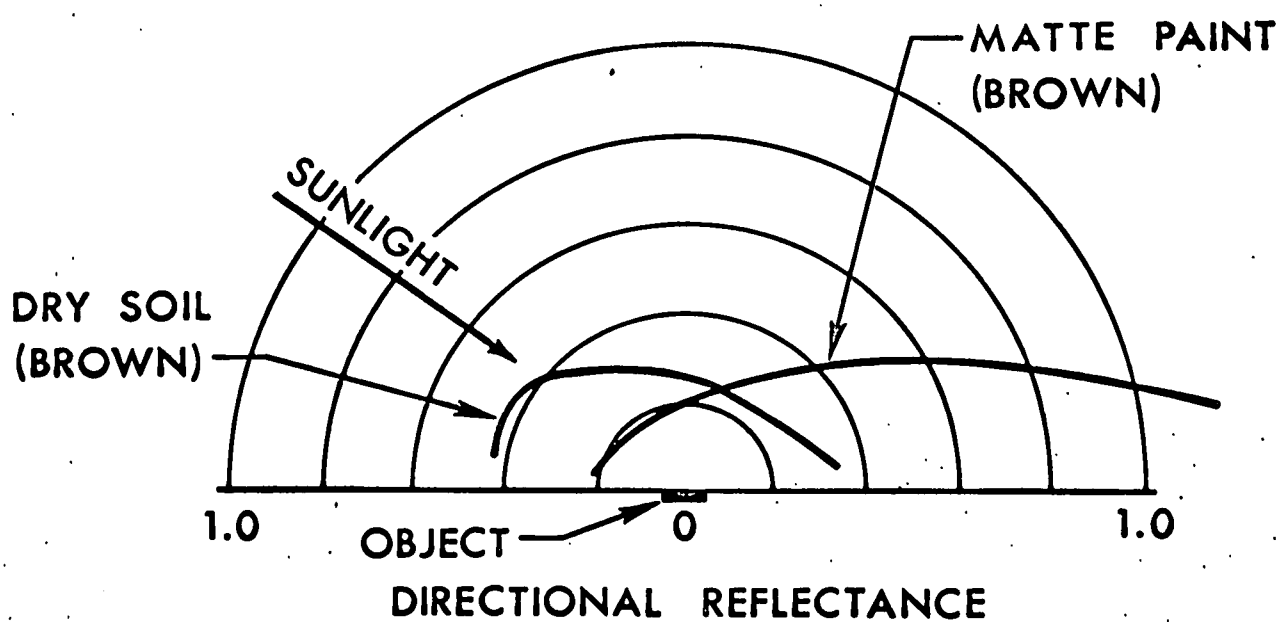

Figure 2.1 Directional reflectance of dry brown soil and matte brown paint, illustrating typical differences.

as shown by Fig. 2.2, the spectral apparent radiance of a maple tree differs markedly from that of a maple leaf (Duntley, 1946, p. 213).

Diffuse reflectors. No natural terrain and no known man-made surface is a perfect diffuse reflector in the sense of appearing equally luminous from all angles of view. A few surfaces, including freshly fallen snow, approximate this condition provided the solar zenith angle is less than 45°, but even fresh snow exhibits marked gloss characteristics when the sun approaches the horizon, an extremely common condition during the snowy season. Man-made surfaces invariably exhibit pronounced gloss characteristics, particularly when the solar zenith angle exceeds 60°. Since large solar zenith angles occur much more commonly than do small ones, very serious errors in visibility calculations can arise from the false assumption that target or background surfaces are perfect diffuse reflectors, i.e., that they obey "Lambert's law of reflection." (O.S.A., 1953, p. 178). Section 3 of this paper presents data on some commonly occurring backgrounds and recommends techniques for calculating the inherent contrast of objects seen against these surfaces.

2.2 Objects

Objects, or visual targets as they are often called, are of every conceivable variety. In general they have complex, three-dimensional shapes producing an intricate pattern of highlights and shadows even if their reflecting characteristics are the same on all of their surfaces, a circumstance which rarely exists. The gloss characteristics of object surfaces show even more variety than do background surfaces. Many glossy objects have mirror-like surfaces that form virtual images of the sun which are often vastly brighter than any portion of the background and, correspondingly, are visible

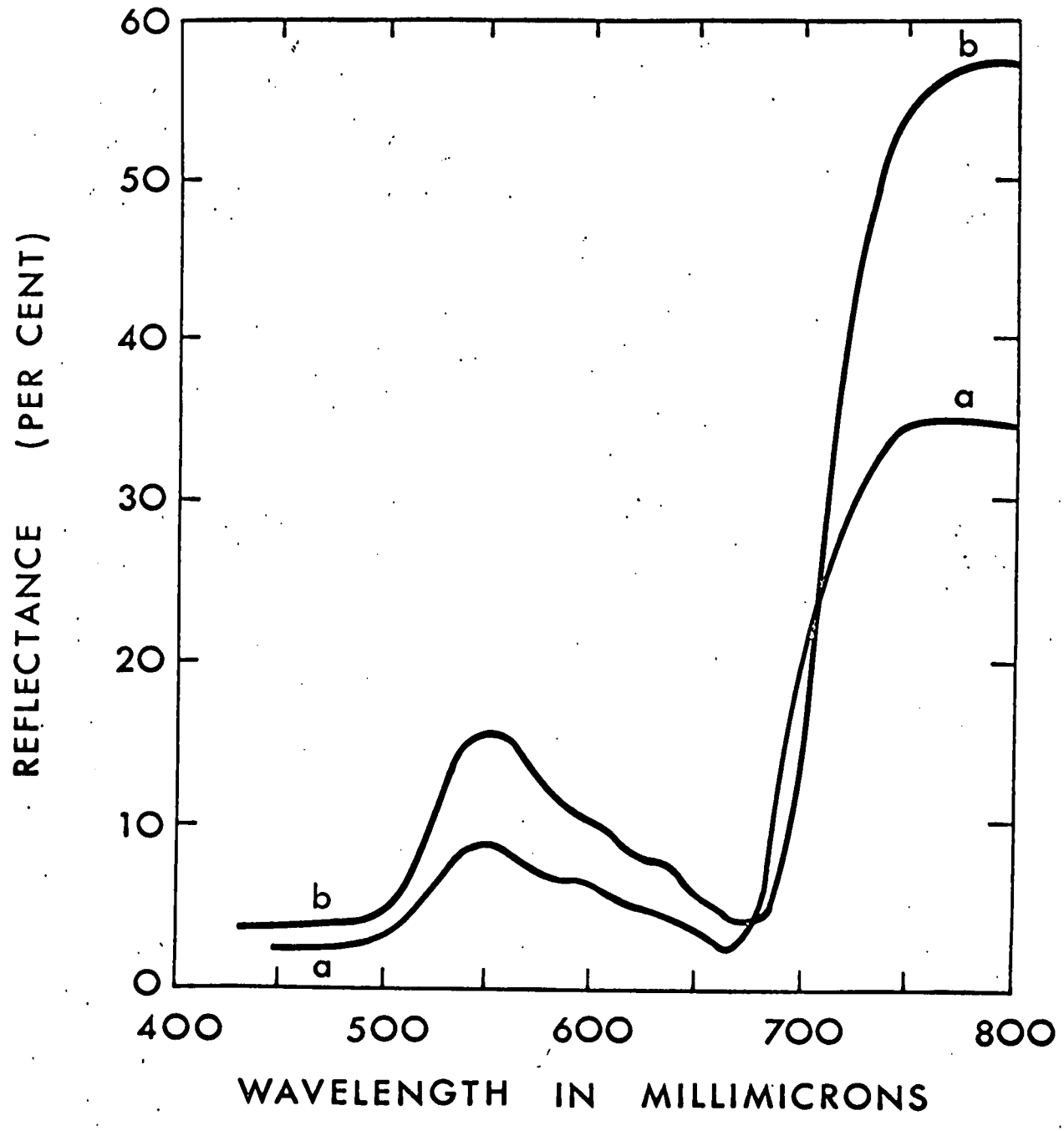

Figure 2.2 Spectrophotometric curves of a maple tree (curve a) and of a maple leaf (curve b)

at much greater range than any other type of surface. Thus it is a common experience while flying to see rivers and bodies of water in the far distance when no other terrain features of like size are visible; this is a consequence of the large positive contrast presented by these bodies of water due to the mirror-like reflections of the sky which they produce.

In virtually every instance of a man-made object viewed against a natural background the disparate gloss characteristics cause the object to undergo marked changes in its appearance and its conspicuity when viewed from various directions, as has been illustrated by Fig. 2.1. Data for a variety of examples of this sort will be found in Sect. 3 of this report.

Obviously any object is visually detectable only if its photometric properties differ from those of its background in the observer's direction of view. Whatever difference does occur constitutes an optical signal. The detectability of such a signal depends upon the properties of the sensor which, in this article, is the human visual system.

2.3 Visual Properties

For more than a century research scientists have produced a voluminous literature concerning the capability of the human visual system to detect minimal optical signals. The discovery that the psychometric function is nearly the same for all visual detection tasks when the photometric nature of the object and its background are specified in terms of contrast (Blackwell - 1946, 1963) enabled the simplification and collation of an enormous body of experimental

facts. Without that simplification, visibility calculations would scarcely be practicable as an engineering procedure. The further discovery that the shape of an object is ordinarily of minor consequence compared with the effect of its angular size provided an additional important simplifying approximation. The experimental result that color contrasts ordinarily have an almost negligible effect (MacAdam, 1946) on the detectability of an optical signal, although they affect the noticeability of supra-threshold objects, constitutes yet another important simplification of visual properties. The fact that under virtually all circumstances geometrically identical objects are equally detectable if their universal contrasts are equal in magnitude even if opposite in sign is perhaps the most important of the first order experimental generalizations; in Sects. 3 and 9 of this report it is demonstrated that this basic result, a dividend of the definition of universal contrast, is of vital importance in visibility calculations.

Under conditions of high (daylight) level adaptation, visual threshold properties are nearly invariant to adapting luminance, are minimal in the central 1^{o} of the visual field (the foveal region), and increase systematically toward the periphery. The smallest detectable optical signal is one for which all of the object flux is concentrated within a circular area only slightly larger than the anatomical dimensions of the foveal cone receptors. All objects of this angular size or smaller, regardless of their actual angular dimension, shape, or pattern are equally detectable if their flux

content is the same; this is known as Ricco's law, which may be written $C\omega$ = constant for the special case of objects having apparent contrast C and subtending a solid angle ω at the eye of the observer but having no angular dimension sufficient to exceed the Ricco domain. The angular diameter within which Ricco's law is obeyed increases somewhat as adaptation luminance is diminished until, in the region of twilight, moonlight, and starlight, the increase is rapid, reaching 15 min of arc at starlight levels of adaptation. Since all objects, regardless of size or shape, which fall within the range of Ricco's law are indistinguishable if their flux content is equal, the resolving power of the human visual system depends upon adaptation level.

Peripheral vision. Maximum object detectability occurs within the rod-free central fovea under conditions of high level (photopic) daytime adaptation conditions, but at twilight (mesoptic) levels, detectability is virtually uniform throughout the fovea, parafovea, and peripheral retina although resolution diminishes toward the periphery. At low light levels, i.e., scotopic adaptation, the sensitivity of the rod-free central fovea effectively vanishes and the greatest sensitivity occurs in the ring-shaped parafovea where rod receptors are dense.

Visual search. In daytime optimum detectability occurs when the object is imaged on the foveal portion of the retina, but this circumstance does not always occur. During visual search, in fact, it is relatively improbable that the image will fall on the fovea. The probability of success in searching some prescribed field

of view for an object can be computed only if detection thresholds for that object in the peripheral portions of the retina are known. It is as if the eye had associated with it a detectivity lobe, greatest on-axis and falling rapidly toward the periphery. This lobe is not a fixed structure but depends markedly upon the angular size and nature of the object and upon its apparent contrast. Thus, lobe shape is governed by the atmosphere, by the directional reflectance characteristics of both target and background, and by the prevailing distribution of natural lighting; it is, therefore, different for each path of sight and for each visual fixation. Details of visual search calculations in which account is taken of the changing nature of the detectivity lobe are discussed in Part 10 of this report.

Recognition and identification. The higher levels of the human visual system are capable of determining object type, class, and identity. Thus, at different levels of visual performance an object may be detected as a shapeless spot, recognized as a ship, classified as a passenger liner, or identified as the Queen Mary. Although quantitative predictions of the limiting circumstances when the higher level functions can be performed involve more variables and greater uncertainties with respect to input data, certain approaches to problems of this class have been made (Harris, 1959).

2.4 Atmospheric Properties

The appearance of distant objects is affected so profoundly by the optical properties of the atmosphere that meteorologists include atmospheric clarity among the meteorological parameters to be

observed, reported, and forecast. Unfortunately the meteorological data are seldom of appreciable usefulness in predicting the visual detectability of specific objects. Quite different optical properties of the atmosphere and its lighting must be known before valid predictions can be made. The literature of visibility contains many examples of attempts to calculate the needed information from models of the atmosphere and its lighting. The success of these attempts is difficult to test or judge unless measurements of real atmospheric and lighting conditions have been made for comparison. Such data are difficult to acquire and are, therefore, exceedingly rare. Section 6 of this report may be the first publication of a sufficiently complete set of measured atmospheric properties to enable valid visibility calculations applicable to a real atmospheric condition to be made. Even so, the Tables in Sect. 6 and the related tabulations in Sect. 3 relate only to conditions which prevailed at one place on one occasion. They are, moreover, incomplete since no radiometric or spectroradiometric data are included. Clearly, a complete photometric and radiometric description of the atmosphere at any one time and place involves the measurement and tabulation of a very large quantity of data. The need is, however, for many such bodies of data representing many places at many times of day and under a variety of atmospheric conditions. Such a compilation would be a well-nigh hopeless task were it not for the capabilities of large electronic computers for which the required bodies of data can be stored on magnetic tape. The creation of such a computer library of atmospheric and lighting conditions is in prospect and will, when

combined with corresponding libraries of visual data, object characteristics, and background information enable major visibility calculations to be carried through quickly, economically, and automatically. Until sufficient data has been collected and stored in computer format, limited visibility calculation studies will doubtless continue to be carried out by procedures like those described later in this report.

The scientific background which underlies the tables in Sects. 3 and 6 of this report and the equations for their use has been published previously (Duntley, Boileau, and Preisendorfer, 1957). Equation (5) on page 500 of that reference (also see Duntley, 1948a, Eq. (12), p. 182) states that all radiance differences are transmitted by the atmosphere with the same attenuation as that experienced by each image-forming ray. This implies that no fine details are obliterated by atmospheric scattering processes. Additional theory by Middleton (1942) and experiments by Duntley (1948a, p. 186) support this implication and the belief that images of distant objects are formed by photons which traverse the intervening media without being scattered. These concepts can be summarized by the modulation transfer function for atmospheric haze.

Atmospheric modulation transfer function. In the absence of atmospheric boil, all non-zero spatial frequencies are attenuated equally, by an amount equal to the beam transmittance of the path of sight (see Eq. (5), p. 500 of Duntley, et al, 1957). The apparent radiance of the zero spatial frequency, however, is, by Eq. (4) of the same reference, the sum of the path radiance and the product of the inherent radiance and beam transmittance. These concepts form the basis of a derivation by James L. Harris of the modulation transfer

function for atmospheric haze, as follows: Consider the inherent radiance of a scene, such as that on the cover of this issue, to be represented by a radiance distribution $N_o(\alpha,\beta)$, where N denotes spectral radiance, the subscript signifies zero observation distance (i.e., inherent radiance), and α,β are rectangular angular coordinates at the eye of the observer. The field of view is rectangular and bounded by the angles $-A/2 < \alpha < A/2$ and $-B/2 < \beta < B/2$. In terms of a two-dimensional Fourier representation, the inherent radiance is

$$N_o(\alpha,\beta) = a_{oo} + \sum_{i=o}^{\infty}{}' \sum_{j=o}^{\infty}{}' a_{ij} \cos\frac{2\pi i\alpha}{A} \cos\frac{2\pi j\beta}{B}$$

$$+ \sum_{i=o}^{\infty} \sum_{j=1}^{\infty} b_{ij} \cos\frac{2\pi i\alpha}{A} \sin\frac{2\pi j\beta}{B}$$

$$+ \sum_{i=1}^{\infty} \sum_{j=o}^{\infty} c_{ij} \sin\frac{2\pi i\alpha}{A} \cos\frac{2\pi j\beta}{B}$$

$$+ \sum_{i=1}^{\infty} \sum_{j=1}^{\infty} d_{ij} \sin\frac{2\pi i\alpha}{A} \sin\frac{2\pi j\beta}{B}$$

where the primes on the first double summation indicate that the term i=j=0 has been eliminated, and where

$$a_{oo} = \frac{1}{AB} \int_{-A/2}^{A/2} \int_{-B/2}^{B/2} N_o(\alpha,\beta)\, d\alpha d\beta \,. \qquad 2.1$$

The corresponding apparent radiance $N_r(\alpha,\beta)$, as seen from observation distance r is

$$N_r(\alpha,\beta) = a_{oo}T_r + T_r \sum_{i=o}^{\infty} \sum_{j=o}^{\infty} g(a_{ij},b_{ij},c_{ij},d_{ij}) + N_r^*$$

where the double summation symbolizes the four components shown above, provided that the beam transmittance $T_r \neq f(\alpha,\beta)$ and the path radiance $N_r^* \neq f(\alpha,\beta)$. These assumptions are described by saying that T_r and N_r^* are decoupled from the scene and represent measures of atmospheric effects.

The non-normalized modulation transfer function for non-zero spatial frequencies is simply $a_{ij}\ T_r/a_{ij}$ and that for the zero spatial frequency is $(a_{oo}\ T_r + N_r^*)/a_{oo}$. Normalization to unity at zero spatial frequency is accomplished by dividing each expression by $(a_{oo}\ T_r + N^*)/a_{oo}$. The normalized modulation transfer function for non-zero spatial frequencies, denoted by τ_r is, therefore,

$$\tau_r = \frac{T_r}{(a_{oo}\ T_r + N_r^*)/a_{oo}} = \frac{1}{1 + N_r^*/a_{oo}\ T_r} \qquad 2.2$$

The symbol a_{oo}, defined by Eq. 2.1, signifies the average inherent radiance of the field of view. Objects occupying only a minor portion of the field and/or differing but slightly in inherent radiance from their surroundings have a negligible effect on a_{oo}. If the object appears against any uniform area of sufficient angular area to render negligible its effect upon a_{oo} for that area, Eq. 2.2 may be written

$${}_b\tau_r = 1/(1 + N_r^*/{}_bN_o\ T_r) \quad , \qquad 2.3$$

where ${}_bN_o$ is called the inherent radiance of the <u>background</u> against which the object appears. The prescript b on ${}_b\tau_r$ signifies that this modulation transfer function for atmospheric haze applies to the specified background. In this case the object is said to be <u>decoupled</u> from the background. Since ${}_b\tau_r$ applies universally to <u>any</u> decoupled target which may appear against background b, it has

been called the universal modulation transfer function for atmospheric haze; this is the proper factor for use in the modulation transfer function products used to describe the performance of optical and photographic systems used to record decoupled targets.

Contrast. Throughout the literature of visibility the ratio of the radiance (or luminance) of any object decoupled from its background to the radiance (or luminance) of its background in the direction of observation, or some function of that ratio, has been referred to as contrast. In this article the ratio defined above will be denoted by ρ and referred to as ratio contrast. Since any function of ρ also represents a form of contrast there are, obviously, a limitless number of possible forms, each of which could be named.

Most of the literature of visibility, both psychophysiological and physical, has made exclusive use of the contrast function $\rho-1$ because it provides important advantages in both disciplines. Fundamentally, the italicized generalization in Section 2.3, which refers to $\rho-1$ or its algebraic equivalent $\Delta B/B$, states that flux increments (ΔB) are as detectable as flux decrements ($-\Delta B$). Since negative contrast ($-\Delta B/B$) can never exceed one in absolute value whereas the magnitude of positive contrast is limitless, objects lighter than their backgrounds can be vastly more detectable than otherwise identical objects darker than their backgrounds. Physically, $\rho-1$ is relatable to the universal modulation transfer function, as may be seen by combining Eqs. (4) and (7) on p. 500 of the paper by Duntley, Boileau, and Preisendorfer (1957) to produce the equation

$$C_r(z,\theta,\phi)/C_o(z_t,\theta,\phi) = 1/\left[1 + N_r^*(z,\theta,\phi)/{}_bN_o(z_t,\theta,\phi)\ T_r(z,\theta,\phi)\right] \qquad 2.4$$

in the notation used in that reference as well as in Sect. 6 of this report. In Eq. 2.4 $C_o(z_t,\theta,\phi)$ denotes the inherent contrast ρ-1 of an object at altitude z_t when viewed along a path of sight defined by zenith angle θ and azimuth angle ϕ; the subscript zero implies zero observation distance, i.e., inherent contrast. Similarly, $C_r(z,\theta,\phi)$ denotes the apparent contrast of the target at viewing distance r from altitude z along the same path of sight θ,ϕ. The same parenthetical modifiers denoting altitude and path of sight appear on the path radiance $N_r^*(z,\theta,\phi)$, the beam transmittance $T_r(z,\theta,\phi)$, and the inherent background radiance ${}_bN_o(z_t,\theta,\phi)$. With the parenthetical modifiers added, the right-hand member of Eq. 2.3 is seen to be identical with the right-hand member of Eq. 2.4. Thus, the universal modulation transfer function for atmospheric haze ${}_b\tau_r$ is identically equal to the ratio C_r/C_o of apparent to inherent contrast when $C_o = \rho$-1 for background b; i.e., in complete notation

$$ {}_b\tau_r(z,\theta,\phi) \equiv {}_bC_r(z,\theta,\phi)/{}_bC_o(z_t,\theta,\phi), \qquad 2.5 $$

where the prescript b specifies that the quantity applies to background b. The ρ-1 type of contrasts in Eqs. 2.4 and 2.5 share with ${}_b\tau_r$ the unique and valuable property of universal applicability to <u>any</u> object which may appear against background b. ${}_bC_r(z,\theta,\phi)$ and ${}_bC_o(z_t,\theta,\phi)$ are, therefore, referred to as <u>universal apparent contrast</u> and <u>universal inherent contrast</u>, respectively. The form ρ-1 is also referred to as <u>universal contrast</u>. The ratio of universal apparent contrast to universal inherent contrast is called universal contrast transmittance and denoted by ${}_b\mathcal{T}_r(z,\theta,\phi)$. Because the form ρ-1 is

used exclusively in this report (except in the following paragraph) and throughout virtually the entire literature of visual science and visibility, the adjective universal has been omitted in the later sections of this report but the universal form of contrast is to be understood unless some alternate form is mentioned by name.

Modulation contrast. Resolution tests and performance analyses of many optical systems, particularly photographic systems, are advantageously described in terms of the ratio $(\rho-1)/(\rho+1)$; this may be called modulation contrast and denoted by $_{12}\overline{\overline{C}}_r$. Algebraically this definition is equivalent to the form $\Delta N/({}_1N + {}_2N)$, a radiometric non-entity in object space, but obviously descriptive of a spatial modulation test object composed of alternating, equally wide bars having radiances ${}_1N$ and ${}_2N$, respectively, and related to the modulation transfer function for atmospheric haze through the relation $a_{oo} = ({}_1N + {}_2N)/2$. Modulation contrast $_{12}\overline{\overline{C}}_r$ shares none of the universal properties of ${}_bC_r$, but simple algebraic interconnections between it and universal contrast exist because of the respective definitions $_{12}\overline{\overline{C}}_r = (\rho-1)/(\rho+1)$ and ${}_bC_r = (\rho-1)$. Simple algebraic relations can readily be found between modulation contrast transmittance $_{12}\overline{\overline{\overline{T}}}_r$ and the pair of universal contrast transmittances ${}_1\mathcal{T}_r$ and ${}_2\mathcal{T}_r$.

Modulation contrast and modulation contrast transmittance have, at present, no usefulness in visibility for at least three reasons: (1) they lack universal applicability to all objects and components of objects, a property essential to the object index concepts described in Sect. 9; (2) they lack the single-valued connection with detection thresholds possessed by the

universal forms and without which the techniques dealt with in Sects. 3, 4, and 10 would be vastly more complicated; (3) virtually no visual threshold data exists in spatial frequency form, although research in this direction has begun (De Palma and Lowry, 1962).

Atmospheric boil. Image transmission by the atmosphere is affected by atmospheric boil in an entirely different manner than by atmospheric haze. Non-zero spatial frequencies are not attenuated equally, resulting in a true loss in resolution. Visibly noticeable temporal variations are produced in the images of distant objects. The contrast transmittance for objects of small angular subtense varies inversely as the third power of the distance in the presence of boil distributed uniformly throughout the path of sight (Duntley, 1963b). (See also Hufnagel and Stanley, 1964).

2.5 Water Properties

Visibility by swimmers is limited by contrast attenuation in a manner somewhat similar to that experienced in a foggy atmosphere. Differences between atmospheric effects and corresponding underwater effects are evident along inclined paths of sight, however, because absorption of visible light, ordinarily absent in the atmosphere, plays a prominent role in even the clearest of waters. Underwater sighting ranges are always short compared with sighting ranges in clear air. Nearly all objects, therefore, subtend so large a visual angle when seen underwater that the exact size of the object is of almost no consequence. Except for very tiny objects or the fine

details of larger ones, underwater sighting ranges depend almost entirely upon the contrast transmittance of the path of sight when ample daylight prevails. The fundamentals of this subject have been treated by Duntley (1963a). Additional discussion, chiefly from the standpoint of input data, is given in Sect. 7 of this report.

2.6 Combining Techniques

Data on objects, backgrounds, atmospheres, and observers must be combined if answers are to be generated for the types of questions raised in the first paragraph of Sect. 1. Such visibility calculations were made initially by iterative numerical procedures which bracketed the final answer as closely as necessary (Duntley, 1946, 1948a, b). Such calculations are cumbersome, time-consuming, and they invite mistakes. Prior to the advent of fast electronic computers, the most promising method to accelerate the calculations appeared to lie in the use of nomographic charts. A series of nomograms for visibility calculations were published by Duntley (1946, 1948b) and were subsequently republished by Middleton (1952) and by various others.

Graphical methods. Alternative graphical procedures have also been devised. One common technique is to prepare a plot of apparent object contrast versus observer distance expressed in terms of the angular diameter of a circular disk having an angular area equal to that of the object. This curve is superimposed upon a plot of threshold contrast for circular objects versus the angular diameter of these objects. The curves intersect at the limiting object diameter and indicate, therefore, the maximum distance at which the

object can be visually detected. The steepness of the intersection of the curves and the spread between them at other object distances provides a valuable indication of the variability of the detection range with observer performance. It must be borne in mind that all of the visual threshold data are averages of the performance of several observers and that there is an important degree of variability throughout the human population.

Visual search. The detection ranges calculated by any of the procedures described in the preceding paragraphs represent the maximum distances achievable. These ranges will only be realized when the object is imaged upon the most sensitive portion of the retina. In most instances the observer is required to search for an object within his field of view. In such a circumstance the probability of the object being imaged on his optimal retinal area may be small and the probability of detection at any given range will depend upon the peripheral sensitivity of his eye. Calculation of detection probabilities in visual search was pioneered by Lamar (1946) and a valuable compendium on visual search techniques is contained in National Academy of Science-National Research Council Publication 712 (1960). Although the principles of visual search calculations have been well-known for about twenty years, their practical application has been compromised in virtually every instance by lack of sufficient data on the optical properties of objects and backgrounds, visual properties, ocular behavior, and atmospheric effects. Even when adequate information is available, the computational task is a staggering one if the data are used properly. A new concept of target

classification described in Sect. 9 may eliminate part of this difficulty. When it is combined with computer techniques, a permanently satisfactory means for visual search calculations should result. Section 10 of this report contains a numerical example of an advanced type of visual search calculation intended to illustrate more completely than has been done heretofore one technique for incorporating real and complete data into a practical visual search calculation.

3. OPTICAL PROPERTIES OF OBJECTS AND BACKGROUNDS

by J. I. Gordon

There are two basic approaches to the description of the optical properties of objects and backgrounds. One is to describe the component properties, such as directional reflectance and lighting distribution. These properties may then be combined with information on the shape and orientation of each pattern element in order to determine its inherent luminance in the direction of any given path of sight. The alternative method is to measure the inherent luminance (or the inherent spectral radiance) under specific natural lighting conditions. It is the latter approach that has been employed almost exclusively in this section, since data in this form are directly useable in practical visibility problems.

Because of space limitations, the data on targets and backgrounds presented in this section will be limited to photopic properties under only one form of natural illumination. Emphasis is placed upon data appropriate for use with the specific atmospheric properties presented in Sect. 6, i.e., a clear day with a moderately high sun at a zenith angle of 41.5°.

3.1 Natural Illumination

The position of the sun and the relative contribution of the sun to the total illuminance have a major effect upon the inherent luminance of objects and backgrounds. The total illuminance on a fully exposed horizontal plane at sea level in clear weather has been

tabulated as a function of the zenith angle of the sun by Brown (1952); a curve plotted from these tables is shown in Fig. 3.1. The same figure also contains data points representing data obtained in the desert near Inyokern, California, on 7 August 1962 by means of a photoelectric illuminometer and shadow intensity meter (see Sect. 8). The measured total illuminance, due to both sun and sky, is denoted by crosses, whereas the component of illuminance due to the sky alone is shown by circled points. Obviously, the contribution due to the sun becomes more important with decreasing solar zenith angle. Fig. 3.2 presents the same data as the ratio of the component of illuminance due to the sky to the total illuminance. The contrast of a shadow on a horizontal, diffusely reflecting background is this ratio minus 1; such contrasts are indicated on the right-hand scale of Fig. 3.2.

On clear days, the total illuminance at a given solar zenith angle shows less variability with air clarity than does the component of illuminance due to the sky, presumably because more sunlight is scattered and redistributed when atmospheric clarity decreases, thus increasing the sky illuminance. Since very little visible light is lost by absorption in the atmosphere unless smoke and dust are present, the redistribution may increase the total illuminance at the very large solar zenith angles, and only slightly decrease the total illuminance when the sun is near the zenith. For example, on the day for which the atmospheric properties are given in Sec. 6, the total illuminance on a horizontal plane at ground level was 5940 lumens/sq. ft. and the ratio of sky component to the total illuminance was 0.235. Thus the total illuminance was only slightly below that for the clear desert

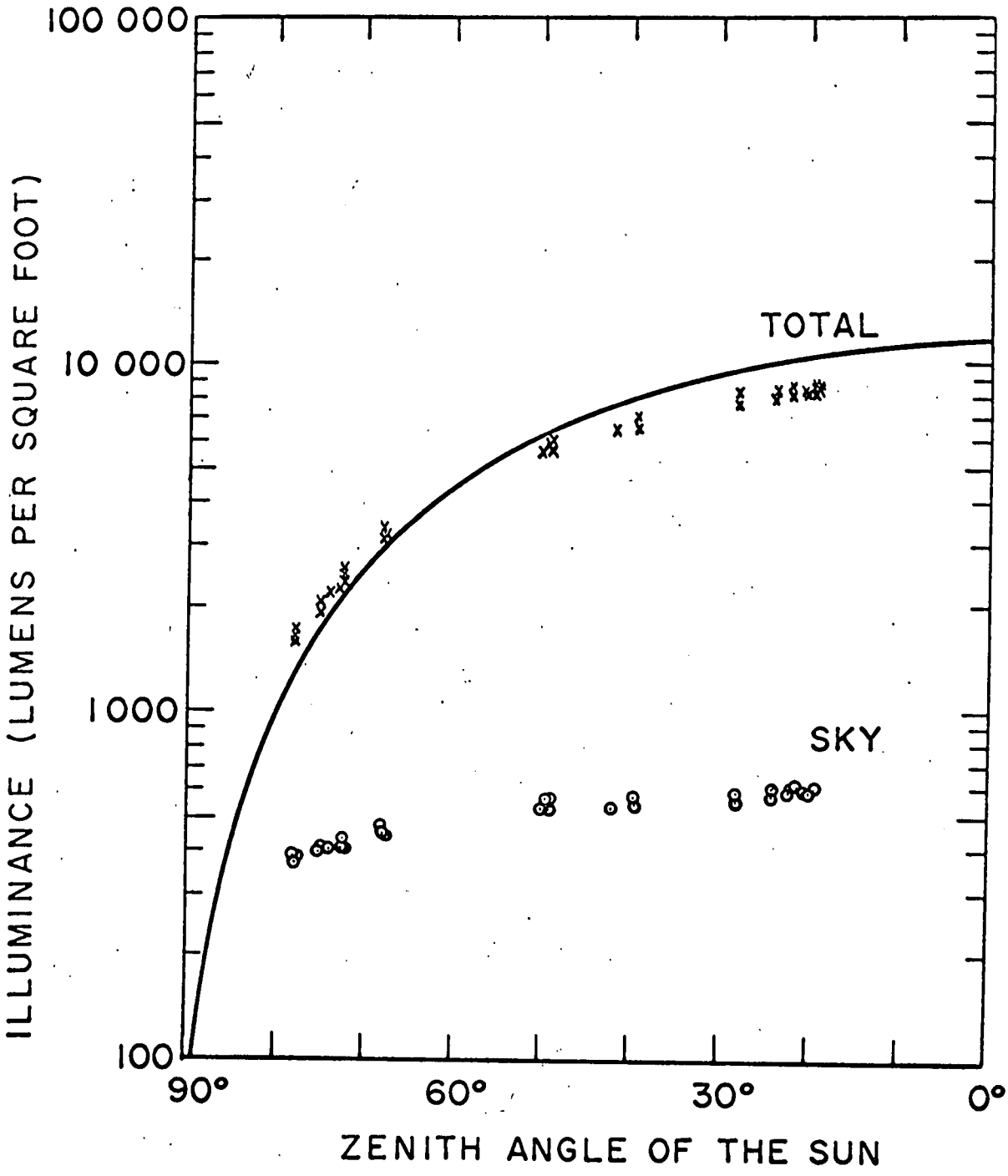

Figure 3.1 Illuminance as a function of sun position; solid curve is from Brown (1952).

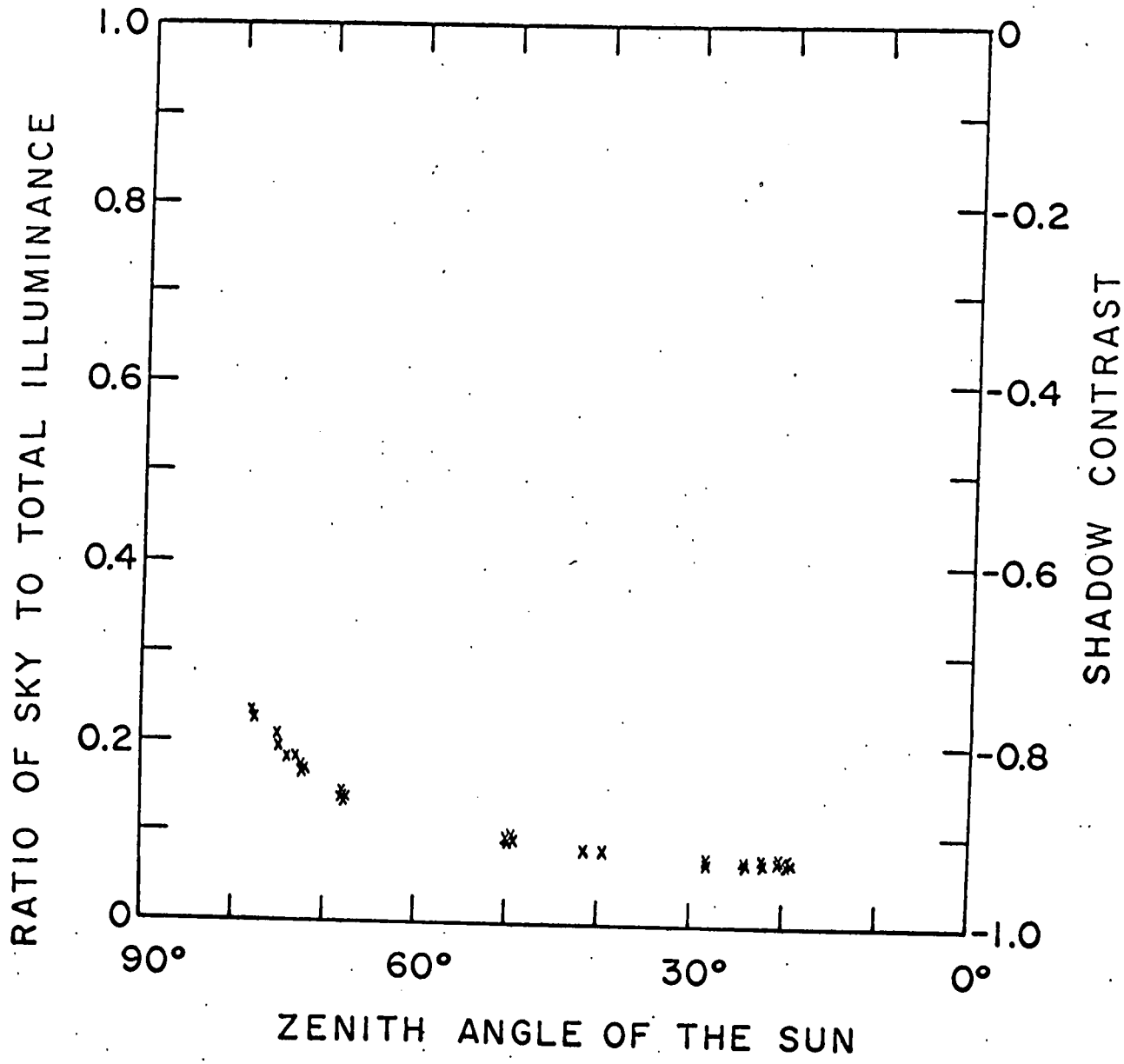

Figure 3.2 Shadow intensity as a function of sun position; ratio presumably goes to 1 when sun has a zenith angle of 90°.

day depicted by the data in Figs. 3.1 and 3.2 but the sky made a much larger relative contribution.

Moonlight. Measurements of the luminance of objects and backgrounds under moonlight are more difficult to make than under sunlight due to the large decrease in illumination. The full moon is approximately the same angular size as the sun and, similarly, serves as the principal source of light. Thus, for the same zenith angle of the sun or moon and the same atmospheric conditions, objects and backgrounds will have the same directional reflectances, and contrasts determined in daylight are, therefore, directly applicable. This is as true for upward and horizontal paths of sight as for downward paths of sight. Moreover, the ratio of the luminance of an object under comparable sunlight and full moonlight conditions is equal to the ratio of the inherent luminances of the sun and the moon.

3.2 Sky Backgrounds

The backgrounds generally encountered on upward-looking paths of sight are skies. Fortunately, the literature contains numerous measurements of sky luminance under a variety of conditions. A most useful compendium by Hulbert (1957) tabulates clear weather sky luminances for nighttime, twilight, and daytime as a function of solar zenith angle, and path of sight. The luminance of overcast skies was treated by Moon and Spencer (1952).

Sky luminance data as a function of altitude and path of sight for a clear day with a solar zenith angle of 41.5° is given in Sect. 6 of this report.

A common background for horizontal paths of sight is the sky near the horizon. Typical horizon sky luminances as a function of time of day or night and type of weather are presented in Table 3.1 from Duntley (1946, 1948b).

Table 3.1 Horizon Sky Luminances

Description	Luminance (Foot Lamberts)
Full daylight	1000
Overcast day	100
Very dark day	10
Twilight	1
Deep Twilight	10^{-1}
Full Moon	10^{-2}
Quarter Moon	10^{-3}
Starlight	10^{-4}
Overcast Starlight	10^{-5}

For horizon sky data for clear weather, nighttime, twilight, and daytime as a function of sun zenith angle and azimuth from the sun, refer to Hulburt (1957). For data coordinated with atmospheric clarity data for sun zenith angle 41.5°, see Sect. 6 of this report.

3.3 Directional Reflectance of Terrains

The characteristic differences in directional reflectance between most man-made surfaces and natural terrains was noted in Sect. 2 of this report. A further example is provided by Fig. 3.3, which depicts weathered aluminum and hard-packed dirt. The latter exhibits prominent backgloss. Table 3.2 gives luminous directional reflectance data for 14 terrains. The first five of these terrains were measured simultaneously with the atmospheric data given in Sect. 6 of this report and are appropriate for use with those data. The remaining nine sets of terrain data were selected as also appropriate for use in the same way. The data in Table 3.2 are ratios of inherent luminance in the direction of the specified path of sight to the total illuminance on a fully exposed horizontal plane at ground level; this was 5940 lumens/sq ft when the atmospheric data given in Sect. 6 were obtained.

Directional reflectance was chosen for tabulation in Table 3.2 to minimize the effect of the change in total illuminance for small changes in sun zenith angle. Only at the paths of sight where the background exhibits a large specular component does a minor change in solar zenith angle cause an appreciable change in directional reflectance. Specular reflectance tends to be most important at angles which reflect the sun and at grazing incidence to the surface.

All the data in Table 3.2 on various terrain backgrounds and other background surfaces, except those for calm water, exhibit the phenomenon of backgloss; i.e., the highest directional reflectance occurs when the path of sight is away from the azimuth of the sun ($\phi = 180^{\circ}$).

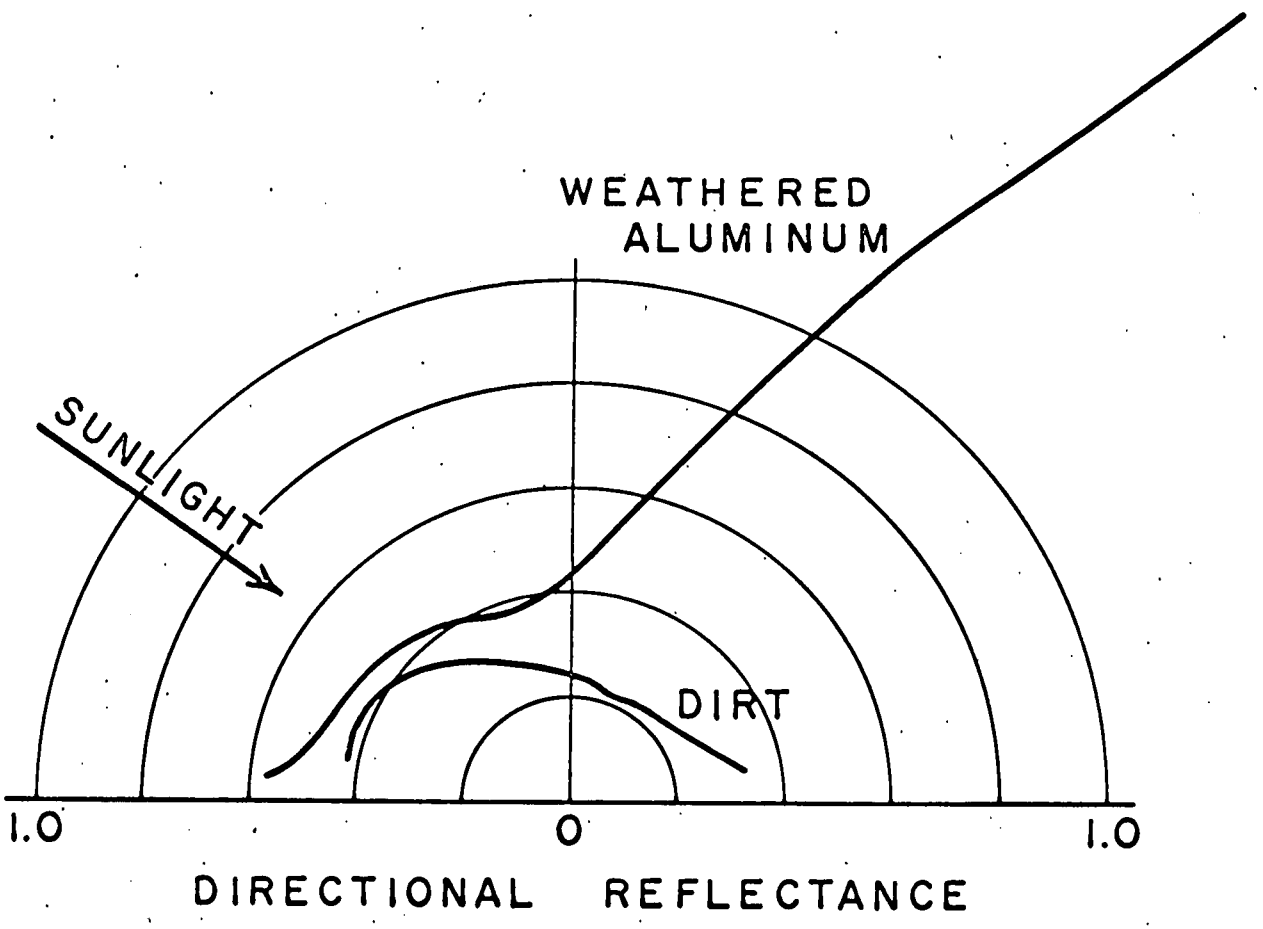

Figure 3.3 Directional luminous reflectance of weathered aluminum (see Table 3.3, object 1) and hard packed yellowish dirt (see Table 3.2, terrain 8).

Description	Sun Zenith Angle	Azimuth of the Path of Sight Relative to the Sun	Zenith Angle of Path of Sight 180	165	150	135	120	105	100	95
1. Pine trees, small uniformly spaced. These data are for the unresolved terrain over which the atmospheric data given in Section 6 were collected .	41.5	0	0.0333	0.0241	0.0214	0.0214	0.0261	0.0379	0.0463	0.0859
		45		0.0222	0.0202	0.0194	0.0210	0.0303	0.0387	0.0549
		90		0.0315	0.0311	0.0317	0.0317	0.0337	0.0387	0.0463
		135		0.0335	0.0382	0.0392	0.0387	0.0438	0.0463	0.0572
		180		0.0402	0.0444	0.0578	0.0640	0.0711	0.0758	0.0825
2. Grass, thick, rather long, pale green, dormant, dryish, little ground showing.*	41.5	0	0.088	0.081	0.076	0.077	0.088	0.094	0.096	0.094
		180		0.098	0.119	0.146	0.150	0.153	0.153	0.160
3. Asphalt, oily, with dust film blown onto oil.*	42.0	0	0.061	0.057	0.058	0.060	0.068	0.090	0.104	0.127
		180		0.067	0.080	0.101	0.090	0.086	0.086	0.088
4. "White" concrete, aged.*	42.2	0	0.266	0.263	0.254	0.254	0.266	0.298	0.320	0.374
		180		0.289	0.313	0.343	0.367	0.350	0.343	0.320
5. Calm water, infinite optical depth. **	41.5	0	0.0222	0.0234	0.0297		0.0569	0.139	0.267	0.461
		45		0.0230	0.0240	0.0272	0.0357	0.107	0.199	0.325
		90		0.0221	0.0222	0.0234	0.0293	0.0711	0.121	0.214
		135		0.0213	0.0212	0.0220	0.0270	0.0665	0.113	0.203
		180		0.0214	0.0212	0.0216	0.0267	0.0718	0.125	0.254

by means of a goniophotometer,

* These terrains were measured on the ground, beneath and during the collection of the data in Section 6.

** Computed from equations by Duntley (1952) for the lighting condition prevailing for items 1 and 2 in this Table.

Description	Sun Zenith Angle	Azimuth of the Path of Sight Relative to the Sun	Zenith Angle of Path of Sight							
			180	165	150	135	120	105	100	95
11. Grass, dry meadow, dense, midsummer.***	45	0	0.0955	0.0897	0.0960	0.0952	0.108	0.129		
	45	90		0.0778	0.0890	0.101	0.111	0.130		
	45	180		0.116	0.131	0.143	0.153	0.170		
	45	270		0.107	0.121	0.134	0.137	0.132		
12. Ilyas, sparse and dry, yellowish grass on sand at end of summer.***	40	0	0.231		0.320		0.342	0.356		
	40	90			0.163		0.176	0.198		
	40	180			0.295		0.353	0.359		
	40	270			0.262		0.237	0.229		
13. Sand Dunes, sharply expressed microrelief dry.***	40	0	0.288		0.183		0.337	0.353		
	40	90			0.284		0.329	0.306		
	40	180			0.246		0.259	0.276		
	40	270			0.278		0.410	0.281		
14. Podsol, ploughed, moist.***	50	0	0.0600	0.0680	0.0646		0.0555			
	50	90		0.0662	0.0953	0.0715	0.0614	0.0761		
	50	270		0.149	(0.180)	0.168	0.168	(0.189)		

*** Luminous directional reflectance for terrains 11 through 14 were computed from spectrophotometric data by Krinov (1947) using C.I.E. Illuminant B.

Parentheses indicate estimates based on incomplete spectral data. Disparity between data for azimuths 90° and 270° "is explained apparently by the direction of shallow furrows in relation to the sun" (Krinov, Belkov, 1953, p.75).

Description	Sun Zenith Angle	Azimuth of the Path of Sight Relative to the Sun	Zenith Angle of Path of Sight 180	165	150	135	120	105	100	95
6. Grass, lush green, closely mowed thick lawn.†	40.4	0	0.100	0.096	0.098	0.108	0.120	0.149	0.168	
	39.6	90		0.103	0.110	0.121	0.138	0.159	0.168	
	39.6	135		0.107	0.125	0.148	0.166	0.178	0.178	
	39.9	180		0.109	0.109	0.119	0.122	0.125	0.125	
7. Macadam, washed off and scrubbed. †	48.5	0	0.113	0.115	0.119	0.128	0.148	0.194	0.229	
	60.1	90		0.110	0.109	0.116	0.122	0.139	0.147	
	46.0	180		0.126	0.141	0.156	0.166	0.172	0.176	
8. Dirt, hard packed, yellowish.†	53.2	0	0.243	0.230	0.229	0.239	0.252	0.300	0.330	
	56.5	90		0.243	0.258	0.260	0.276	0.300	0.304	
	51.1	180		0.272	0.313	0.370	0.422	0.432	0.434	
9. Mixed green forest, deciduous (oak) and evergreen (pine).††	39.0	0	0.0360	0.0325	0.0291	0.0205	0.0205	0.0342		
	37.0	180		0.0410	0.0493	0.0493	0.0820	0.263		
10. Pine Forest††	33.5	0	0.0385	0.0385	0.0308	0.0246	0.0246	0.0200		

†Data taken with a goniophotometer, 10 October 1956.
††Data taken with a photoelectric telephotometer from a helicopter at 300-ft. altitude, mountain forested area near Julian, California, 23 September 1959.

3.4 Objects

The most accurate method of determining the optical characteristics of a three-dimensional object is to measure the optical properties of the actual object or a scale model with optically equivalent surface characteristics on the actual background under natural illumination, thus obtaining the effect of the appropriate interreflections between surfaces. A less precise but simpler approach is to measure the directional reflectance of a flat surface oriented in a series of directions appropriate to the object for the paths of sight in question. The data reported in this section utilized the latter procedure. The number of surface orientations was limited to angle increments of 45°. Thus, a 17-sided figure represents surfaces appropriate for most downward paths of sight, and a 26-sided figure represents surfaces for all paths of sight.

The designation of "object" and "background" is somewhat arbitrary, since what is background in one case may be an object in another. For instance a road may be the background for a vehicle or it may be the object when viewed against the surrounding terrain. Similarly, what is an object in one case may become a background in another. A vehicle may itself be the object, or some surface of the vehicle may be the background against which lettering is to be discerned. In Table 3.2 horizontal, natural and man-made surfaces are arbitrarily called "backgrounds." Just as arbitrarily, man-made surfaces placed in the various orientations described above are termed "objects" in Table 3.3.

The data in Table 3.3 are appropriate for use with the backgrounds in Table 3.2. The three man-made objects are weathered aluminum, an

Object	Sun Zenith Angle	Azimuth of the Path of Sight Relative to the Sun	Normal From Surface: Zenith Angle	Normal From Surface: Azimuth	Zenith Angle of Path of Sight: 180	165	150	135	120	105	100	95
1. Weathered Aluminum**	56.5	0	0	0	0.440	0.62	1.18	3.65	9.2	3.75	3.30	3.03
	56.2	0	45	180	0.255	0.245	0.245	0.350	1.03	0.86	0.92	1.08
	56.2	0	45	0	1.00	0.76	0.72					
	57.2	0	45	±90	0.380	0.405	0.51	0.70				
	56.4	0	90	180		0.231	0.269					
	55.8	90	0	0	0.440	0.465	0.445	0.451	0.475	0.52	0.55	0.56
	56.2	180	0	0	0.440	0.392	0.400	0.440	0.460	0.485	0.52	0.58
	56.1	180	45	0	1.00	1.80	5.9	3.80	1.62	0.99	0.87	0.80
	56.1	180	45	180	0.255	0.275	0.328					
	57.2	180	45	±90	0.380	0.380	0.420	0.470				
	57.3	180	90	±45				0.58	0.61	0.64	0.65	0.66
	56.2	180	90	0		0.455	0.51	0.60	0.70	0.76	0.82	0.88
Weathered Aluminum (Shadowed)**	56.0	0	0	0	0.206	0.206	0.245					
	56.0	180	0	0	0.206	0.223	0.261	0.290	0.290	0.310	0.330	0.415

*Sky condition: Clear
**Data taken with a goniophotometer, January 1959.

Table 3.3 Directional Luminous Reflectance of Objects

Object	Sun Zenith Angle	Azimuth of the Path of Sight Relative to the Sun	Normal From Surface: Zenith Angle	Normal From Surface: Azimuth	Zenith Angle of Path of Sight: 180	165	150	135	120	105	100	95
2. Aluminum Paint **	56.5	0	0	0	0.362	0.420	0.64	1.35	3.45	3.45	3.38	3.45
	55.9	0	45	180	0.198	0.193	0.220	0.340	0.97	0.83	0.93	1.07
	55.9	0	45	0	0.77	0.64	0.58					
	57.0	0	45	±90	0.292	0.292	0.345	0.490				
	56.5	0	90	180		0.180	0.222					
	55.8	90	0	0	0.362	0.362	0.370	0.380	0.385	0.420	0.440	0.440
	56.5	180	0	0	0.362	0.355	0.400	0.460	0.490	0.50	0.50	0.50
	55.8	180	45	0	0.77	1.06	1.58	1.45	1.20	0.82	0.75	0.68
	55.8	180	45	180	0.198	0.220	0.270					
	57.0	180	45	±90	0.292	0.310	0.345	0.410				
	57.5	180	90	±45				0.52	0.57	0.56	0.56	0.56
	56.3	180	90	0		0.460	0.52	0.65	0.71	0.74	0.73	0.72
Aluminum Paint (Shadowed)**	56.1	0	0	0	0.180	0.183	0.210					
	56.1	180	0	0	0.180	0.200	0.240	0.246	0.242	0.271	0.285	0.299

Luminous

Table 3.3 Directional Reflectance of Objects

Object	Sun Zenith Angle	Azimuth of the Path of Sight Relative to the Sun	Normal From Surface: Zenith Angle	Normal From Surface: Azimuth	Zenith Angle of Path of Sight: 180	165	150	135	120	105	100	95
3. Glossy White Paint**	57.2	0	0	0	0.92	0.92	0.95	1.38	4.40	1.85	1.50	1.40
	55.9	0	45	180	0.248	0.245	0.274	0.395	1.01	0.87	0.99	1.10
	55.9	0	45	0	1.59	1.49	1.33					
	56.8	0	45	±90	0.72	0.74	0.78	0.82				
	56.3	0	90	180		0.236	0.290					
	55.0	45	0	0	0.92	0.91	0.90	0.89	0.89	0.82	0.79	0.75
	55.5	90	0	0	0.92	0.91	0.90	0.89	0.86	0.78	0.70	0.64
	55.0	135	0	0	0.92	0.91	0.90	0.89	0.84	0.72	0.64	0.54
	57.2	180	0	0	0.92	0.92	0.94	0.99	1.06	0.95	0.89	0.83
	55.9	180	45	0	1.59	1.68	2.85	1.83	1.69	1.62	1.63	1.63
	55.9	180	45	180	0.248	0.257	0.315					
	56.9	180	45	±90	0.72	0.74	0.81	0.85				
	57.5	180	90	±45				1.30	1.32	1.33	1.32	1.32
	56.2	180	90	0		1.20	1.43	1.50	1.50	1.46	1.46	1.42
Glossy White Paint (Shadowed)**	56.3	0	0	0	0.223	0.216	0.240					
	56.3	180	0	0	0.223	0.240	0.290	0.285	0.290	0.352	0.400	0.490

aluminum painted surface, and a glossy white painted surface. Diagrams depicting the orientation of the surfaces and the zenith angle and azimuth (θ,ϕ) of the normal from each surface are presented in Fig. 3.4. The top part of the figure is for the path of sight toward the azimuth of the sun, $\phi = 0^\circ$; as shown on the right, the path of sight has various zenith angles from 180° (straight downward) to 95° (nearly horizontal). Similarly, the bottom portion of Fig. 3.4 is for the paths of sight looking away from the sun. These diagrams are to be used as aids in interpreting the data presented in Table 3.3.

3.5 Inherent Contrast

A graphical method for representing the inherent contrast of objects and backgrounds for various paths of sight is illustrated by Fig. 3.5, wherein data from Tables 3.2 and 3.3 for terrain 8 (dirt) and object 1 (weathered aluminum), respectively, are plotted in semilogarithmic form. Consider first the two solid curves. The (small) vertical separation between them is a direct (logarithmic) measure of the ratio of the directional reflectance of the two surfaces along all downward inclined paths of sight in the plane away from the sun. Similarly, the (large) vertical separation between the two dotted curves shows graphically the magnitude of the ratio of the corresponding directional reflectances for paths of sight toward the plane of the sun (azimuth 0°).

A semilogarithmic plot of the vertical separations between the two pairs of curves in Fig. 3.5 is shown in Fig. 3.6. The object-to-background ratios (separations) are plotted on the logarithmic scale at the right in Fig. 3.6. The scale on the left is for contrast, which is simply the object-to-background ratio minus one.

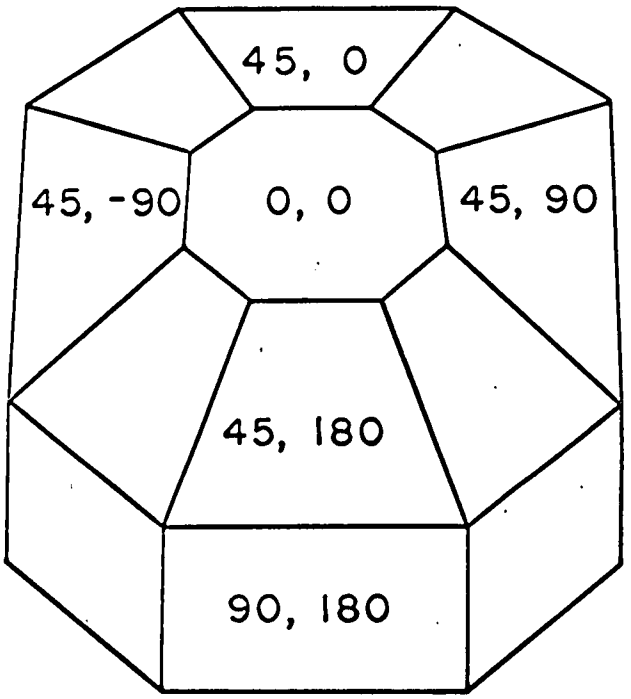

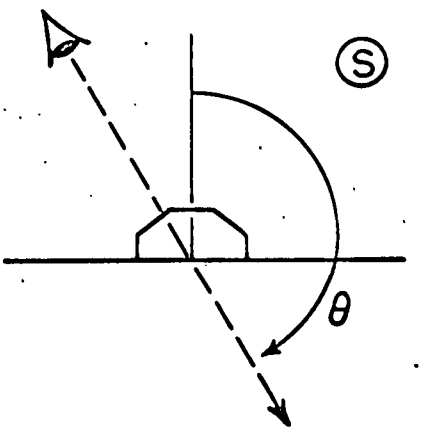

AZIMUTH OF PATH OF SIGHT 0°

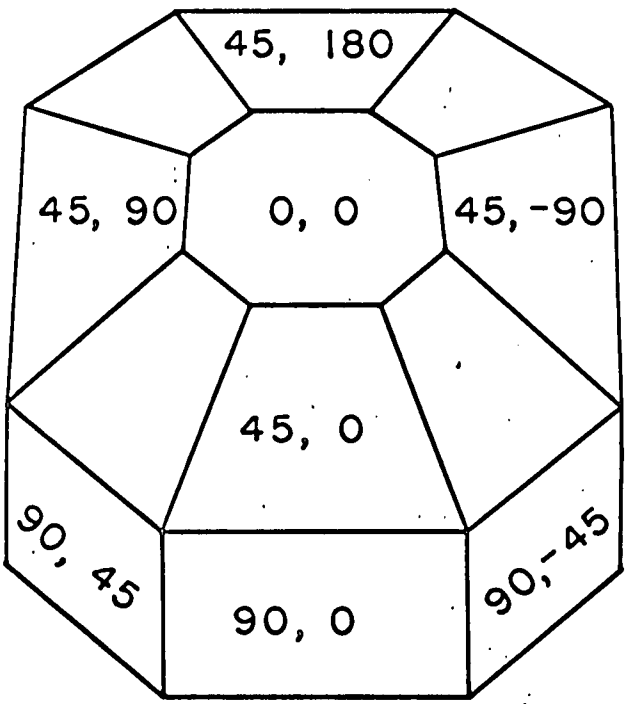

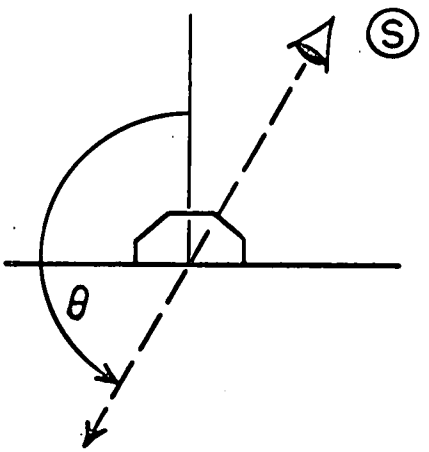

AZIMUTH OF PATH OF SIGHT 180°

Figure 3.4 Surfaces of three-dimensional objects; each number pair refers to the zenith angle and azimuth from the plane of the sun of the normal from the surface, respectively.

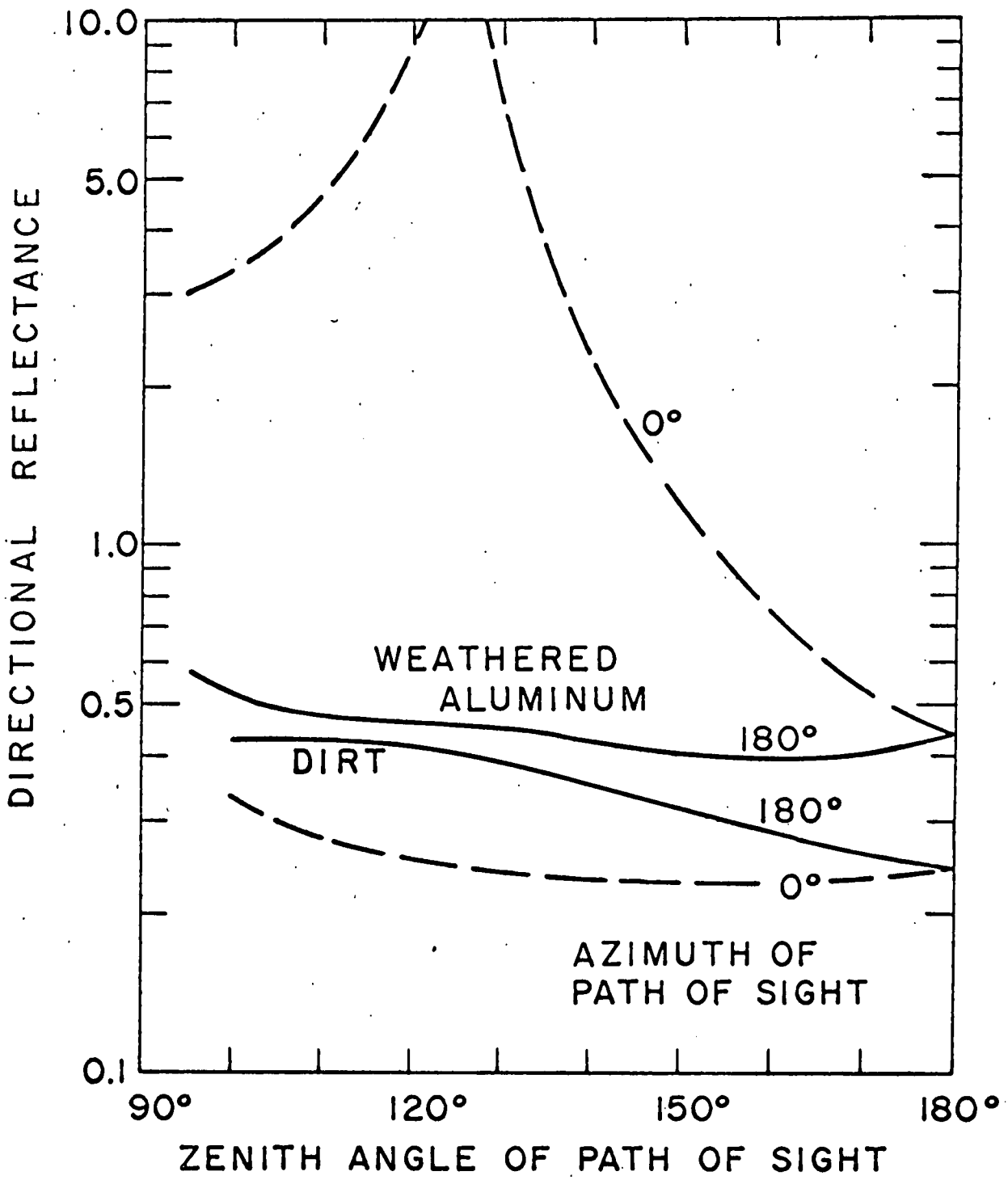

Figure 3.5 Reflectance of object and background.

Practical convenience is often served by a ruler bearing a logarithmic reflectance-ratio scale marked in contrast. When such a ruler is used, zero contrast is always placed on the curve of background reflectance and contrast is read from the curve of target reflectance vertically above or below, depending upon whether the contrast is positive or negative.

If, for a given three-dimensional object for one azimuth of the path of sight, the contrasts of all of the surfaces are plotted in similar fashion on one graph, a quick picture is obtained of the range of contrast contained within the complex object. This form for plotting contrast has the additional advantage of duplicating the precision of the initial measurements.

3.6 Contrast Control

The above techniques are of direct usefulness to problems of contrast control. Either contrast minimization, or contrast maximization may be desired.

To a first approximation it can be assumed that a paint can be found with approximately the same directional characteristics as the object surface but lower or higher in reflectance. A reflectance curve of such a paint would have the same characteristics as shown in Fig. 3.5 but displaced above or below the curve depending on whether the reflectance has been raised or lowered. Therefore the contrast curve in Fig. 3.6 can be assumed to depict the contrast of the new paint but with the curve displaced above or below the present curve. Instead of moving the curve, the zero contrast line may be moved with the same result.

In selecting a new reference line it is desirable to minimize (or maximize) the absolute value of the contrast, since the human eye

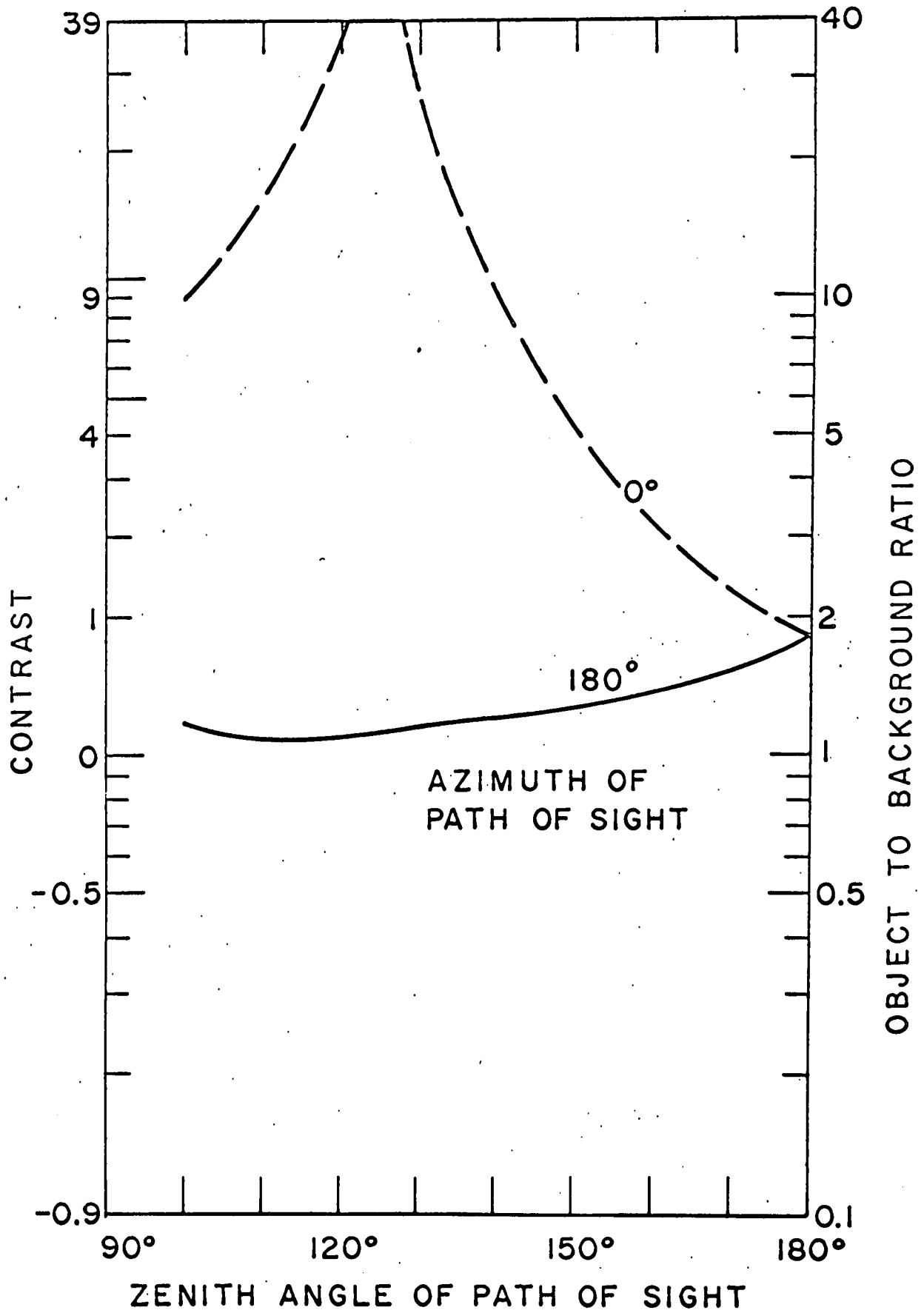

Figure 3.6 Contrast of object and background

responds equally to positive and negative contrast of the same absolute value. Often the best reduction (or increase) in the absolute contrast can be achieved by the minimization (or maximization) of the area between the zero contrast line and the contrast curves when the curve is plotted on a linear contrast scale. One way to achieve minimization is to have as large a portion of the contrast curve lie on or near zero contrast as possible. This also usually means that the areas under the curve are fairly equally divided between positive and negative contrast.

In carrying out the above procedures, several cautions should be noted:

First, the coordinates used for plotting the contrast curves in Fig. 3.6 gravely distort the contrast picture. On this grid equal distances above and below the contrast line do not constitute equal absolute contrasts. The grid completely masks the fact that negative contrast has a maximum value of minus one, whereas positive contrast can be infinitely large. For this reason, in evaluating a change in reference line it is important to use a movable contrast scale to measure the new absolute values of contrast achieved.

The second factor to be noted while minimizing (or maximizing) contrast is the relative importance of portions of the contrast curves. These must be evaluated in terms of the size of the projected area of the object which has this particular contrast. Consider, for instance, a horizontal surface. The maximum area is seen when the path of sight is normal to the surface, a zenith angle of 180°. At 120° zenith angle the projected area has been reduced to 50 percent of its maximum. Therefore, for horizontal surfaces the most important portion of the

contrast curve lies on the right-hand side of the graph in Fig. 3.6, and the contrasts for the more slanted paths of sight (zenith angles less than 120^{o}) can be ignored.

The third caution concerns the achievability of the paint reflectance needed to produce the desired contrast change. The minimum achievable reflectance for black paint depends upon whether a dull or glossy finish is desired.

The reflectance of the desired paint is obtained by dividing the reflectance of the object surface by the factor by which the zero reference line has been raised or multiplying by the factor by which it has been lowered.

The final step necessary to complete the engineering procedure for contrast minimization (or maximization) is to obtain contrast curves for paints believed to have the required directional reflectance characteristics. This requires directional measurements of the paint under appropriate lighting conditions.

4.0 THE USE OF VISUAL PERFORMANCE DATA IN VISIBILITY PREDICTION

by

John H. Taylor

The optical signal which reaches the observer, after modification by the optics of the environment and the transmission properties of any interposed devices (magnifiers, photographic or video links and the like), constitutes the raw material of visual discrimination. The visual performance capabilities of the observer will, accordingly, govern whether the available signal provides an adequate basis for the discrimination of interest. While the properties of the human visual apparatus have been extensively studied in terms of anatomy, histology, chemistry and electrophysiology, studies of visual performance have proven to be far more useful in the prediction of visibility. This report will be concerned with certain visual performance data which are now available, with the techniques used in applying these data to visibility problems, and with one or two examples in which it has recently been verified that these techniques lead to useful predictions. Human vision has, because of its overwhelming importance in human behavior, been studied intensively by behavioral scientists from the earliest days of recorded scientific history. Since the birth of experimental psychology all aspects of visual experience have been subjected to ever more rigorous and quantitative experimentation. As a result, the scientific literature abounds in data relating to the visual process. On close inspection, unfortunately, it becomes clear that only a very small proportion of these data are useful in formulating predictive techniques, and that only a relative handful of quite recent data

are sufficiently precise or systematic to allow quantitative estimates over a useful range of conditions. There are two major reasons for this difficulty. On one hand, those data which have been collected for traditional reasons of basic research come usually from carefully controlled and abstracted laboratory experiments which, quite properly, have been designed to isolate and study single parameters of visual performance or, at most, a few interrelated ones. In general these studies have produced the most elegant quantititive data, have investigated the effects of varying physical attributes of the stimulus over very wide ranges, and are, except for rare instances, difficult to apply directly in solving applied visibility problems. The second main body of data which is available come from frankly applied experiments. In these studies great pains may have been taken to simulate the real situation, not only as regards the appearance of the stimulus, but extending to the purposeful inclusion of extraneous stimuli, fatigue, stress, reward, punishment, and whatever other condition that the experimenter may believe to be an important determinant or modifier in the real situation. This class of studies has yielded results which, depending upon the ingenuity of the investigator in selecting the salient aspects of the problem situation, tend to be directly useful in prediction for a specific situation, and which all too often disappear into limbo as soon as the emergent problem has been solved.

This, then, is the dilemma which confronts anyone seeking to predict visual performance in any but the very simplest of real situations. It is highly unlikely that his specific problem has been studied previously, so that no adequate data for direct application are to be found. Further, the large body of quantitative data from abstracted laboratory experiments

may seem to have little predictive value when referred to the complex visual tasks of ordinary occurrence. Nevertheless, it is generally believed that these basic visual performance data will ultimately, as more and better data accrue, allow any visibility question to be answered most accurately and expeditiously. And it is owing to this conviction that the new science of visibility is developing ever more potent predictive techniques. To be sure, tremendous lacunae still exist in the visual performance data, and we are many years away from being able to handle certain classes of problems in a confident way; for these we must still appeal to simulation or be content with approximate solutions. For the increasing variety of problems which have been posed, there is becoming available an increasing body of quantitative laboratory data to assist us in giving better answers over a wider range of situations. Some of the most useful visual performance data will first be presented, and then the manner of interrelating them will be shown, some considerations in making the jump from laboratory to real life will be listed, and, finally, a specific problem and its mode of solution will be described.

4.1 Contrast discrimination data

By far the most widely known and utilized body of data which has been used in visibility prediction came from studies conducted during and after World War II at the Tiffany Foundation, and which were reported by Blackwell (1946). These data indicate the dependency of target detection upon the angular extent of the stimulus (circles) and upon the level of background luminance to which the observer is adapted. More recently, these data have been supplemented to include the case of larger targets (Taylor, 1960a and 1960b) than the six-degree ones of the earlier study.

The data now in use are a composite of the two studies, and are shown in Figure (4.1). Despite the manifest limitations of this fund of data, they remain our single most comprehensive indicator of the manner in which luminance contrast requirements vary with target size and background level. It will be shown later that these same data have been used, with others, in formulating constructs which help in treating more complicated stimulus situations.

Despite the extensiveness of the Tiffany data, it must be remembered that, rigorously speaking, they refer only to the special case of uniform circular targets against uniformly luminous backgrounds, by uncontrolled binocular vision, and with effectively infinite viewing time. The time of occurrence of the stimulus was known to the observers, as was their location. It is necessary, therefore, to evaluate the importance of such additional properties of the visual signal as shape, location in space and time, discontinuities either of luminance or of duration, as well as the properties of the background. A considerable number of studies are to be found which bear upon one or another of these variables, and some of those which have yielded usefully quantitative data will be cited. No attempt will be made to provide an extensive catalogue of relevant data (for this the reader is encouraged to consult the sources listed in the final section of this report), but those in common use in visibility problem solving will be described.

4.1.1 Target duration. A recent study by Blackwell and McCready (1958) provides comprehensive data concerning the influence of stimulus duration upon detection. The experiments were carried out with seven values of target duration ranging from 1.00 second to 0.001 second. Background luminance was varied over six orders of magnitude from 100 ft-L down to

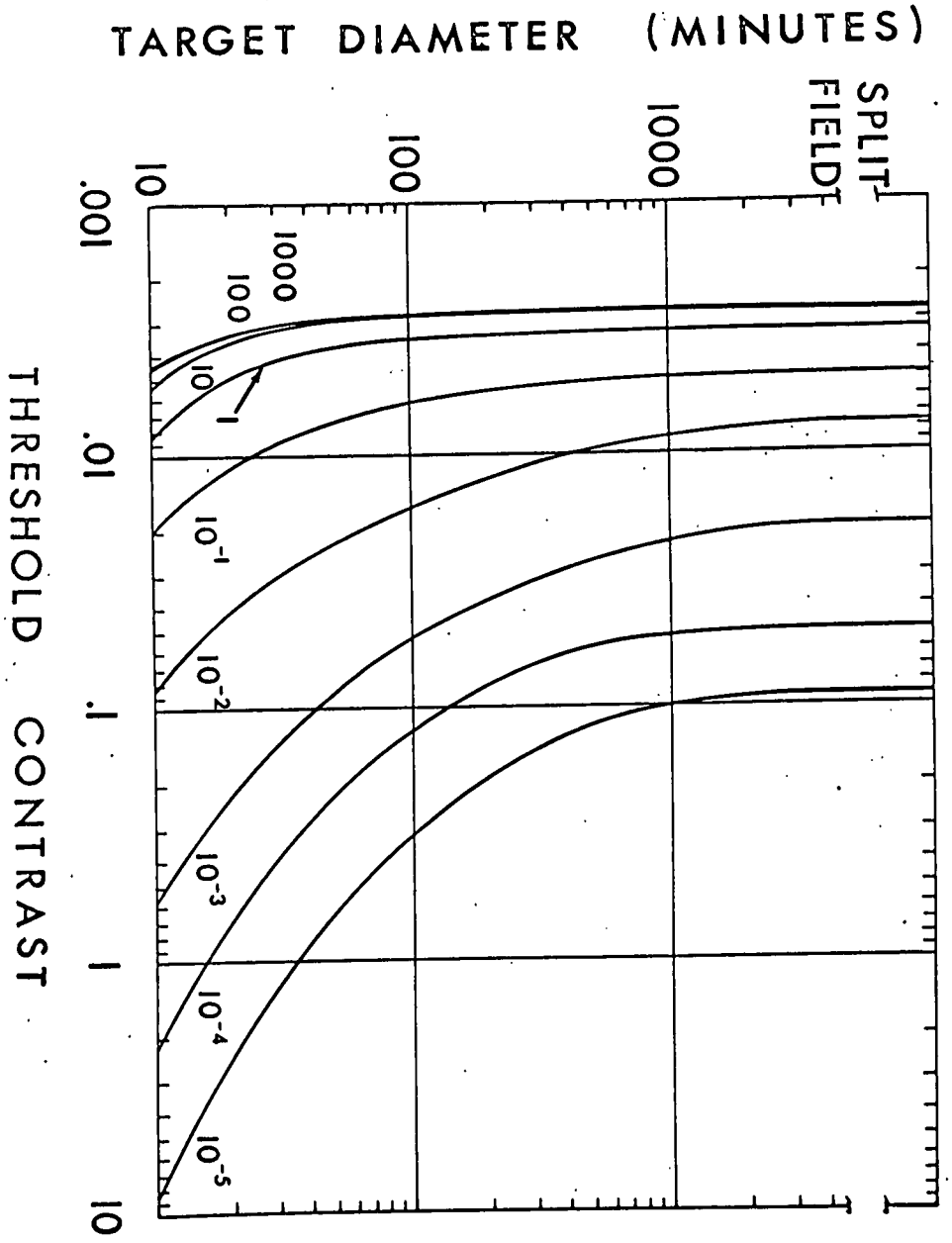

Figure 4.1 Threshold contrast as a function of the diameter of a uniform circular target. This figure represents an extension of the Tiffany data based upon experiments referred to in the text. The assumption was made that asymptotic values of contrast would be reached in the case of a "split field," i.e., with a target of infinite radius. Each curve refers to a different adaptation luminance level, expressed here in ft-L.

0.001 ft-L, and four sizes of circular targets were used, subtending 0.80, 3.2, 12.8, and 51.2 arc minutes. Uniformly luminous circular stimuli, again, were displayed against uniform backgrounds. All observations were made using foveal vision, however, so that direct application of the data may be made only to axial lines of sight. Since many visibility problems involve initial target detection along paraxial optical paths, supplementary data for peripheral vision are clearly needed, and a recent study by this Laboratory will later be described which represents a beginning step in meeting this need. For the special case of stimuli of very brief duration, the so-called "laws" of Bunsen and Roscoe and of Bloch, and the equations of Blondel and Rey are frequently useful engineering approximations in visibility prediction. The limitations of both are well discussed in papers by Barlow (1958) and by Neeland, Laufer and Schaub (1938).

One region of the stimulus duration continuum is of unique interest in visibility. A recent study by Ford, White, and Lichtenstein (1959) and a succeeding one by White and Ford (1960) have shown that the dwell time in visual search (the time that the eyes remain stationary between fixations) of a field of average complexity tends toward a value of about 1/3 second. This finding has created an enhanced interest in the visual performance data which refer to approximately this stimulus duration. Generally speaking, then, visibility problems are likely to center upon target durations of three categories: very brief flashes, as signal beacons, flashers, etc; moderately short glimpses, as in visual search, or; essentially unlimited viewing times.

4.1.2 Target location. The data so far cited as being sufficiently extensive for use in problem solving share the common limitation that they refer only to vision on the line of sight. (An exception to this occurs

in the Tiffany data for low background levels, where the direction of fixation was indeterminate.) Since various regions of the human retina show great differences in sensitivity, and because target detection in ordinary seeing is most frequently first accomplished in the peripheral visual field, the laboratory data for strictly central vision are of limited applicability. The central visual field is most sensitive at high levels of adapting luminance, but this advantage becomes progressively less as the levels are reduced. At some value of prevailing luminance (circa 0.001 ft-L) all parts of the visual field are approximately equisensitive, and at still lower levels central vision becomes (except for extreme reds) strongly subordinate to off-axis vision. These facts, with others, have led to a great deal of experimental work on contrast sensitivity as a function of target location in the visual field. Again, however, these studies have not yielded sufficient systematic quantitative data of useful generality, although they are of tremendous value in showing the relative magnitudes and interactions of certain effects.

An appropriate case in point is provided by a study by Blackwell and Moldauer (1958), who investigated the dependence of contrast threshold upon location of the target within the field of view. Nine levels of adapting luminance were used, and targets were presented centrally and at five eccentric positions out to 12° in the field. The stimulus was an effective point source (subtending 1 minute of arc) presented in a 0.01-second flash, both of which conditions limit the direct applicability of the data to a very few visibility problems. Nevertheless, until quite recently the Blackwell-Moldauer data have had to be appealed to as our best index of quantitative sensitivity changes with target location, and over a wide range of luminance levels. Not long ago, because of certain misgivings

about the legitimacy of using existing data for problems involving visual search, a study was made using a range of target sizes from 1 minute to 120 minutes of arc. The stimuli were presented at seven positions in the visual field, from the center to a distance of 12.5 degrees from the fovea along one meridian. A single value of photopic adaptation luminance was used (75 ft-L), and the targets were exposed for 0.33 second in order to approximate the search situation. The data from this study (Taylor, 1961) are presented in Figure 4.2. While the experiment was limited to a single background luminance and to only 12.5 degrees off-axis, the range of target sizes selected embraces most objects in the natural visibility situation.

4.1.3 Target shape. Up to this point the detection data relating to brightness contrast discrimination have come from studies using uniformly bright circular stimuli. Since ordinary objects are rarely so simple, there has been considerable effort applied to evaluating the effects of target shape upon detectability. A promising approach was suggested by Graham et al.(1939) and has been elaborated by several recent workers (for a summary, see Blackwell, 1963). Very simply stated, it is found that spatial summation of stimulus energy occurs within the visual system, and that an empirical weighting function can be found by experiment which can then be applied to the prediction of a considerable range of stimulus shapes. The basic data used in deriving this summation function are obtained by extensive studies of circular targets of varying size, and the nature of the function is found to depend upon such factors as adaptation luminance, position in the field, and the time of presentation. A specimen of such data is shown in Figure 4.3 and Table 4.1, which present the results of a recent study from this Laboratory in which we sought to provide

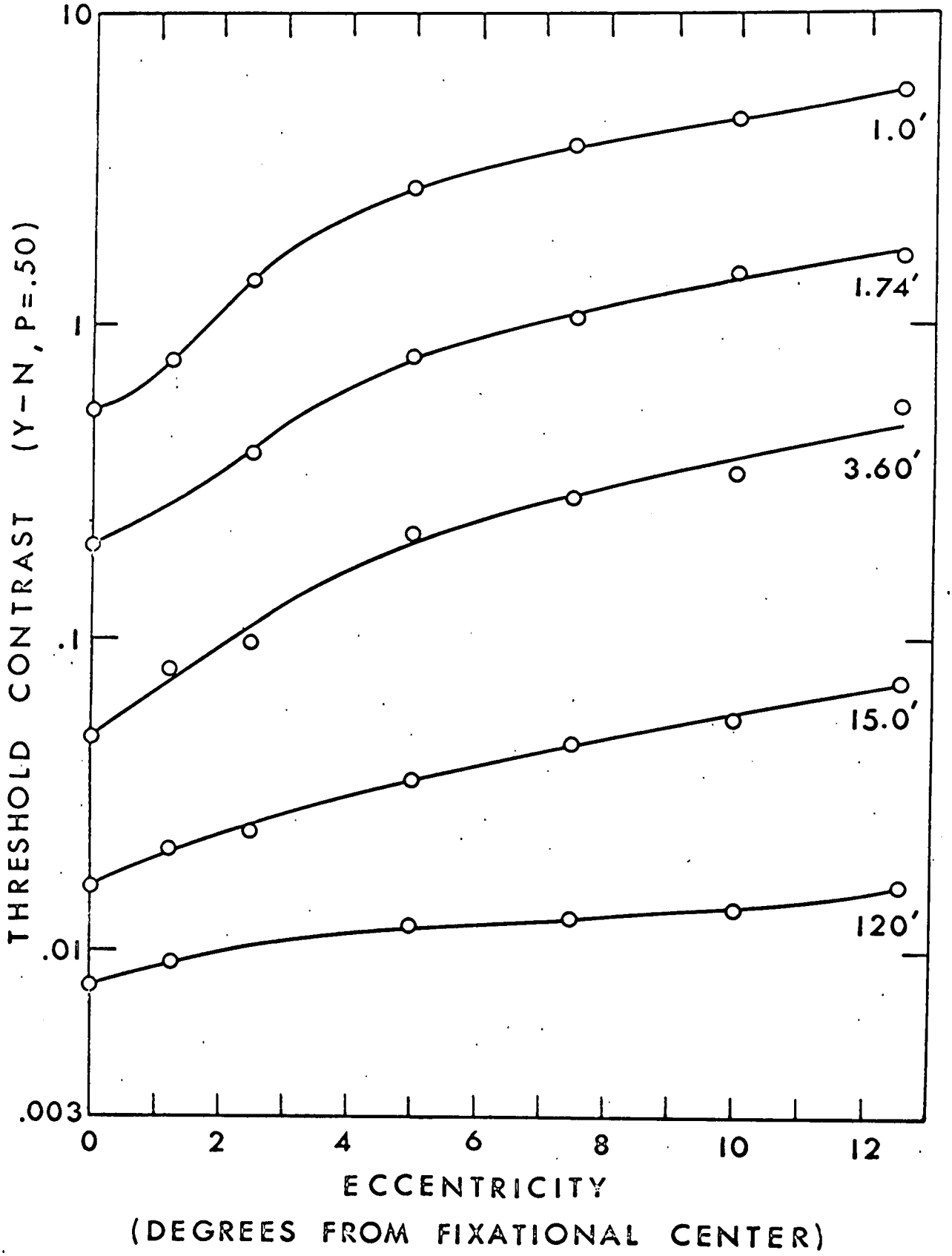

Figure 4.2 Threshold contrast as a function of retinal position and target size for binocular photopic vision. Adaptation level was 75 ft-L, and the target duration was 0.33 second. The curves are labelled to indicate the angular diameter of the uniform circular stimuli. Four observers, for which the plotted average values represent 0.50 probability of detection in a 'yes-no' experiment. Each data point is based upon 2400 observations.

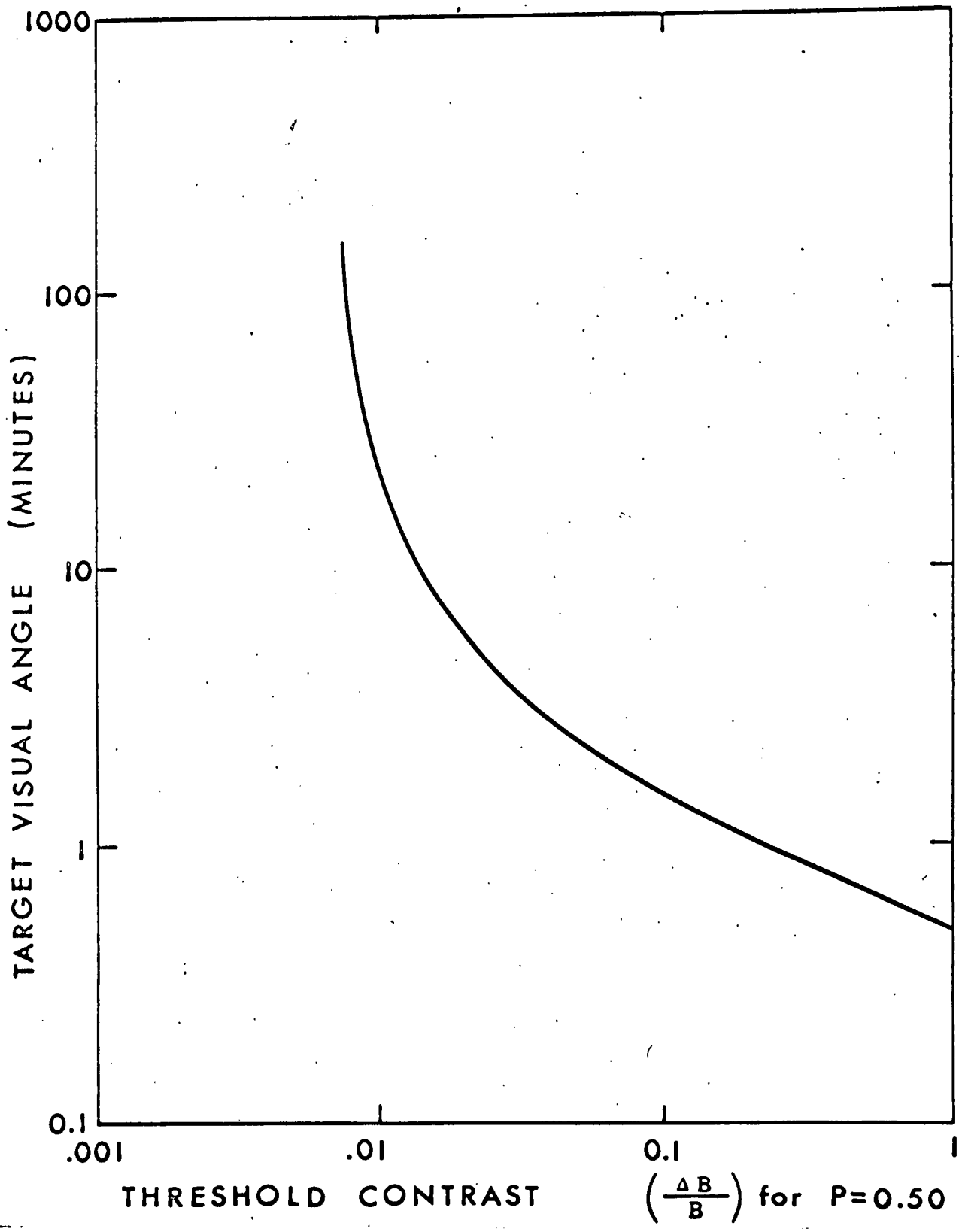

Figure 4.3 A redetermination of the target size and threshold contrast dependency made under controlled conditions of central foveal fixation and an invariant target duration of 0.33 second. Background luminance constant at 75 ft-L. The forced-choice temporal psychophysical method was used, and the data represent averages from 5 observers, who made a total of 45,000 observations, using 18 target sizes. (See Table 4.1)

Table 4.1 Values of threshold contrast as a function of target diameter for a stimulus duration of 0.33 second, binocular viewing, foveal fixation, and forced-choice temporal method. These values are averages from the large-scale plots of four observers, and hence represent smoothed data.

TABLE 4.1

Target Diameter (Min of Arc)	Threshold Contrast	Target Diameter (Min of Arc)	Threshold Contrast	Target Diameter (Min of Arc)	Threshold Contrast	Target Diameter (Min of Arc)	Threshold Contrast
120.0	0.00763	8.20	0.0158	3.32	0.0320	1.95	0.0650
82.5	0.00785	7.80	0.0163	3.22	0.0331	1.92	0.0670
62.5	0.00810	7.40	0.0168	3.15	0.0341	1.88	0.0690
51.0	0.00835	7.00	0.0174	3.07	0.0352	1.85	0.0710
43.5	0.00860	6.75	0.0179	3.00	0.0362	1.82	0.0735
37.0	0.00890	6.45	0.0184	2.90	0.0373	1.78	0.0760
32.5	0.00915	6.10	0.0191	2.82	0.0384	1.75	0.0780
29.5	0.00940	5.90	0.0196	2.75	0.0396	1.73	0.0800
23.5	0.0100	5.65	0.0202	2.70	0.0404	1.70	0.0830
21.5	0.0103	5.40	0.0208	2.61	0.0422	1.67	0.0855
19.0	0.0107	5.15	0.0216	2.55	0.0436	1.64	0.0883
17.5	0.0110	5.00	0.0222	2.49	0.0450	1.61	0.0910
16.5	0.0113	4.80	0.0229	2.43	0.0464	1.58	0.0940
15.0	0.0117	4.60	0.0236	2.39	0.0478	1.56	0.0965
14.2	0.0120	4.45	0.0243	2.33	0.0492	1.53	0.100
13.2	0.0124	4.30	0.0251	2.29	0.0504	1.51	0.102
12.5	0.0127	4.15	0.0258	2.24	0.0522	1.48	0.106
11.5	0.0132	4.00	0.0267	2.19	0.0541	1.46	0.108
10.8	0.0136	3.90	0.0275	2.15	0.0558	1.44	0.112
10.2	0.0140	3.75	0.0283	2.11	0.0573	1.42	0.116
9.70	0.0144	3.65	0.0292	2.06	0.0592	1.39	0.119
9.10	0.0149	3.50	0.0301	2.03	0.0610	1.38	0.122

TABLE 4.1 (Cont.)

Target Diameter (Min of Arc)	Threshold Contrast	Target Diameter (Min of Arc)	Threshold Contrast	Target Diameter (Min of Arc)	Threshold Contrast	Target Diameter (Min of Arc)	Threshold Contrast
8.70	0.0153	3.41	0.0311	1.99	0.0630	1.35	0.127
1.33	0.131	0.945	0.264	0.671	0.530		
1.32	0.134	0.930	0.272	0.660	0.550		
1.29	0.138	0.920	0.280	0.651	0.565		
1.27	0.143	0.905	0.288	0.642	0.583		
1.25	0.148	0.890	0.297	0.633	0.600		
1.23	0.152	0.880	0.306	0.622	0.620		
1.21	0.157	0.865	0.316	0.615	0.635		
1.19	0.162	0.855	0.326	0.604	0.660		
1.18	0.166	0.840	0.337	0.596	0.680		
1.16	0.172	0.830	0.347	0.588	0.700		
1.14	0.178	0.815	0.358	0.579	0.720		
1.12	0.183	0.805	0.369	0.569	0.745		
1.11	0.189	0.790	0.380	0.560	0.770		
1.09	0.195	0.780	0.392	0.552	0.795		
1.08	0.200	0.765	0.405	0.545	0.815		
1.06	0.207	0.759	0.415	0.537	0.840		
1.04	0.213	0.745	0.428	0.528	0.870		
1.03	0.220	0.735	0.442	0.519	0.900		
1.02	0.226	0.725	0.455	0.512	0.925		
1.00	0.233	0.713	0.470	0.505	0.950		
0.990	0.240	0.701	0.485	0.497	0.985		
0.975	0.248	0.692	0.500				

detailed data for a specific set of viewing conditions. Studies are now in progress which test the adequacy of this approach to predict visibility ranges. One special case of contemporary interest is that of very long and very thin objects, such as wires or roads seen from aircraft or space vehicles. The sightings reported by our astronauts, especially by Major Gordon Cooper, were thought by some to have been unlikely in view of existing laboratory data. Close analysis of the reports, however, and their comparison with appropriate data for extended targets (e.g., Hecht and Mintz, 1939) reveal that the sightings were entirely possible.

4.1.4 Non-uniform backgrounds. A large proportion of visibility problems involve backgrounds which have luminance gradients. The systematic study of this problem has proven a formidable one, and only a few beginnings have been made. Blackwell and Bixel (1960) have used the concept of "effective contrast" --derived from equivalent uniform background data--with some success in cases where the structural elements of the target and background are of comparable size. Hamilton and Blackwell (1957) investigated the effect of the presence of a single luminance gradient, such as an horizon. In connection with an air-sea rescue problem involving searchlights with non-uniform beam intensities, an experiment was performed here which simulated the beam, the surrounding dark ocean, and the targets of interest. The results of this study are shown in Figure 4.4, and are typical of the limited sorts of data which must occasionally be obtained by direct simulation for want of adequate general information. The data suggest that the immediate target background luminance is the prime determinant of the threshold, although no generality is assumed for this result.

Fixation at	Target location within non-uniform field				
	A	B	C	D	E
C	7.90	2.23	0.616		
D		3.13	1.28	0.763	
E			3.11	2.03	1.64

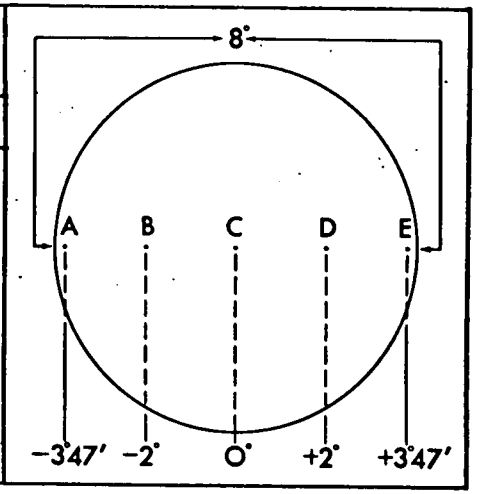

Figure 4.4 Threshold contrasts for 1-minute circular targets seen against an 8° circular background of non-uniform luminance with a dark surround. The background has a central luminance of 1 ft-L which fell off in approximate accordance with the cosine law until the edge luminance was 0.1 ft-L. Eye fixations and stimulus locations are given in terms of the notation in the sketch to the right of the figure. The data, while limited to a single specific case, indicate that the two variables interact in a manner too complicated to predict from ordinary data for uniform backgrounds of large angular extent.

4.2 Field factors

Visual response data collected in the laboratory generally represent contrast sensitivities which will never be exceeded in the field situation, and which must therefore be converted into values which are of useful predictive value in visibility calculations. There are two kinds of conversion which are usually made; the first based upon the statistical nature of the laboratory data and the mode of their collection, and the second necessitated by the fact that, in the laboratory, the observer is typically given more or less complete information about the stimulus, including its size, shape, location, duration, and time of occurrence. These two sorts of conversion are combined into a so-called "Field Factor" which, for a specific case, is a multiplier which is directly applied to the basic data when expressed in terms of contrast. A complete Field Factor will also, of course, account for individual differences in observer training, fatigue, abnormal physiological states, and psychological variables, but these higher-order effects are usually treated after the fundamental engineering visibility calculation has been completed.

4.2.1 Probability conversions. Nearly all laboratory data now in use are from experiments done by the psychophysical methods of constant stimulus. The primary results are obtained by presenting fixed values of stimulus magnitude (size, contrast, intensity) over a range which will result in frequencies-of-seeing ranging from essentially zero to 100 per cent. It is found, upon plotting many hundreds of such stimulus presentations, that the probability of target detection rises with stimulus magnitude in accordance with an ogival curve which is well fitted by a normal gaussian integral. Statistically, the best determined point of the ogive is

the point of inflection, i.e., where the probability of correct discrimination is 0.50, and this is the value of threshold contrast of prime interest in laboratory studies. In real life, of course, one is usually interested in probabilities which are near 1.00, or essential certainty of correct discrimination. Owing to a nearly invariant relationship between obtained thresholds and the steepness of the ogive (see, for example, Blackwell, 1963) it is possible to apply a conversion factor which will yield any desired probability level. The confidence with which this may be done depends heavily upon the original method of data collection, and is most satisfactory when applied to so-called 'forced-choice' data; other constant stimulus methods yield data which show non-systematic variability in the relationship. An example of the sorts of conversion factors which may be applied to forced-choice data is given in Table 4.2, taken from Blackwell and McCready (1958). These values, while somewhat variant

TABLE 4.2

To obtain detection probability	Multiply value of contrast at P = 0.5 by
0.90	1.50
0.95	1.64
0.99	1.91

between observers and for different visual tasks, are useful approximations in visibility calculations.

4.2.2 Task-dependent conversions. As suggested above, the laboratory observer tends to have more or less complete information

about the stimuli which are to confront him. In practical situations, his foreknowledge of the spatial and temporal aspects of the target may range from essentially complete to utterly lacking. Studies by Blackwell and his colleagues (1958, 1959) have provided some quantitative estimates of the effects of lack of knowledge about target location, size, duration, and time of occurrence, as well as of various combinations of these. The results of these experiments have been summarized in Table 4.3. It must be emphasized that these values, which are multiplicative factors to be applied to threshold contrast data from experiments where complete knowledge was available to the observers, are derived from very limited experiments and should therefore be used with caution. At the present state of the art they are best estimates, and probably meet the accuracy requirements of many practical visibility problems. Certain anomalous

TABLE 4.3

Target Properties				Correction Factor
Location ±4° or more	Time of Occurrence	Size (3 used)	Duration (3 used)	↓
+	+	+	+	1.00
+	−	+	+	1.40
+	−	+	−	1.60
+	−	−	+	1.50
+	−	−	−	1.45
−	+	+	+	1.31

results were obtained, and are discussed by Blackwell (1958). For example, it is indicated in Table 4.3 that the factor needed when time, size and duration information are all lacking is smaller than that obtained when either

size or duration information was given, provided the time of occurrence was not known. Unknown location was studied in a separate experiment, and it is not established whether the obtained factor is valid in the presence of other uncertainties; a conservative approach at present requires its inclusion.

The special case of targets which occur infrequently over very long periods of time involves the problem of 'vigilance', which has been investigated for a variety of visibility cases. The correction factor needed for vigilance will be very task-dependent, and the recent review article by Jerison and Pickett (1963) should be consulted. For general use, a contrast correction factor of 1.19 for vigilance alone has been recommended (Blackwell, 1958). This factor is probably satisfactory when the stimuli occur randomly and with an average frequency of one or two in twenty minutes; higher occurrence rates requiring less correction.

Trained observers perform better than inexperienced ones, and the magnitude and time course of practice effects are greater for more complex visibility tasks. A recent study by Taylor (1964), indicates the character of the practice effects found in a simple laboratory detection experiment, and shows that a correction factor of 1.90 in contrast will compensate for the difference between trained and naive observers. This value is in excellent agreement with the factor reported by Blackwell (1959) of 2.00 for a different data collection method.

At this point, it is well to give an example of how a Field Factor is determined for a real case, and how it may be used to arrive at a realistic estimate of observer performance under field conditions. Let it be assumed that an observer must confidently detect the occurrence of a stimulus of known duration and size but of unknown location within a circular display

area with a diameter of 8°. The target will be present at infrequent intervals, say once every 15 minutes or so, and he can be allowed to miss only 5 per cent of the occurrences. He is brand new at the task, and our problem is to arrange the contrast of the target so that this 95 per cent criterion will be met. We begin by consulting the laboratory data, which tells us that, for our target size and duration and for the prevailing adapting luminance, the required contrast for 50 per cent correct discrimination by practiced observers in a forced-choice experiment was found to be 0.0061. To correct, respectively, for confidence level, unknown location, vigilance, and lack of training we multiply this contrast value by 1.64, 1.31, 1.19, and 2.00, i.e., by 5.12. The needed target contrast, therefore, is 0.031 for our problem.*

4.2.3 Special conversions. Additional contributions to the Field Factor may occasionally occur. These tend to be even more highly individual, and generally derive from special environmental conditions and observer states, e.g., oxygen deprivation, dietary factors, acceleration, vibration, fatigue, distraction, toxic atmospheres, glare, anxiety, sensory deprivation, abnormal thermal levels, and a host of others. Only fragmentary data can be adduced in most cases, and it is commonly found necessary to assess these effects by means of specific experiments.

*It should be noted that this estimate refers to the 0.95 confidence level in forced-choice terms. An additional factor of 1.2 in contrast may be used to approximate ordinary seeing. It is often necessary to use laboratory threshold data from "yes-no" experiments; in this case a rough rule of thumb is sometimes used which calls for doubling the liminal contrast value.

4.3 An example of visual performance data applied to a problem in meteorology

The estimation of meteorological visibility is frequently made by direct visual observation of distant objects at known distances, and is, at best, subject to extreme variability and uncertainty. The situation becomes even worse as ambient luminance levels decrease (as seen in Figure 4.1), and especially if the adaptive state of the observer is unknown or is fluctuating. In order to reduce the uncertainty involved in the estimation of night-time meteorological visibility, a system has been devised which takes advantage of the existing visual performance data by preventing the adaptation of the observer from changing (Taylor and Rennilson, 1962). Briefly, the meteorologist is provided with a luminous field of constant value (1 ft-L) against which he sees an array of luminous points of closely controlled intensity. These bright points, which are positioned at different distances from the observer in real space, are so arranged that a simple counting procedure suffices to give a good estimate of meteorological range. The important point is that the laboratory visual performance data become directly useful once the adaptive state has been specified and maintained.

4.4 Summary, and some recommended reading

It is impossible to do more than indicate a few of the sources and uses of visual performance data in these few pages. Since it is evident that visibility problems continue to crop up with increasing frequency and complexity, it is not surprising that the demand for performance data for the human observer is increasingly urgent. Largely because of

this urgency, which was first strongly felt during the second World War but has since derived from man's ventures into unfamiliar environments and his passion for traveling at high velocities, there have appeared several compendia of quantitative data and state-of-the-art summaries. Of these, the interested reader is encouraged to consult the following:

Stevens' (1951) Handbook of Experimental Psychology well summarizes the quantitative data from visual performance studies in Chapters 22, 23, and 24. For the special problems of night-time seeing, the volume by Jayle and Ourgaud (1950), La Vision Nocturne et ses Troubles, is invaluable as a source of data available until that date. In more recent years there has appeared the proceedings of a Symposium on Physiological Optics (1963) which contains an excellent collection of papers on contemporary research. At the applied level Wulfeck's Vision in Military Aviation (1958) provides a wealth of useful quantitative information as well as an extensive bibliography. The various approaches to problems of form discrimination which have been made are discussed by their champions in Wulfeck and Taylor's Form Discrimination (1957). Finally, the dawn of space travel has stimulated the appearance of Miller's Visual Problems of Space Travel (1962) and Baker's special issue of Human Factors (1963) dealing with the role of man's visual capabilities in extra-terrestrial operations. It will soon become clear that, while visual performance is usefully predictable in many problems, many more laboratory studies are needed in order to build up our fund of quantitative information, and, in consequence, to improve our predictive ability in present and future visibility problems.

5. OCULAR BEHAVIOR IN VISUAL SEARCH

by

Carroll T. White
U.S. Navy Electronics Laboratory, San Diego, California

The characteristics of the eyes' activity in various visual search situations, and the relevance of this to the general problem of visibility, are discussed briefly.

One aspect of the problem of visibility that deserves consideration is the nature of ocular activity during visual search situations. This has been a perennial problem in experimental psychology, with many techniques having been devised to record the eyes' behavior. These various techniques have been described and evaluated many times already (Alpern, 1962) so they need not concern us at this time. On the basis of all the work on the nature of eye movements a number of general statements can be made which would be appropriate to the problem at hand.

When a person is performing a visual task his eyes do not scan smoothly over the area being studied. Instead, his eyes perform a series of rapid jumps ("saccadic movements") separated by brief pauses ("fixations"). For all practical purposes only the fixational pauses need be considered when predictions regarding visibility are being made. During the rapid movements between fixations not only is the retinal image blurred, but there appears to be some inhibitory process in the central nervous system that tends to reduce visual sensitivity (Volkmann, 1962).

There has been general agreement in regard to the nature of these fixational pauses. In the free-search situation, when one is looking

for the presence of some object in a relatively homogeneous field, the average duration of such pauses is about 0.25 second, while the briefest pauses are practically never less than 0.10 second (Ford, White, and Lichtenstein, 1959). Because of the time taken by the saccadic movements between fixational pauses it turns out that on an average we can expect a maximum of only about three fixations per second in free-search situations.

As the field to be searched becomes more complex it has been found that the average duration of the fixational pauses increases. For example, when an observer is searching for targets on an otherwise empty radar screen, with only the rotating scan-line present, the average fixation duration was found to have increased to a value of 0.35 second (White and Ford, 1960). In even more complex situations, where the basic visual problem is one of pattern discrimination rather than target detection, the duration increases even more, with values of one second or more having been reported (Gerathewohl, 1952).

The spatial distribution of the fixations over the field being scanned is also of interest in regard to the problem of visibility. As would be expected, the shape of the field of search will influence the spatial distribution of fixations. When corners are present they seem to attract more than their proper share of attention. Another general finding has been that the extreme edges of the field of search are avoided. In the empty-field situations the center of the field is fixated less often than an area roughly midway between the center and the edge of the field.(Ford, White, and Lichtenstein, 1959). In the case of complex visual fields, such as reconnaissance photographs,

this latter finding does not hold, however (Enoch, 1959).

It has been shown that the spatial distribution of fixations in radar watching, determined by the shape of the display and other physical characteristics such as the presence of the rotating scan line, is an important factor in determining the probability of detection of targets appearing at various positions on the radar screen (White and Ford, 1960; Baker, 1958). The distribution of fixations undoubtedly influences the probability of detection in other visual search situations, but nothing more definite can be said about this at present. The fact that the physical characteristics of a field of search can influence the observers' pattern of search, perhaps in a way that is detrimental, would suggest that more effort be made to determine and train observers to practice the most effective search procedure in any given situation.

6. ATMOSPHERIC PROPERTIES

by Almerian R. Boileau

Representative data from Visibility Laboratory Flight 74, Eglin Air Force Base, Florida, are shown in Figs. 6.1, 6.2, and 6.3 and Tables 6.1 through 6.12 inclusive. The flight was made mid-day 28 February 1956. The day was "clear," that is cloudless, but with pronounced haze in the first 4000 ft altitude. Recording of data by airborne photometers was commenced at 1036 Central Standard Time (CST) at an altitude of 20 000 ft and was terminated at 1326 CST at an altitude of 1000 ft. Data were recorded simultaneously at sea level by duplicate photometers installed on an instrumented van beneath the flight pattern.

Beam Transmittance. The measured attenuation length $L(z)$, recorded during Flight 74, is plotted as a function of altitude in Fig. 6.1. This shows the laminar structure of the atmosphere. Also shown in Fig. 6.1 is a plot of equivalent attenuation length $\bar{L}(z)$. This quantity is a pseudo attenuation length which, when combined with its altitude z, can be used directly in the equation

$$T_r(z,\theta) = \exp\left\{-\left[z/\bar{L}(z)\right]\sec\theta\right\} \tag{6.1}$$

to permit easy calculation of the atmospheric beam transmittance between sea level and altitude z for a path of sight inclined θ° from the vertical. (See Elterman, 1963.)

Example: What is the beam transmittance for a path of sight between sea level and 5000 ft when the path of sight is inclined 60°

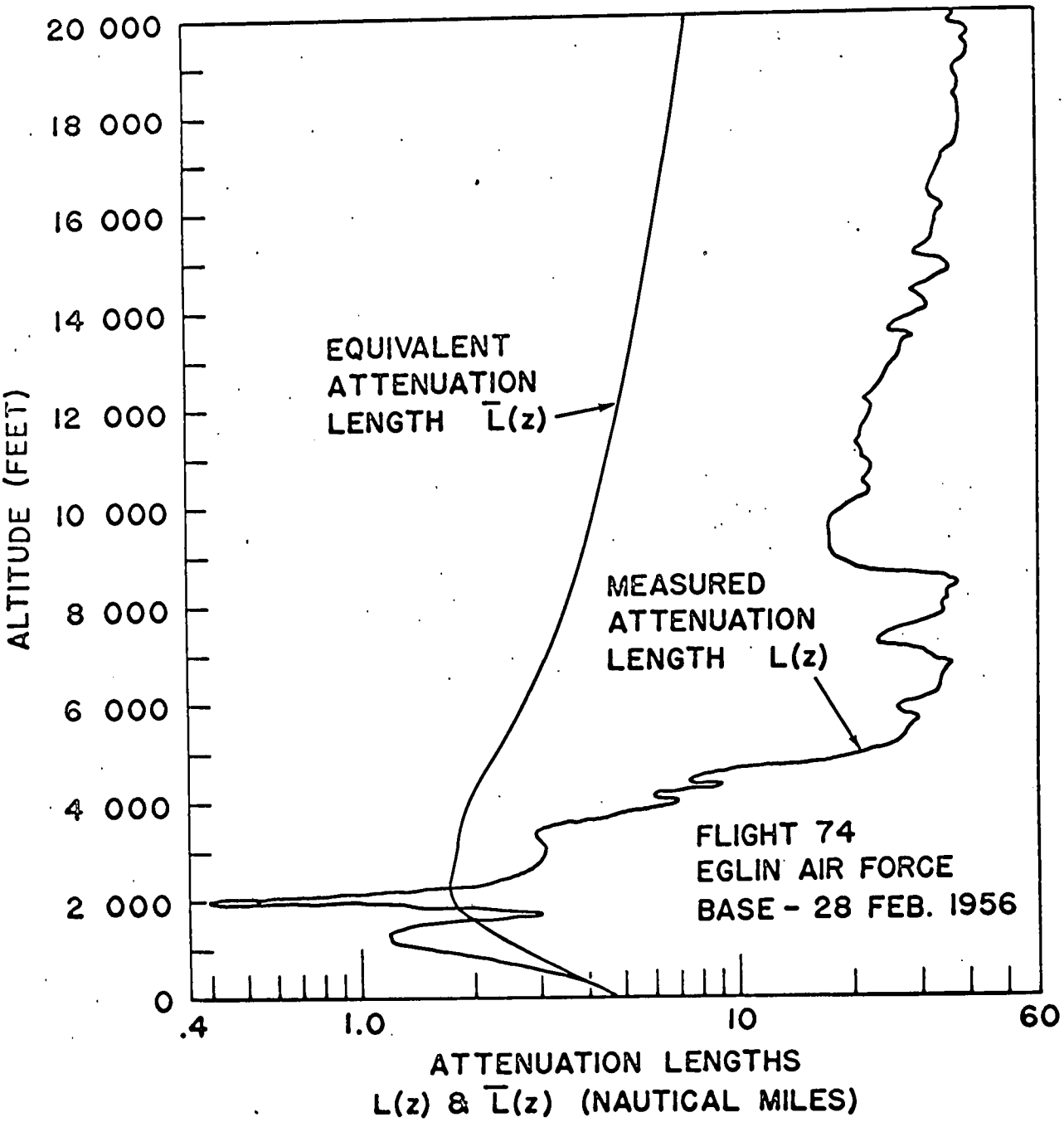

Figure 6.1 Attenuation length L(z) was measured continuously during 1000 ft per minute descent with aircraft held in level attitude. Equivalent attenuation length $\bar{L}(z)$ is computed.

from the vertical, i.e., with a zenith angle of either 60° or 120°? The equivalent attenuation length $\bar{L}(z)$ for 5000 ft is 2.32 nautical miles; the ratio of 6080 ft/nautical mile must be introduced in the equation because the altitude and equivalent attenuation length must be in the same units; the secant of 60° is 2.00 (hence the path length $r = z \sec \theta$ is 10 000 ft); so the beam transmittance found by Eq. 6.1 is

$$T_{10\ 000}\ (0,60^\circ) = \exp\left\{-\left[5000/2.32 \times 6080\right] 2.00\right\}$$

$$= \exp\ -.708$$

$$= 0.493\ .$$

$T_{10\ 000}\ (0,60^\circ)$ is the notation for the beam transmittance for the upward-looking case. The beam transmittance for the downward-looking case $T_{10\ 000}\ (5000,\ 120^\circ)$ has the same numerical value.

Table 6.1 is a table of the data shown in Fig. 6.1 augmented by extrapolated values of attenuation length from 20 000 to 60 000 ft. The value of the dimensionless ratio $z/\bar{L}(z)$ as a function of altitude is also tabulated. Figures 6.2 and 6.3 show beam transmittances computed from the data in Table 6.1. The curves are plotted on log-log graph paper, in the case of the vertical coordinates to expand the data at low altitude and compress the data at the higher altitudes and, in the case of the horizontal coordinate, to permit the curves to be used for graphical determination of beam transmittance between altitudes. An example of how this is done follows.

The beam transmittances given by the curves in Fig. 6.2 and 6.3 are between sea level and the indicated altitude. The beam transmittance between two altitudes is found as the ratio of the two beam transmittances

TABLE 6.1. MEASURED AND EQUIVALENT ATTENUATION LENGTHS, AND RATIO OF ALTITUDE TO EQUIVALENT ATTENUATION LENGTH

Alt (Feet)	Measured $L(z)$[a] (Naut. Miles)	Equivalent $\bar{L}(z)$[b] (Naut. Miles)	$z/\bar{L}(z)$[c]
0	4.60	4.60	.000
1 000	1.50	2.65	.062
2 000	.40	1.75	.188
3 000	3.10	1.71	.289
4 000	7.00	1.96	.356
5 000	22.0	2.32	.354
6 000	28.5	2.74	.361
7 000	31.0	3.15	.365
8 000	34.0	3.55	.371
9 000	17.5	3.92	.378
10 000	19.5	4.25	.387
11 000	21.5	4.58	.395
12 000	22.5	4.90	.403
13 000	26.5	5.22	.410
14 000	31.5	5.54	.416
15 000	30.0	5.86	.421
16 000	34.5	6.18	.426
17 000	34.0	6.48	.431
18 000	38.0	6.80	.436
19 000	39.0	7.10	.440
20 000	35.0	7.40	.445
25 000	44.9	8.85	.465
30 000	53.8	10.3	.481
35 000	64.9	11.6	.495
40 000	81.7	13.0	.507
45 000	104.	14.4	.515
50 000	132.	15.8	.522
55 000	168.	17.1	.528
60 000	214.	18.5	.533
100 000	262.	29.9	.550
200 000	274.	59.3	.551
∞	∞	----	.551[d]

a. Attenuation length $L(z)$ was recorded continuously as a function of altitude from 20 000 feet to 1 000 feet during descent of airplane at 1 000 feet per minute, with the zero altitude value recorded simultaneously in an instrumented van beneath the flight pattern. These data are shown in Fig. 6.1. Attenuation lengths above 20 000 feet are extrapolated, using density ratios calculated from "The ARDC Model Atmosphere, 1959" (see Minzner, Champion, and Pond, 1959).

b. The quantity $1/\overline{L}(z)$ is equal to Elterman's mean attenuation coefficient $K_a(h)$ and the two quantities $z/\overline{L}(z)$ and $K_a(h) : h_1$ may be used interchangeably in Eq. 6.1. (See Elterman, 1963.)

c. In the dimensionless ratio the quantities z and $\overline{L}(z)$ must be expressed in like units.

d. The value of "$z/\overline{L}(z)$" where $z = \infty$ was calculated from the sea level-to-space transmittance obtained from measured and extrapolated attenuation length data.

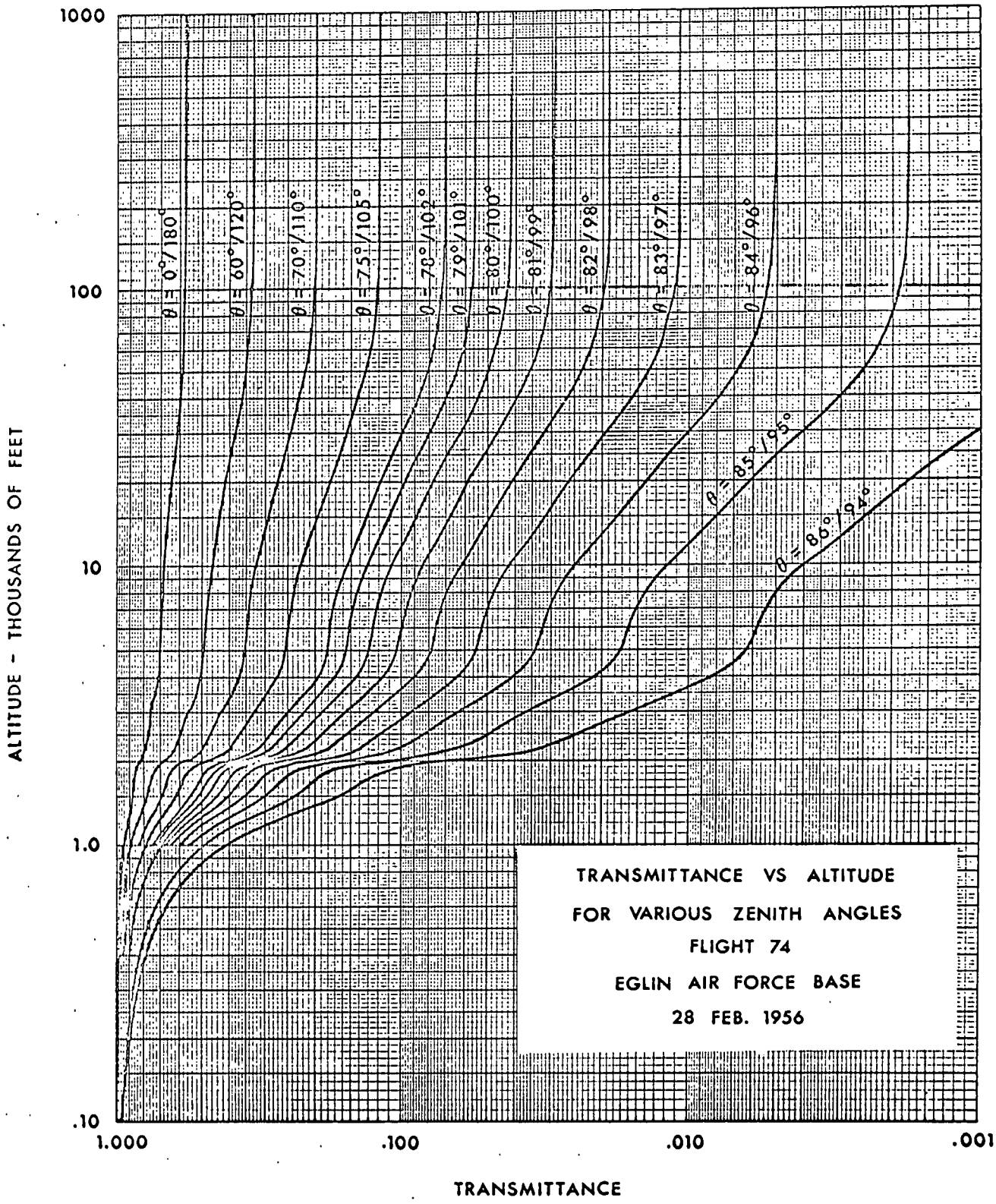

Figure 6.2 Atmospheric beam transmittances, graphs of Eq. 6.1, for various zenith angles from 0°/180° to 86°/94° as indicated.

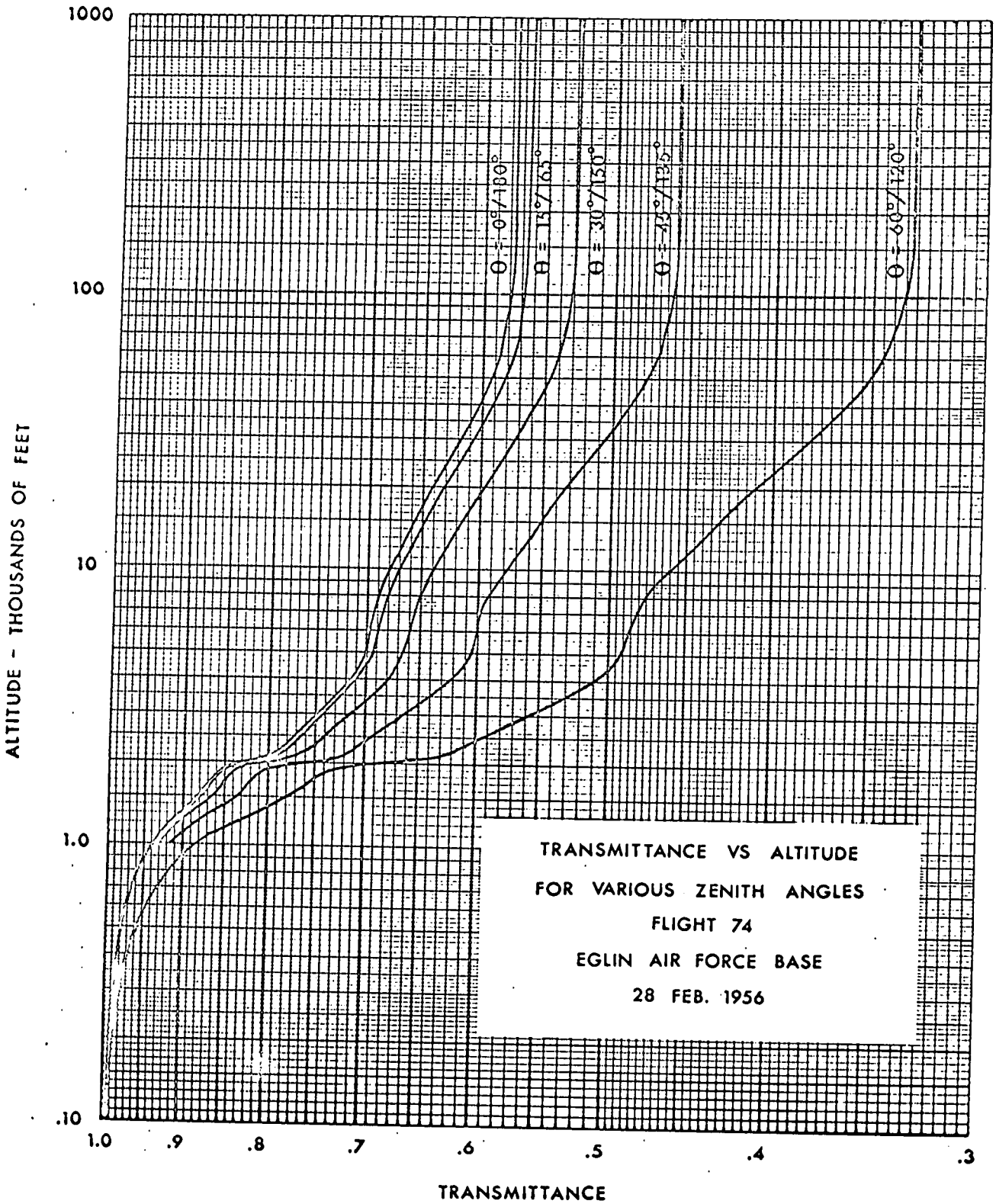

Figure 6.3 Transmittances for various zenith angles from 0°/180° to 60°/120° on expanded horizontal scale.

between sea level and the two altitudes. When the data are plotted on a logarithmic scale the difference between the log values of the beam transmittances is the log of this ratio. As an example, it is desired to find the beam transmittance between 5000 ft and 60 000 ft for a path of sight with a zenith angle of 60° or 120°. The transmittance curve for $\theta = 60^\circ/120^\circ$ indicates transmittances as

$$T_{120\ 000}(60\ 000,\ 120^\circ) = 0.345$$

and

$$T_{10\ 000}(5000,\ 120^\circ) = 0.493 \quad .$$

Then the ratio of these two

$$\begin{aligned} T_{120\ 000}(60\ 000,\ 120^\circ)/T_{10\ 000}(500,\ 120^\circ) &= T_{110\ 000}(60\ 000,\ 120^\circ) \\ &= 0.245/0.493 \\ &= 0.700 \end{aligned}$$

this being the beam transmittance between 60 000 ft and 5000 ft, either upward or downward for a path of sight with a zenith angle of either 60° or 120°. To determine this graphically from Fig. 6.3, the horizontal distance between the intersections of the $\theta = 60^\circ/120^\circ$ transmittance curve with the 5000-ft and 60 000-ft altitude abscissas is transferred to the horizontal base line (preferably with dividers) with the left end of the interval, or difference, placed at the 100 °/o transmittance point at which time the right end of the interval indicates on the base line the beam transmittance in question.

Path Luminance. Tables 6.2 through 6.6 tabulate the sky luminances for inclined paths of sight ranging from the vertically upward (zenith angle 0°) to horizontal (zenith angle 90°), at azimuths with respect to the sun of 0°, 45°, 90°, 135°, and 180°. For these paths of sight, sky luminance and path luminance are numerically equal since the stellar contribution to the apparent luminance of the daytime sky is negligible. Tables 6.7 through 6.11 tabulate the path luminances for paths of sight ranging from directly downward (zenith angle 180°) to 5° below the horizontal (zenith angle 95°) for the same azimuths of 0°, 45°, 90°, 135°, and 180°. In Tables 6.2 through 6.6 the luminances are for paths of sight from the observer's altitude to outer space.

In Tables 6.7 through 6.11 the path luminances are for paths of sight from the observer's altitude to sea level, the length of the path indicated by the subscript r equals z sec θ (see p. 501 of Duntley, et al, 1957). The increase in the length of the path of sight due to the curvature of the earth is less than 5 % in all cases except $\theta = 95°$. When $\theta = 95°$ the path of sight from 60 000 ft is increased by earth curvature by 25 %. Accordingly, the path luminances for that zenith angle were not extrapolated above 20 000 ft.

TABLE 6.2. SKY LUMINANCE $B(z,\theta,0^\circ)$,[a] UPPER SKY, IN AZIMUTH OF SUN.[b]

ALT. (Feet)	Sky Luminance (ft-L) for Zenith Angle θ[c,d,e]							
	$\theta=0^\circ$	15°	30°	60°	75°	80°	85°	90°
0	950	1300	3000	3850	3500	4350	4600	4600
1000	820	1200	2500	3400	3400	3500	3600	4000
2000	680	1180	2250	3200	2900	3100	3200	3800
3000	600	1150	2050	3100	2650	2750	2920	3600
4000	536	1120	1900	3000	2400	2500	2700	3500
5000	510	1100	1810	2900	2200	2300	2530	3300
6000	490	1080	1720	2850	2010	2150	2400	3200
7000	475	1050	1650	2800	1900	2000	2300	3100
8000	465	1000	1620	2750	1820	1920	2220	2980
9000	450	950	1590	2650	1780	1880	2180	2850
10000	420	900	1530	2550	1720	1810	2100	2800
11000	390	840	1500	2480	1690	1770	2050	2750
12000	365	780	1460	2390	1650	1710	2000	2700
13000	345	725	1430	2300	1610	1680	1990	2650
14000	325	680	1400	2250	1590	1650	1930	2650
15000	305	625	1390	2190	1580	1610	1900	2600
16000	289	582	1380	2120	1550	1590	1890	2600
17000	272	539	1350	2090	1530	1570	1850	2550
18000	260	495	1330	2020	1520	1550	1830	2550
19000	248	458	1320	2000	1500	1520	1810	2550
20000	236	420	1300	1950	1500	1500	1810	2550

a. Parenthetical symbols: photometer altitude z, zenith angle θ, and azimuth applicable to Table.

b. Average zenith angle of sun during flight 41.5°.

c. Sky luminances were recorded by airborne equipment, during descent, at five altitudes, viz., 20 000, 8500, 7000, 4000, and 1000 feet. Simultaneous records were made in instrumented van. The data for the different azimuths and zenith angles were plotted against altitude and interpolated graphically so that the tabulated values could be read from the graphs.

d. Extrapolated path luminances for an observer above 20 000 ft may be calculated as the products of 20 000-ft values and appropriate pressure ratio from Table 6.12. This assumes that the character of the aerosol at

20 000 ft and above is unchanged and that the total number of scattering particles in a vertical path of sight above 20 000 ft is proportional to the pressure.

e. Sky luminances at zenith angle of 45° were near the sun and exceeded the range of photometer and are not available.

TABLE 6.3. SKY LUMINANCE $B(z,\theta,\pm 45^{\circ})$,[a] UPPER SKY, 45° FROM AZIMUTH OF SUN.[b]

ALT. (Feet)	Sky Luminance (ft-L) for Zenith Angle θ[c,d]							
	θ=15°	30°	45°	60°	75°	80°	85°	90°
0	1180	1410	1760	1740	2600	3190	3220	2400
1000	1030	1230	1550	1520	2080	2220	2520	2400
2000	920	1100	1350	1320	1780	1960	2380	2400
3000	810	985	1280	1260	1530	1740	2100	2400
4000	725	900	1060	1040	1360	1580	1980	2400
5000	678	860	1000	980	1290	1510	1900	2340
6000	645	835	965	945	1230	1460	1830	2290
7000	610	810	930	920	1200	1400	1780	2220
8000	600	795	880	870	1180	1350	1730	2200
9000	580	770	840	840	1130	1310	1690	2150
10000	550	730	800	800	1090	1270	1640	2110
11000	530	690	765	765	1050	1220	1600	2090
12000	500	655	735	735	1010	1180	1550	2060
13000	480	620	700	700	960	1130	1510	2020
14000	455	580	675	675	920	1100	1460	2000
15000	432	550	645	645	880	1060	1420	1980
16000	412	515	620	620	840	1020	1380	1970
17000	390	485	590	590	800	980	1330	1950
18000	370	455	570	570	770	940	1290	1940
19000	352	430	545	545	730	900	1230	1930
20000	332	400	530	530	700	870	1200	1920

a,b,c,d. See footnotes, Table 6.2.

TABLE 6.4. SKY LUMINANCE $B(z,\theta,\pm 90^{\circ})$,[a] UPPER SKY, 90° FROM AZIMUTH OF SUN.[b]

ALT. (Feet)	Sky Luminance (ft-L) for Zenith Angle θ[c,d]							
	θ=15°	30°	45°	60°	75°	80°	85°	90°
0	925	910	990	1110	1580	1850	2090	1450
1000	780	740	780	875	1200	1380	1630	1500
2000	645	615	660	740	1080	1290	1600	1560
3000	545	530	570	660	1000	1270	1580	1600
4000	475	470	495	600	930	1260	1520	1660
5000	450	435	470	575	900	1250	1500	1680
6000	430	410	445	555	880	1220	1480	1700
7000	410	395	425	545	860	1190	1450	1730
8000	400	385	410	530	810	1030	1410	1760
9000	380	365	395	510	775	950	1370	1800
10000	362	345	380	490	750	920	1330	1810
11000	345	328	360	475	715	895	1300	1810
12000	328	310	345	455	695	865	1270	1820
13000	310	295	330	440	670	840	1230	1820
14000	295	280	312	420	645	815	1200	1830
15000	280	265	300	405	625	785	1170	1830
16000	262	252	283	390	605	760	1130	1840
17000	250	240	270	370	590	740	1100	1840
18000	235	230	256	350	570	720	1060	1850
19000	222	219	242	335	555	700	1030	1850
20000	210	210	232	320	540	680	1000	1860

a,b,c,d. See footnotes, Table 6.2

TABLE 6.5. SKY LUMINANCE $B(z,\theta,\pm 135^{\circ})$,[a] UPPER SKY, 135° FROM AZIMUTH OF SUN.[b]

ALT. (Feet)	Sky Luminance (ft-L) for Zenith Angle θ[c,d]							
	θ=15°	30°	45°	60°	75°	80°	85°	90°
0	690	640	690	880	1450	1720	1980	1470
1000	610	560	580	740	1220	1410	1820	1570
2000	540	500	530	675	1120	1440	1790	1660
3000	486	450	490	630	1060	1300	1780	1720
4000	440	400	450	595	1000	1290	1780	1780
5000	415	382	435	580	975	1280	1770	1780
6000	395	359	419	570	950	1270	1720	1790
7000	375	355	400	560	940	1260	1690	1800
8000	370	349	395	540	910	1200	1600	1890
9000	358	335	380	520	880	1160	1560	1960
10000	340	319	360	495	860	1130	1550	2000
11000	323	302	342	475	840	1110	1520	2020
12000	306	289	325	460	815	1090	1500	2050
13000	290	275	310	440	790	1060	1480	2100
14000	272	260	292	420	780	1030	1460	2110
15000	254	248	276	400	740	1000	1430	2130
16000	249	235	262	380	715	980	1410	2160
17000	222	222	248	365	690	950	1390	2190
18000	209	210	233	348	665	920	1360	2200
19000	194	198	220	330	645	895	1340	2220
20000	185	189	210	315	625	865	1320	2280

a,b,c,d. See footnotes, Table 6.2

TABLE 6.6. SKY LUMINANCE B(z,θ,180°),[a] UPPER SKY, 180° FROM AZIMUTH OF SUN.[b]

ALT. (Feet)	Sky Luminance (ft-L) for Zenith Angle θ[c,d]							
	θ=15°	30°	45°	60°	75°	80°	85°	90°
0	700	640	660	950	1600	1900	2500	1500
1000	620	570	600	800	1500	1800	2300	1600
2000	550	510	550	745	1390	1750	2210	1700
3000	490	460	510	710	1310	1710	2150	1780
4000	450	420	480	680	1250	1700	2100	1850
5000	430	405	460	660	1200	1700	2080	1930
6000	415	392	440	640	1180	1690	2030	1980
7000	400	380	420	620	1150	1680	2000	2000
8000	390	365	405	605	1120	1620	1920	2130
9000	370	350	390	590	1080	1590	1900	2230
10000	355	335	370	570	1020	1510	1850	2290
11000	335	320	355	550	980	1450	1810	2300
12000	319	305	340	525	940	1400	1800	2330
13000	300	289	325	500	900	1350	1790	2350
14000	282	272	310	480	860	1300	1750	2380
15000	265	258	295	455	830	1280	1750	2390
16000	250	242	279	435	800	1220	1750	2390
17000	235	230	262	410	770	1200	1750	2400
18000	220	215	249	390	750	1180	1750	2400
19000	208	201	235	370	720	1120	1750	2400
20000	195	190	220	350	700	1100	1750	2400

a,b,c,d. See footnotes, Table 6.2

TABLE 6.7. PATH LUMINANCE $B_r^*(z,\theta,0^\circ)$,[a] LOWER SKY, IN AZIMUTH OF SUN.[b]

ALT.[e] (Feet)	Path Luminance (ft-L) for Zenith Angle θ[c,d]							
	$\theta = 180^\circ$	165°	150°	135°	120°	105°	100°	95°
1000	60.9	60.9	81.8	88.7	123	223	398	750
2000	134	132	158	163	214	461	727	1140
3000	192	204	229	236	298	676	998	1400
4000	233	259	298	305	371	868	1210	1590
5000	264	281	318	340	414	973	1300	1690
6000	291	301	344	381	469	1070	1390	1780
7000	313	327	377	434	545	1180	1470	1890
8000	341	366	419	496	671	1290	1530	2020
9000	367	388	445	531	732	1360	1580	2110
10000	388	399	459	545	749	1380	1610	2140
15000	484	457	532	610	823	1510	1780	2310
20000	603	510	604	672	896	1660	1980	2500
25000	710	557	674	731	967	1790	2150	
30000	798	596	731	779	1020	1890	2270	
40000	928	653	815	848	1110	2040	2440	
50000	1010	689	867	891	1150	2120	2540	
60000	1060	710	899	917	1180	2170	2590	

a. Parenthetical symbols: photometer altitude z, zenith angle θ, and azimuth applicable to Table.

b. Average zenith angle of sun during flight 41.5°.

c. Path luminances from 0 to 20 000 ft-altitudes for zenith angles from 95° to 180° were calculated as follows:

(1) Path functions for 1000 ft-altitude $B_*(1000,\theta,\varphi)$ were calculated from flight data and Eq. 10 of Duntley, Boileau, and Preisendorfer, 1957.

(2) Path functions for sea level $B_*(0,\theta,\varphi)$ were recorded in the van.

(3) Path luminances for first 1000 ft-altitude $B_r^*(1000,\theta,\varphi)$ were calculated by means of Eq. 17 of Duntley, Boileau, and Preisendorfer, 1957.

(4) Inherent background luminances (groundcover luminances) ${}_bB_o(0,\theta,\varphi)$ were calculated by means of Eq. 6.2 (see Eq. 4 of Duntley, Boileau, and Preisendorfer, 1957).

(5) Path luminances for other than first 1000-ft altitude were calculated by means of Eq. 6.2.

d. Path luminances for altitudes above 20 000 ft were extrapolated as follows:

(1) Path functions for 20 000 ft $B_*(20\,000,\theta,\varphi)$ were calculated from flight data and Eq. 10 of Duntley, Boileau, and Preisendorfer, 1957.

(2) Path functions above 20 000 ft $B_*(z,\theta,\varphi$ were calculated, in 100-ft increments, in proportion to atmospheric density.

(3) Path luminances above 20 000 ft $B_T^*(z,\theta,\varphi)$ were calculated by means of Eq. 17 of Duntley, Boileau, and Preisendorfer, 1957.

e. In using these Tables, it has been found, that above 10 000 ft, altitude increments of 5000 and 10 000 ft are satisfactory.

TABLE 6.8. PATH LUMINANCE $B_r^*(z,\theta,\pm 45^\circ)$,[a] LOWER SKY, 45° FROM AZIMUTH OF SUN.[b]

ALT.[e] (Feet)	Path Luminance (ft-L) for Zenith Angle θ[c,d]						
	θ=165°	150°	135°	120°	105°	100°	95°
1000	86.2	103	110	128	259	359	650
2000	159	183	192	244	473	692	964
3000	220	252	262	331	639	837	1190
4000	267	308	318	391	771	1100	1310
5000	299	335	365	444	854	1180	1450
6000	324	356	406	484	935	1270	1570
7000	340	371	441	525	956	1320	1640
8000	375	417	487	606	1020	1390	1700
9000	401	447	518	645	1070	1450	1780
10000	417	463	534	678	1100	1480	1800
15000	495	541	607	755	1280	1600	1920
20000	587	628	689	856	1470	1760	2100
25000	671	707	763	947	1630	1910	
30000	740	772	824	1020	1760	2010	
40000	841	866	912	1130	1930	2160	
50000	903	925	967	1190	2040	2240	
60000	941	961	1000	1230	2110	2280	

a,b,c,d,e. See footnotes, Table 6.7.

TABLE 6.9. PATH LUMINANCE $B_r^*(z,\theta,\pm 90^\circ)$,[a] LOWER SKY, 90° FROM AZIMUTH OF SUN.[b]

ALT.[e] (Feet)	Path Luminance for Zenith Angle θ[c,d]						
	θ=165°	150°	135°	120°	105°	100°	95°
1000	69.7	77.8	82.8	109	203	359	595
2000	138	156	174	226	389	562	833
3000	195	226	245	325	540	722	990
4000	238	279	298	404	665	867	1110
5000	268	306	339	462	744	975	1190
6000	293	328	372	508	810	1090	1260
7000	321	344	403	549	881	1170	1310
8000	351	383	439	580	932	1190	1380
9000	376	409	463	607	963	1240	1410
10000	393	426	481	628	1000	1270	1450
15000	479	516	571	739	1160	1420	1600
20000	582	609	670	873	1310	1580	1800
25000	675	694	759	993	1450	1730	
30000	751	763	831	1090	1560	1830	
40000	864	864	936	1230	1710	1980	
50000	934	926	1000	1314	1800	2060	
60000	976	964	1040	1370	1860	2100	

a,b,c,d,e. See footnotes, Table 6.7.

TABLE 6.10. PATH LUMINANCE $B_r^*(z,\theta,\pm 135^\circ)$,[a] LOWER SKY, 135° FROM AZIMUTH OF SUN.[b]

ALT.[e] (Feet)	Path Luminance (ft-L) for Zenith Angle θ[c,d]						
	θ=165°	150°	135°	120°	105°	100°	95°
1000	93.4	120	137	137	336	486	693
2000	161	207	241	282	494	677	951
3000	218	278	315	385	625	813	1100
4000	259	326	375	462	729	910	1230
5000	292	358	414	525	804	1000	1290
6000	323	385	440	573	885	1090	1310
7000	344	401	466	609	936	1170	1400
8000	364	427	497	630	1040	1290	1520
9000	395	458	523	652	1140	1390	1650
10000	417	485	560	694	1170	1450	1700
15000	531	620	691	861	1350	1660	1910
20000	634	724	856	995	1470	1780	2050
25000	725	818	1000	1120	1590	1890	
30000	802	895	1130	1220	1670	1980	
40000	915	1010	1300	1360	1790	2090	
50000	986	1080	1410	1440	1860	2150	
60000	1030	1120	1480	1490	1900	2180	

a,b,c,d,e. See footnotes, Table 6.7.

TABLE 6.11. PATH LUMINANCE $B_r^*(z,\theta,180^\circ)$,[a] LOWER SKY, 180° FROM AZIMUTH OF SUN.[b]

ALT.[e] (Feet)	Path Luminance (ft-L) for Zenith Angle θ:[c,d]						
	θ=165°	150°	135°	120°	105°	100°	95°
1000	65.9	94.3	106	144	228	485	860
2000	138	193	227	274	496	763	1140
3000	198	276	327	382	682	935	1270
4000	241	341	407	451	815	1040	1330
5000	264	364	450	512	867	1130	1380
6000	285	386	484	570	920	1230	1450
7000	316	417	515	617	987	1360	1480
8000	387	453	539	659	1110	1450	1680
9000	448	485	558	681	1220	1500	1770
10000	472	509	583	705	1250	1540	1800
15000	575	637	721	816	1420	1750	2000
20000	699	792	867	944	1620	1970	2200
25000	816	943	997	1060	1810	2170	
30000	912	1070	1100	1160	1960	2330	
40000	1050	1250	1260	1300	2160	2530	
50000	1140	1360	1350	1380	2280	2650	
60000	1190	1430	1410	1430	2350	2710	

a,b,c,d,e. See footnotes, Table 6.7.

Table 6.12 lists the ratios of the pressure at various altitudes z to the pressure at 20 000 ft. These ratios can be used for extrapolating the path luminances listed in Tables 6.2 through 6.6 above 20 000 ft.

The following equation describes the apparent luminance of an object seen through the atmosphere (see Eq. 1, p. 500 of Duntley, Boileau, and Preisendorfer, 1957)

$$B_r(z,\theta,\varphi) = B_o(z,\theta,\varphi)\ T_r(z,\theta) + B_r^*(z,\theta,\varphi) \quad . \qquad (6.$$

From this equation it can be seen that the path luminance $B_r^*(z,\theta,\varphi)$ is equal to the difference between the apparent luminance $B_r(z,\theta,\varphi)$ and the product of the inherent luminance $B_o(z,\theta,\varphi)$ and the beam transmittance $T_r(z,\theta)$. Hence, in all cases the path luminance for a path of sight between two altitudes is the difference between the path luminance at the observer's altitude (obtained from the appropriate Table) and the product of the path of sight beam transmittance and the path luminance at the object altitude.

Example: Consider a path of sight at 45° from the azimuth of the sun and inclined downward at a zenith angle of 120°. The path luminance between 5000 ft and 60 000 ft is the difference between the measured path luminance at 60 000 ft and the product of the beam transmittance of the path of sight from 5000 ft to 60 000 ft and the measured path luminance at 5000 ft. In Table 6.8, for azimuth of ± 45°, the path luminance for 60 000 ft and a zenith angle of 120° is listed as 1230 foot-lamberts (ft-L). The same table gives the corresponding path luminance for 5000 ft as 444 ft-L. The beam transmittance for the path of sight previously determined is 0.700. Hence the path luminance for the downward-looking path of sight between the

TABLE 6.12. PRESSURE RATIOS, PRESSURE AT ALTITUDE z TO PRESSURE AT 20 000 FEET

Altitude (Feet)	Ratio of Pressures[a]
20 000	1.000
25 000	0.808
30 000	0.647
40 000	0.404
50 000	0.250
60 000	0.155

a. Ratios are for pressures given by "The ARDC Model Atmosphere, 1959."

60 000-ft and 5000-ft altitudes is

$$B^*_{110\ 000}\ (60\ 000,\ 120^\circ, 45^\circ) = 1230 - (444)(0.700) = 919\ \text{ft-L}.$$

This is the quantity denoted by $B^*_r(z,\theta,\varphi)$ in Eq. 6.2.

Apparent Luminance of an Object. Once the beam transmittance and path luminance have been found for the assumed path of sight, the apparent luminance ${}_tB_r(z,\theta,\varphi)$ of an object having an inherent luminance of ${}_tB_o(z_t,\theta,\varphi)$ can be readily predicted with the aid of Eq. 6.2.

Example: If an aircraft flying at an altitude of 5000 ft has an inherent luminance of 2500 ft-L in the direction of the path of sight, its apparent luminance at the upper end of the path is

$${}_tB_{110\ 000}(60\ 000, 120^\circ, 45^\circ) = (2500)\ (0.700) + 919 = 2669\ \text{ft-L}.$$

It is interesting to note that if in this case the object had an inherent luminance of 3063 ft-L its apparent luminance would also be 3063 ft-L; this is the effective equilibrium luminance for this path of sight (Duntley, Boileau, and Preisendorfer, 1957). If, however, the object had an inherent luminance greater than 3063 ft-L, the apparent luminance would be reduced by this path of sight. Thus an object having an inherent luminance of 4000 ft-L will have an apparent luminance of only 3719 ft-L since the 1200 ft-L loss of transmitted inherent luminance exceeds the 919 ft-L path luminance gain.

Apparent Contrast. Because the detectability of any given object depends on its apparent contrast, the illustrative example from the preceding paragraph should be extended to illustrate the calculation of the apparent contrast at the end of the path of sight.

Example: Let it be assumed that the low-flying aircraft appears against a uniform groundcover of small, fairly closely-spaced pine trees on flat terrain. This was the type of groundcover over which Flight 74 took place. Table 3.2 gives the directional luminous reflectance of this groundcover as seen from the assumed direction ($\theta = 120^{\circ}$; $\varphi = 45^{\circ}$) as 0.021. During Flight 74 the illumination on a fully exposed horizontal plane at ground level was measured as 5940 lumen ft^{-2}. Thus the inherent luminance of the groundcover is (5940)(0.021) = 125 ft-L. Equation 6.2 can now be used with the transmittance from Fig. 6.3 (previously determined to be 0.345) and the path luminance from Table 6.8 (previously determined to be 1230 ft-L) to calculate the apparent luminance of the background against which the aircraft appears. Thus, as seen from an altitude of 60 000 ft, the apparent luminance of the background is

$$ {}_{b}B_{120\ 000}(60\ 000, 120^{\circ}, 45^{\circ}) = (125)(0.345) + 1230 = 1273 \text{ ft-L} $$

and the apparent contrast of the low-flying aircraft against the pine-covered terrain as seen from 60 000 ft is

$$ C_{110\ 000}(60\ 000, 120^{\circ}, 45^{\circ}) = \frac{2669 - 1273}{1273} = 1.097 \ . $$

Inherent Contrast. The inherent contrast of the low-flying aircraft against the same groundcover can be found by using the inherent luminance of the aircraft and, as the background luminance, the apparent luminance of the groundcover as seen from 5000 ft along the assumed directional path of sight.

Example: The inherent luminance of the groundcover has been determined as 125 ft-L. The beam transmittance for the appropriate path of sight has already been determined as 0.493. Table 6.8 gives the path luminance for the assumed path of sight as 444 ft-L. Thus the apparent luminance of the background as seen from 5000 ft along the path of sight would be

$$ {}_bB_{10\,000}(5000,120^\circ,45^\circ) = (125)(0.493) + 444 = 506 \text{ ft-L} . $$

Then the inherent contrast of the low-flying aircraft would be

$$ C_o(5000,120^\circ,45^\circ) = \frac{2500 - 506}{506} = 3.941 . $$

Contrast Transmittance. In the preceding illustration the inherent contrast of 3.941 has been reduced to 1.097 by atmospheric attenuation of the optical signal and the addition of path luminance. Thus, contrast has been reduced by the factor

$$ C_{110\,000}(60\,000,120^\circ,45^\circ)/C_o\,(5000,120^\circ,45^\circ) = 1.097/3.941 = 0.278 . $$

The ratio of the apparent contrast to the inherent contrast, $C_r(z,\theta,\varphi)/C_o(z,\theta,\varphi)$, is called the Contrast Transmittance. It is also computable by any of the three following equations:

$$ C_r(z,\theta,\varphi)/C_o(z,\theta,\varphi) = T_r(z,\theta)\ {}_bB_o(z_t,\theta,\varphi)/{}_bB_r(z,\theta,\varphi) \tag{6.3} $$

$$ \frac{C_r(z,\theta,\varphi)}{C_o(z_t,\theta,\varphi)} = \frac{1}{1 + B_r^*(z,\theta,\varphi)/T_r(z,\theta)\ {}_bB_o(z,\theta,\varphi)} \tag{6.4} $$

$$ C_r(z,\theta,\varphi)/C_o(z_t,\theta,\varphi) = 1 - B_r^*(z,\theta,\varphi)/{}_bB_r(z,\theta,\varphi) \tag{6.5} $$

Example: Equation 6.3 shows that the contrast transmittance may be calculated from the beam transmittance and the inherent and apparent background luminances. The beam transmittance has been determined to be 0.700. The inherent background luminance, that is, the background luminance used in the determination of the inherent contrast, ${}_bB_{10\ 000}(5000, 120^\circ, 45^\circ)$, is 506 ft-L. The apparent background luminance as seen from 60 000 ft is 1273 ft-L. Accordingly, $C_{110\ 000}(60\ 000, 120^\circ, 45^\circ)/C_o(5000, 120^\circ, 45^\circ) = (0.700)(506)/1273 = 0.278$.

Equation 6.4 relates the contrast transmittance to path luminance, beam transmittance, and inherent background luminance. The path luminance, previously determined, is 919 ft-L. The beam transmittance and inherent background luminance are, as before, 0.700 and 506 ft-L, respectively. Then the contrast transmittance is

$$C_{110\ 000}(60\ 000, 120^\circ, 45^\circ)/C_o(5000, 120^\circ, 45^\circ) = 1/\left[1 + 919/(0.700)(506)\right] = 0.278 .$$

When Eq. 6.5 is used to determine the contrast transmittance, only two quantities are required, viz., path luminance and apparent background luminance. These two quantities are 919 ft-L and 1273 ft-L. Then

$$C_{110\ 000}(60\ 000, 120^\circ, 45^\circ)/C_o(5000, 120^\circ, 45^\circ) = 1 - 919/1273 = 1 - 0.722 = 0.278 .$$

It is highly significant and important to note that none of the three equations used to calculate the contrast transmittance involves any photometric property of the object. The contrast transmittance applies, therefore, to any object which may appear against the prevailing background and, for this reason, has been specified as the universal contrast transmittance. The contrasts, the ratio of which is the universal contrast transmittance, are termed universal apparent contrast

and universal inherent contrast to distinguish them from other forms of contrast, e.g., ρ or $(\rho-1)/(\rho+1)$, which do not share this useful property. It will be shown in Sect. 9 that visual object classification techniques are possible only in terms of universal contrast. Throughout this article the word "contrast" denotes universal contrast; all other forms of contrast are specifically identified by name, e.g., ratio contrast ρ or modulation contrast $(\rho-1)/(\rho+1)$.

The contrast transmittance nomogram, Fig. 6.4, constructed by Jacqueline I. Gordon, is a device for solving Eq. 6.4 graphically. From this nomogram one can quickly determine (a) the beam transmittance for a horizontal path of sight from the attenuation length and range, (b) the ratio of path luminance to beam transmittance from the two separate quantities, and (c) the contrast transmittance from the above ratio and the inherent background luminance.

Upward Paths of Sight. The foregoing example concerned a path of sight inclined downward with a zenith angle of 120° and azimuth of 45°. Now let us consider the reciprocal path of sight, the inclined upward path of sight, with a zenith angle of 60° and azimuth of -135°. This would be the path of sight for an observer in the low-flying aircraft looking in the direction of the aircraft at 60 000 ft. Again the contrast transmittance can be calculated by Eq. 6.3, Eq. 6.4, or Eq. 6.6.

Example: The beam transmittance of the path of sight as previously determined is 0.700. The inherent background luminance, the product of the 20 000-ft altitude sky luminance from Table 6.5 and the 60 000-ft pressure ratio factor from Table 6.12, is 48.8 ft-L. The apparent background luminance is read directly from Table 6.5 as 580 ft-L. The path luminance is the difference between the apparent background luminance and the attenuated inherent background luminance, or is the difference between 580 ft-L and 0.700 x 48.8 ft-L which is 545.8 ft-L.
Then the contrast transmittance calculated by Eqs. 6.3,

Figure 6.4 - Contrast Transmittance Nomogram. The solving of Eq. 6.4 is done in three steps as follows:

Step 1. Determine beam transmittance. For horizontal path of sight use attenuation length $L(z)$ and range r. For other than horizontal sight use equivalent attenuation length $\bar{L}(z)$ and range $r = z \sec \theta$. Place straight edge across appropriate values of scales 1 and 2 and read transmittance on scale 3. If $L(z)$ or $\bar{L}(z)$ is less than one or greater than ten nautical miles (N.M.) multiply attenuation length and range by same factor to get on scale. Example: What is transmittance for upward path of sight from 5000 ft to 60 000 ft with $\theta = 60^{\circ}$? (The nomogram is used to determine transmittances between sea level and various altitudes, hence the transmittance between two altitudes is found as the ratio of two transmittances determined from the nomogram.) For $T_{120\ 000}(0,60,\varphi)$: determine from Table 6.1 that $\bar{L}(z)$ is 18.5 N.M.; range $r = 60\ 000 \times \sec \theta = 120\ 000$ ft; multiply both quantities by factor 0.1; place straight edge on 1.85 (scale 1) and 12 000 (scale 2) and read transmittance of 0.345 on scale 3. In a similar manner $T_{10\ 000}(0,60,\varphi)$ is determined to be 0.493. The ratio $0.345/0.493 = 0.700$, the transmittance $T_{110\ 000}(5000,60,\varphi)$.

Step 2. Determine the path luminance - beam transmittance ratio. Place straight edge across appropriate values of scales 3 and 4 and read ratio on scale 5. The units of scales 4 may be any photometric units, the units of scale 4 determining the units of scale 5. Example: With a beam transmittance of 0.700 and a previously determined path

Figure 6.4 - (cont.)

luminance of 545.8 ft-L, the ratio is found to be 780 ft-L.

Step 3. Determine contrast transmittance. Place straight edge across appropriate values of scales 5 and 6 and read contrast transmittance on scale 7. The units of scales 5 and 6 may be any photometric units provided the same units are used for both scales; they need not be the same units used in step 2 above. If the value of the inherent background luminance is less than 100 or more than 3000 it is necessary to use an appropriate factor to get on scale; in that case use the same factor for scales 5 and 6. Example: A previously determined background luminance is 48.8 ft-L. The ratio of path luminance to beam transmittance determined in step 2 is 780 ft-L. Scale 6 has a 100 ft-L lower limit so use a factor of 10. Enter scales 5 and 6 with 7800 ft-L and 488 ft-L and read contrast transmittance on scale 7 as 0.059.

Modulation contrast. This nomogram may also be used for obtaining modulation contrast by entering the inherent background luminance scale, scale 6, with the properly averaged luminance (see Eq. 2.1).

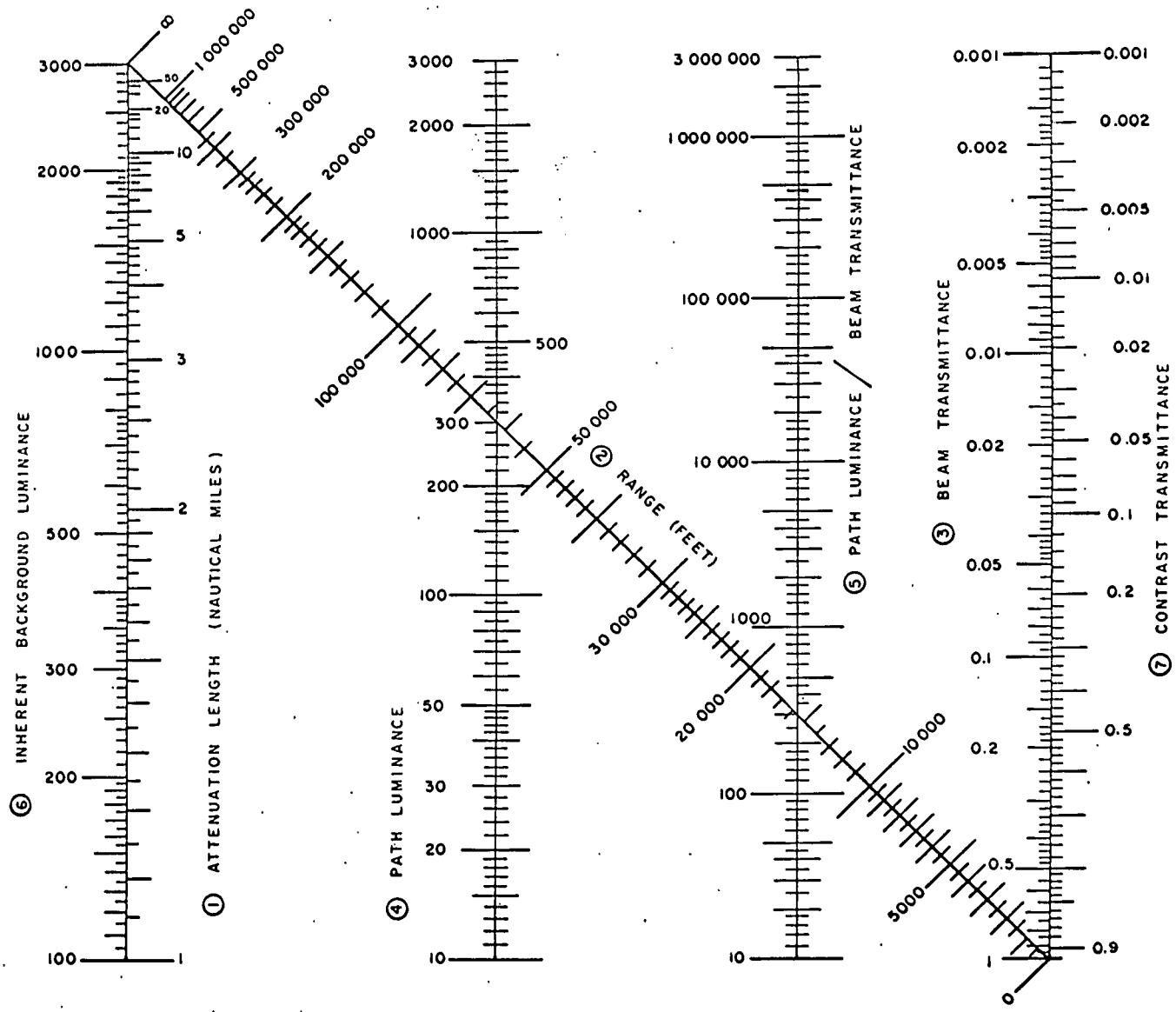
⑥ INHERENT BACKGROUND LUMINANCE
3000
2000
1000
500
300
200
100
① ATTENUATION LENGTH (NAUTICAL MILES)
∞
1 000 000
500 000
300 000
200 000
100 000
50 000
30 000
20 000
10 000
5000
1
② RANGE (FEET)
④ PATH LUMINANCE
3000
2000
1000
500
300
200
100
50
30
20
10
⑤ PATH LUMINANCE / BEAM TRANSMITTANCE
3 000 000
1 000 000
100 000
10 000
1000
100
10
③ BEAM TRANSMITTANCE
0.001
0.002
0.005
0.01
0.02
0.05
0.1
0.2
0.5
1
⑦ CONTRAST TRANSMITTANCE
0.001
0.002
0.005
0.01
0.02
0.05
0.1
0.2
0.5
0.9
0

Figure 6.4

6.4, and 6.5, respectively, is

$$C_{110\ 000}(5000,60^\circ,-135^\circ)/C_o(60\ 000,60^\circ,-135^\circ) = (0.700)(48.8)/580 = 0.059$$

$$C_{110\ 000}(5000,60^\circ,-135^\circ)/C_o(60\ 000,60^\circ,-135^\circ) = 1/\left[1 + 545.8/(0.700)(48.8)\right] = 0.059$$

$$C_{110\ 000}(5000,60^\circ,-135^\circ)/C_o(60\ 000,60^\circ,-135^\circ) = 1 - 545.8/580 = 0.059 .$$

Inasmuch as the contrast transmittances apply to specific background luminances the two factors 0.278 and 0.059 calculated in the foregoing examples may, in accordance with Sect. 1 of this article, be written as

$$506\mathcal{T}_{110\ 000}(60\ 000,120^\circ,45^\circ) = 0.278 \quad \text{(path inclined downward)}$$

and

$$82.1\mathcal{T}_{110\ 000}(5000,60^\circ,-135^\circ) = 0.059 \quad \text{(path inclined upward)} .$$

Note that while the beam transmittances for the reciprocal paths of sight are identical, the contrast transmittances are not. This is because the path luminances for reciprocal paths of sight may, and usually do, differ greatly.

Material as developed in this section is combined with physiological data of the human eye and other pertinent data such as search or recognition factors in the treatment of visibility problems. How this is done is described in another section.

7. DISTRIBUTIONS OF SKY LUMINANCE

by J. I. Gordon

The upper and lower sky luminances measured during Flight 74, 28 February 1956 (see Sec. 6), are presented in map form in Figs. 7.1 through 7.6. Sky luminance distributions are given for ground level, for 5000 feet, and for 20 000 feet. At the time of Flight 74 the lower atmosphere contained a heavy haze layer below 5000 feet, as shown by the curve of attenuation length versus altitude in Fig. 6.1.

The telephotometers used to measure these luminances had a 5° field of view. Near the sun the luminance distribution is not well defined using this resolution and no attempt has been made to depict the rapid change in luminance in the solar aureole. The apparent sun luminance given is the average for the solar disk and thus represents a value appropriate for a field of view of approximately $1/2^{\circ}$.

The lower sky luminance distribution for ground level has a discontinuity from 90° to 92.5°. This is also a portion of the sky having a large luminance gradient.

These sky maps illustrate the increase in apparent luminance of the lower hemisphere and the decrease in luminance of the upper hemisphere as the observer ascends in altitude. They define the distribution of lighting on all non-self luminous objects at the three altitudes. They also provide a means for determining the background luminance at these altitudes for any angle of sight not in the Tables of data presented in Sec. 6.

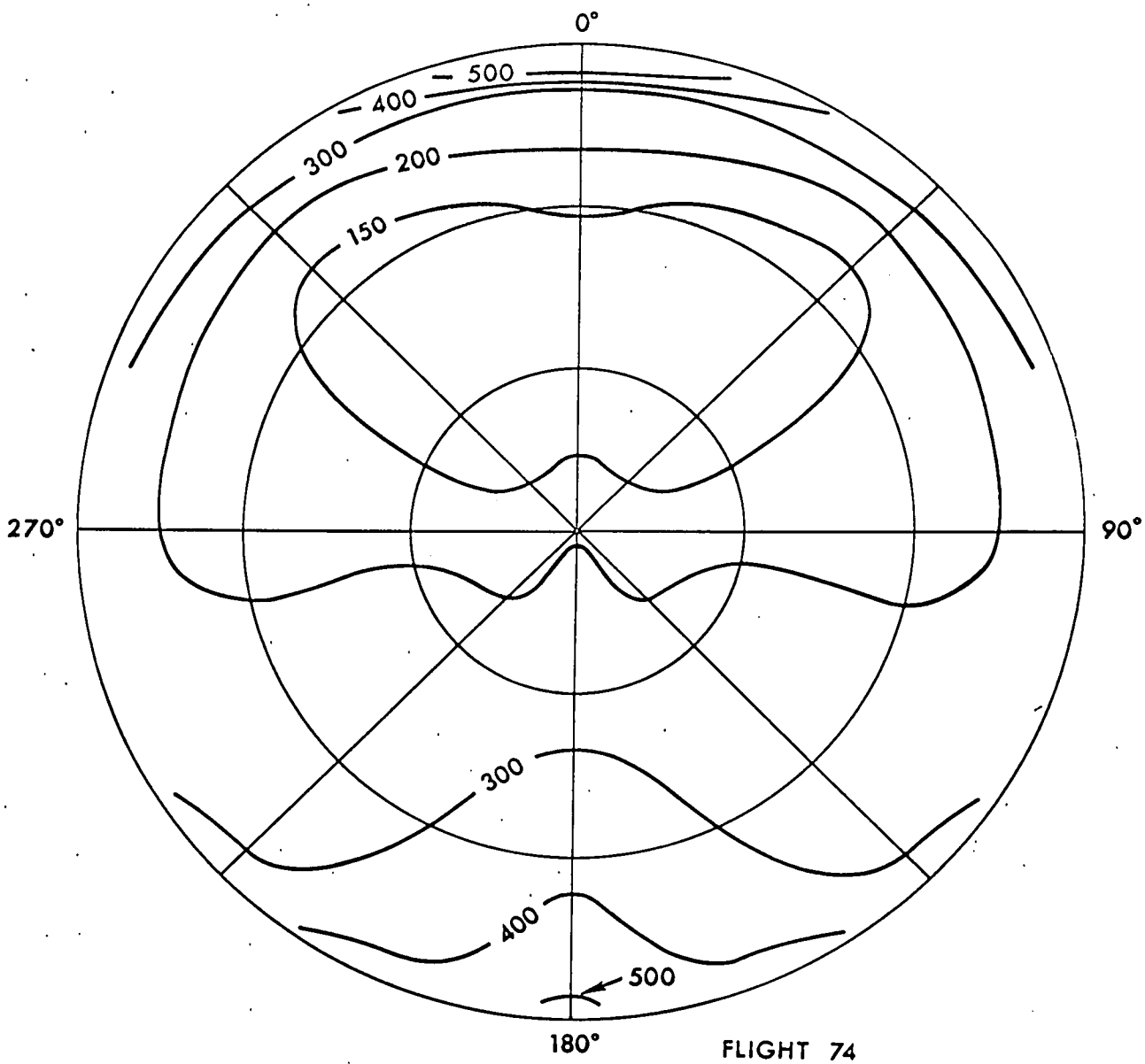

FLIGHT 74

LOWER SKY LUMINANCE
(Foot-Lamberts)

ALTITUDE - Ground Level

FIGURE 7.1

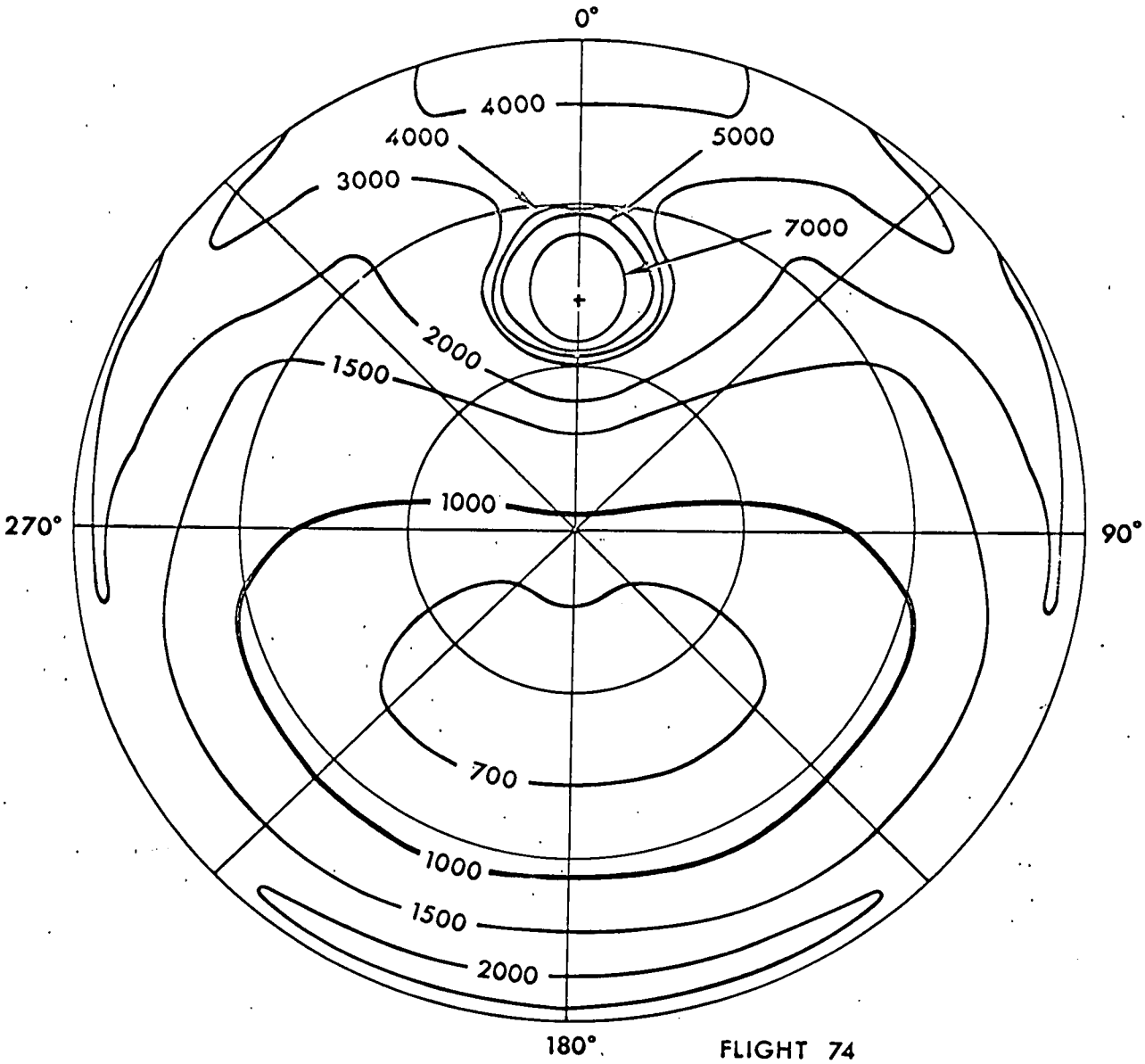

+ SUN ZENITH ANGLE 41.5°
APPARENT LUMINANCE OF THE SUN
2.79×10^8 FOOT LAMBERTS

FLIGHT 74
UPPER SKY LUMINANCE
(Foot-Lamberts)
ALTITUDE - Ground Level

FIGURE 7.2

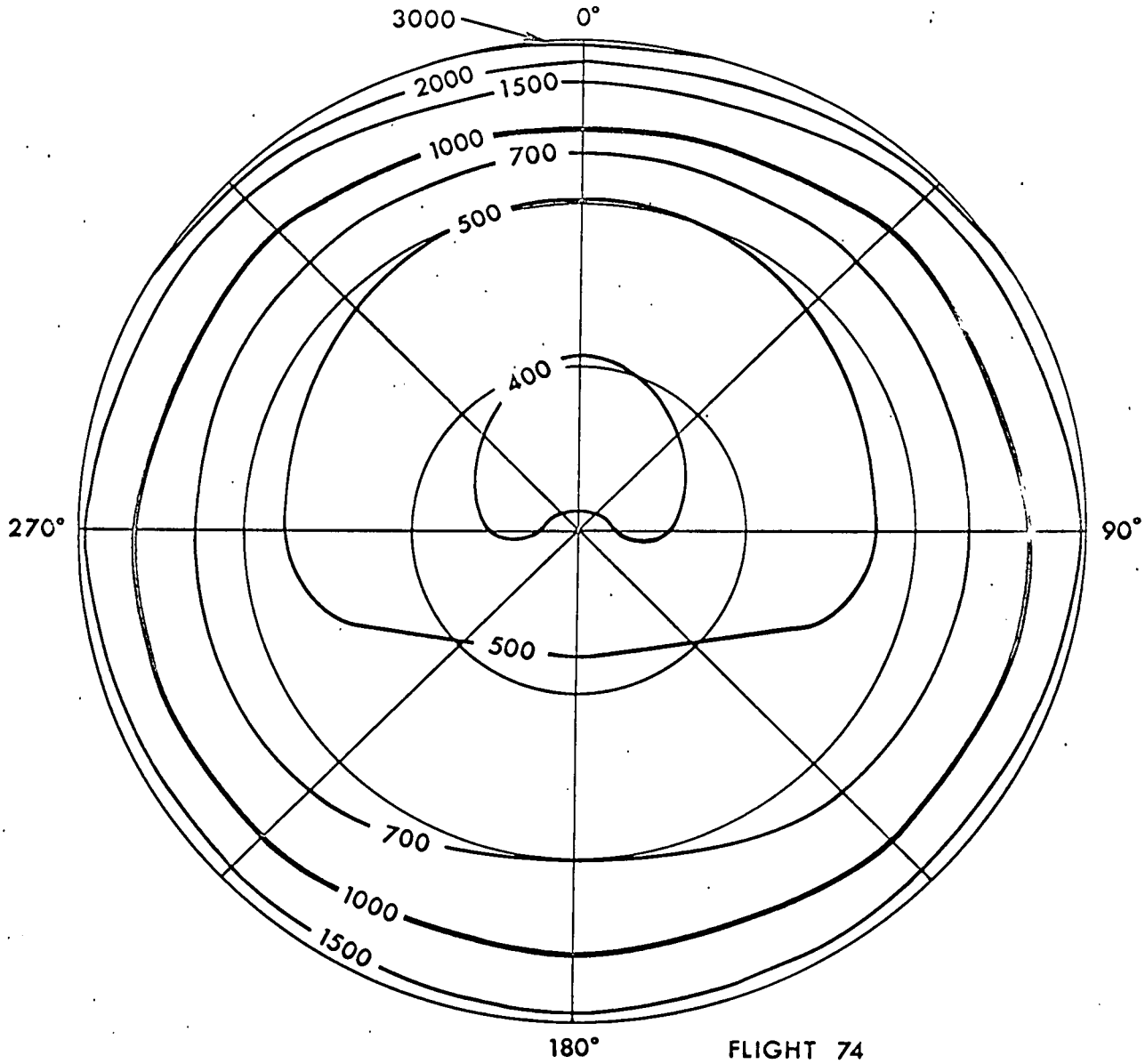

FLIGHT 74
LOWER SKY LUMINANCE
(Foot-Lamberts)
ALTITUDE - 5,000 feet

FIGURE 7.3

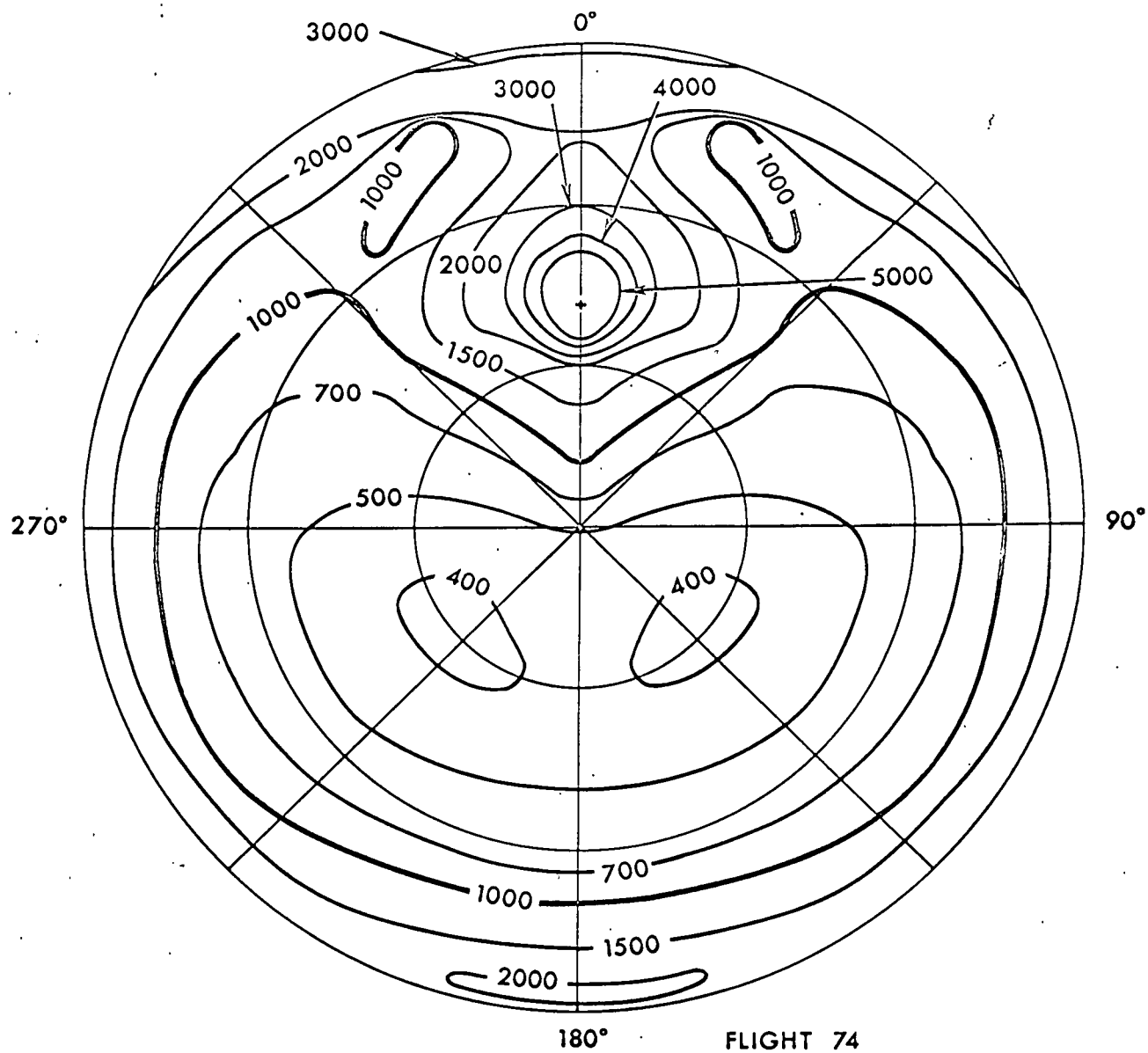

+ SUN ZENITH ANGLE 41.5°
APPARENT LUMINANCE OF THE SUN
4.45×10^8 FOOT LAMBERTS

FLIGHT 74
UPPER SKY LUMINANCE
(Foot-Lamberts)
ALTITUDE - 5,000 feet

FIGURE 7.4

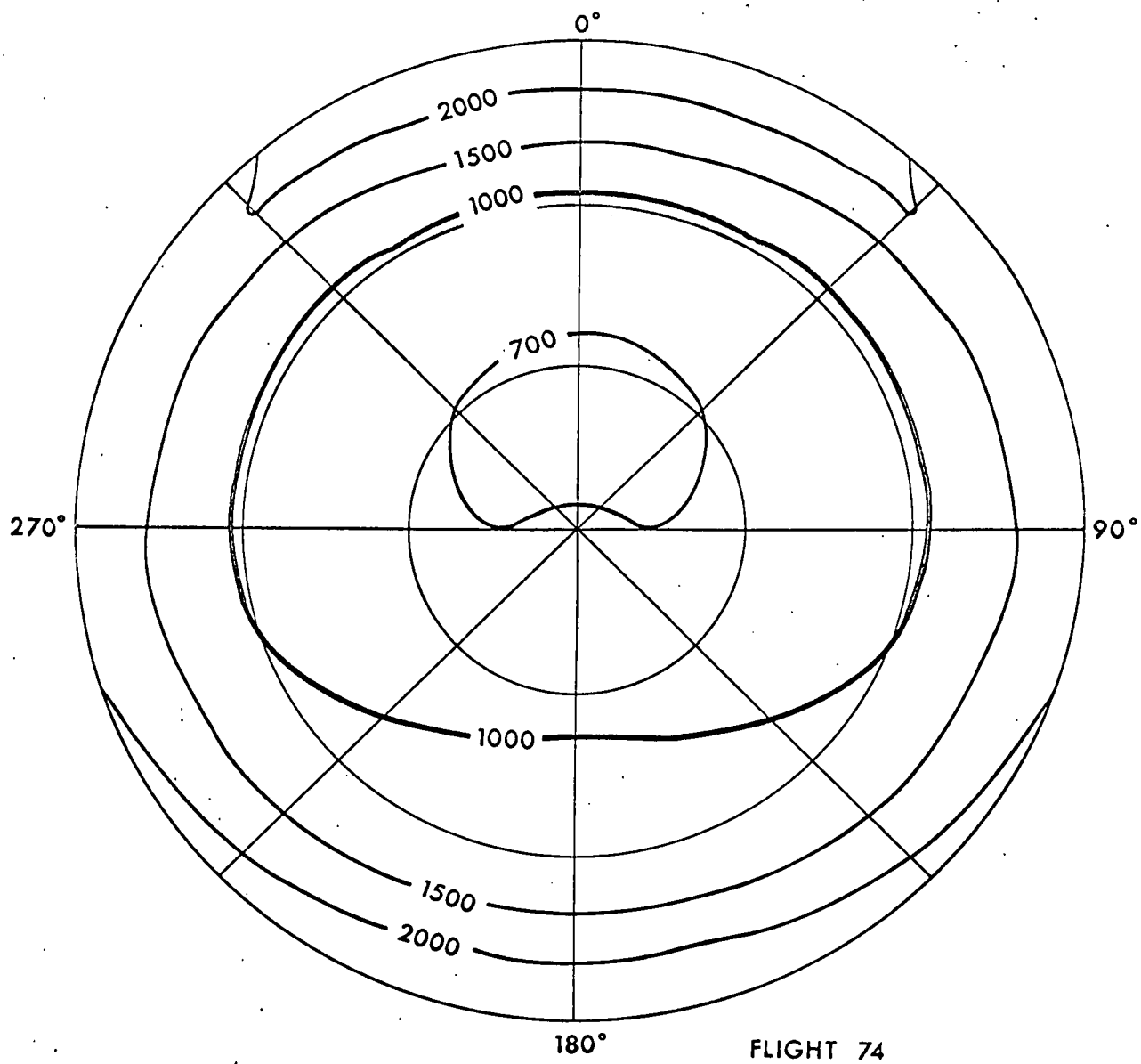

FLIGHT 74
LOWER SKY LUMINANCE
(Foot-Lamberts)
ALTITUDE – 20,000 feet

FIGURE 7.5

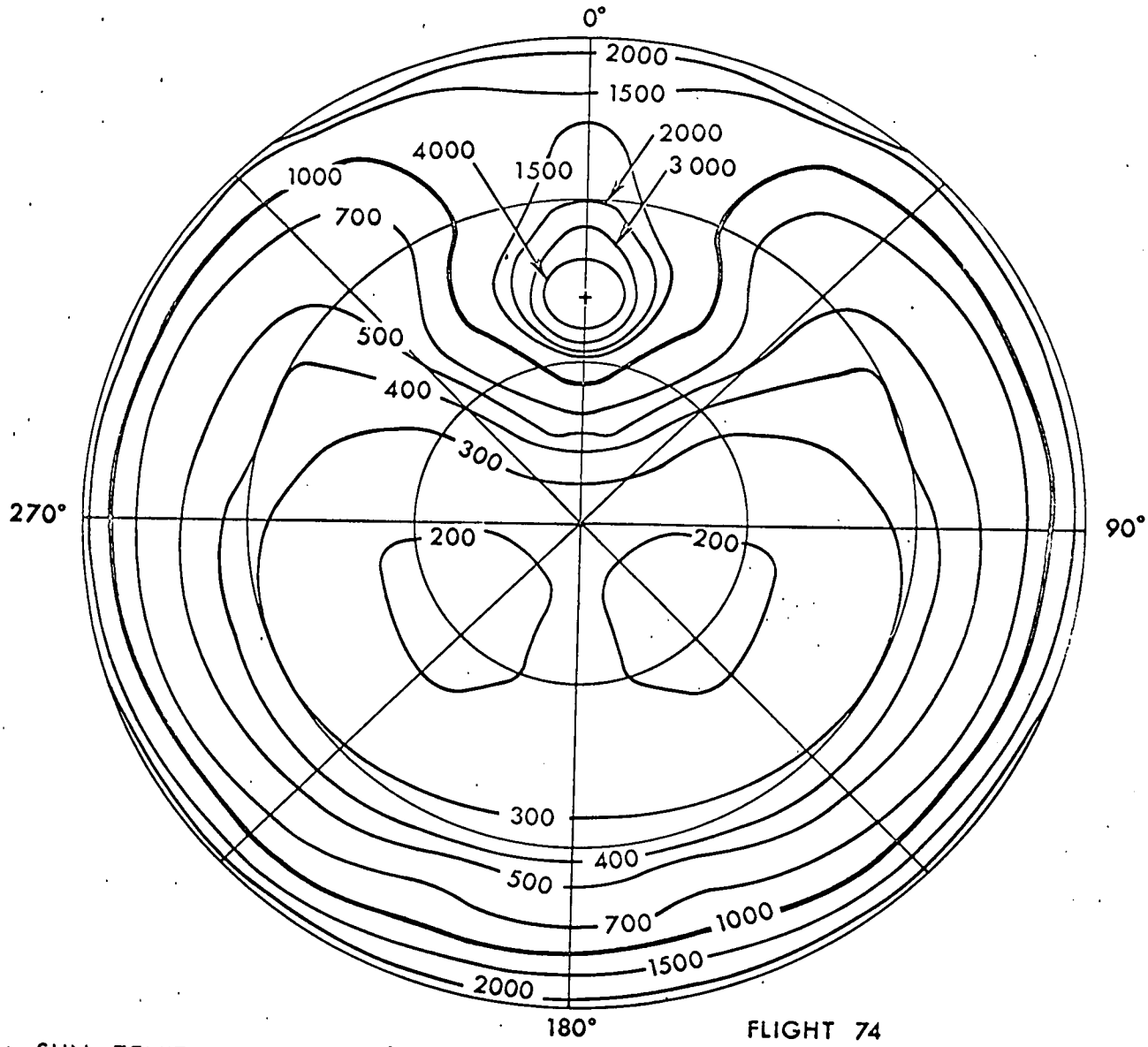

+ SUN ZENITH ANGLE 41.5°
APPARENT LUMINANCE OF THE SUN
5.05×10^8 FOOT LAMBERTS

FLIGHT 74
UPPER SKY LUMINANCE
(Foot–Lamberts)
ALTITUDE – 20,000 feet

FIGURE 7.6

8.0 TECHNIQUES OF MEASUREMENT

by Roswell W. Austin

The acquisition of data for solving visibility problems requires equipment which measures optical properties of objects, backgrounds, and the environment under conditions specified by the problem. Data of the type used in this report can be obtained with instruments of more or less conventional design or by using specialized instruments which for the most part have been adequately described in previous literature, as by Middleton (1952) and by Duntley, et al (1957). Most of the instruments have in common the ability to obtain the relative or absolute magnitude of light flux in order to measure some intrinsic property of an object, such as a reflectance or transmittance, or in order to measure an extrinsic property, such as a luminance or illuminance. Many of the principles used in the photometric calibration of such instruments are covered by Walsh (1958). However, considerable insight, skill, and ingenuity are called for to assure that all instruments involved in obtaining data for use in a problem solution are calibrated in a manner that will lead to internally consistent results.

As the techniques involve photometry, it would be well to examine the properties of some of the sensors commonly used for this purpose and their problems and pitfalls. We will summarize these and describe a few examples of instruments which have been used to advantage in obtaining data for visibility problem solution.

8.1 Photometers

Two basic divisions of photometry are visual and physical. In visual photometry the eye does not make absolute measurements with an accuracy that is satisfactory for anything but a gross assessment of light level. However, two adjacent luminous fields of like spectral quality can be compared and equated with considerable precision if there is sufficient time and operator skill. Most visual photometers use this principle. They compare the unknown with an internal standard of proper spectral quality. Their use is usually restricted to the laboratory or to cases where other methods cannot be used.

Physical photometers may be classified as photographic and photoelectric, according to the sensor used. With due consideration for their spectral sensitivity they can measure or compare light fields and sources with great rapidity and, with adequate precautions, with accuracy suitable for most environmental measurements. The chief advantage of photographic photometry is that it can record a vast amount of information quickly on a single piece of film. However, all facets of the procedure must be carefully controlled and known if any accurate photometric information is to be obtained. Mees (1944, p. 884), states, "Hardly any type of measurement contains so many pitfalls for the unwary as photographic photometry."

In addition to the usual sensitometric controls of the film development and printing processes many other factors must be considered. These include: spectral sensitivity of the film for the development used; spectral transmittance of the lens, filters, and windows; flare characteristics of camera system for the illumination conditions under which photograph was taken; vignetting and $\cos^4\theta$ transmission losses of the lens for off-axis

images; uniformity of negative material and its development; Eberhard and other adjacency effects; suitability of type of density measurement-- specular or diffuse-- for the use to which the measurement is to be put. The ratio of these densities, the Callier Q factor, may be as large as 1.7 depending upon gamma and density (Mees, 1944, p. 642). The care with which all of the above factors are measured and taken into consideration will determine the accuracy of the photometric information which can be obtained from a photographic system of photometry. It is unfortunate that far too often the apparent simplicity of the system leads to its use with only a superficial appreciation of the many attendant problems.

The photoelectric sensors used in photometers can be divided into three sub-classes: photoconductive, photovoltaic, and photoemissive. The application of photoelectric sensors to photometry is well covered in the literature and the reader is referred to sources such as Zworykin and Ramberg (1949) for details and further bibliographic references. We will make a few general observations about their application and mention some of the problems and limitations affecting the choice of sensor.

The photoconductive cell is well known as a detector of infrared energy and varieties of photoconductive devices, mostly of the cadmium sulphide type, have found some application to photometry. They are

limited in their usefulness due to their slow time response characteristics and the dependence their chacteristics have on light—level and temperature. However, in certain situations where their spectral response, non-linearity, slow response and temperature sensitivity can be tolerated or adequately compensated for, their size, high sensitivity, and relatively low cost make them suitable choices as detectors.

The photovoltaic device has had wide application for many years and still finds a place where a simple photometer of moderate sensitivity and capability will suffice. Its problems of non-linearity, fatigue, and temperature coefficient of its sensitivity can usually be kept within tolerable limits if the resistive load into which it operates can be held to a value which is small compared with its internal resistance.

This implies that an optimum method of use would be to measure the short-circuit current output from the cell, a technique that is essentially feasible with modern electronic microammeters. Still other useful techniques are given by Rittner (1947), Moon and Laurence (1941) and Wood (1936). Many new developments have occurred in this field as a result of the requirement for solar energy conversion devices and with the great emphasis on semiconductor research in the past few years. The selenium cell, however, is still the most widely used photovoltaic detector for general photometry. These cells are capable of supplying short circuit output currents as high as 850 microamperes per lumen, are available in convenient sizes, and can be obtained hermetically sealed with an inert gas for improved stability in field environments.

The photoemissive detector in the form of the multiplier phototube is currently the most widely used sensor for environmental photometry. The modern tube owes much of its development to the requirements of nuclear science for scintillation counters. As a result, much of the literature on recent studies and developments on multiplier phototubes will be found in nuclear science journals. Specifically the annual Proceedings of the Scintillation Counter Symposia (1958), (1960), (1962) are excellent sources of relevant tube information. Fortunately, many of the requirements placed on the tubes for scintillation counting are compatible with their use as photometers. As a result, tubes are available in a number of styles and sizes with various cathode spectral sensitivities (Engstrom 1960) to fit many photometer applications. There are also special tubes which can be used at temperatures as high as 150°C (Causse, 1960) and ruggedized tubes for high vibration and acceleration environments.

A valuable feature of the multiplier phototube is its integral electron multiplier which provides an inexpensive yet fast and versatile amplifier for the photocathode current. This results in a minimum of noise being added to that of the cathode current and provides a convenient method of varying the gain of the tube, hence its output current. For "DC" photometers where the flux on the cathode is not modulated, the dark current is a prime factor in determining the sensitivity of the photometer along with the quantum efficiency of the cathode surface. Tubes are available that have equivalent anode dark current inputs as low as 10^{-12} lumens. This can be reduced even further by cooling the cathode to reduce its thermionic emission.

For all its many virtues, the multiplier phototube has some serious problems that one must design around or take into account if it is to be used as a sensor for a stable, reliable photometer. These will be listed with references and a remark about their significance.

Non-uniformity of the sensitivity of the photocathode surface. (See Ingrao and Pasachoff, 1961). Photometer optical systems should not form images of anything in object space on the photocathode or image motion will be interpreted as a flux change. Also, all absolute calibrations must use the same area of cathode as the measurement.

Large anode sensitivities of thousands of amperes per lumen can result in serious temporary or permanent changes in tube characteristics if the tube is accidentally exposed to too large amounts of flux. Dynode resistors can sometimes be chosen to preclude the possibility of damaging currents. Alternatively, the tube can be used in a circuit which will, as the cathode current is increased, automatically reduce the dynode voltage to keep the anode current constant. A frequently used circuit of the type was described

by Sweet (1950).

Anode sensitivity changes with time and temperature - Anode fatigue effects can be either increases or decreases in sensitivity with time after an exposure to flux. Their magnitude depends upon processing in tube manufacture, magnitude of dynode current, and temperature (Cathey, 1958), (Marshall, Coltman and Hunter, 1947). Operation of the tube at low anode currents (<1 μa) will often maintain fatigue effects below a significant value. However, there are significant tube-to-tube variations and this effect should always be looked for. Fatigue effects can be greatly reduced by using cesium-free tubes, since they are usually caused by a redistribution of the cesium in the tube due to temperature or high current density.

Non-conformity of the spectral response with the manufacturer's curve. This can be of major significance in equipment having a broad spectral sensitivity such as those corrected to have photopic response. Gross errors can result if an improperly corrected photometer is calibrated using a standard lamp at color temperature of, say, 2854°K and is then used to measure scenes having color temperatures from 5000° to 15,000°K. Individual tube spectral responses should be measured and filters determined accordingly.

Spectral response changes with temperature. (See Murray and Manning (1960) and Young (1963)). This effect is of much greater magnitude in Cs-Sb cathodes than is generally realized. A reduction in temperature causes a small increase in sensitivity from the blue through the green region and a marked decrease in sensitivity in the red. Fig. 8.1 presents data obtained in this laboratory showing the changes which can occur with modest changes in temperature. Remedies: (1) temperature control, (2) use of the multialkali S-20 photocathode which, although it contains cesium, shows less temperature dependence out to 700 mμ or (3) use of a cesium-free tube.

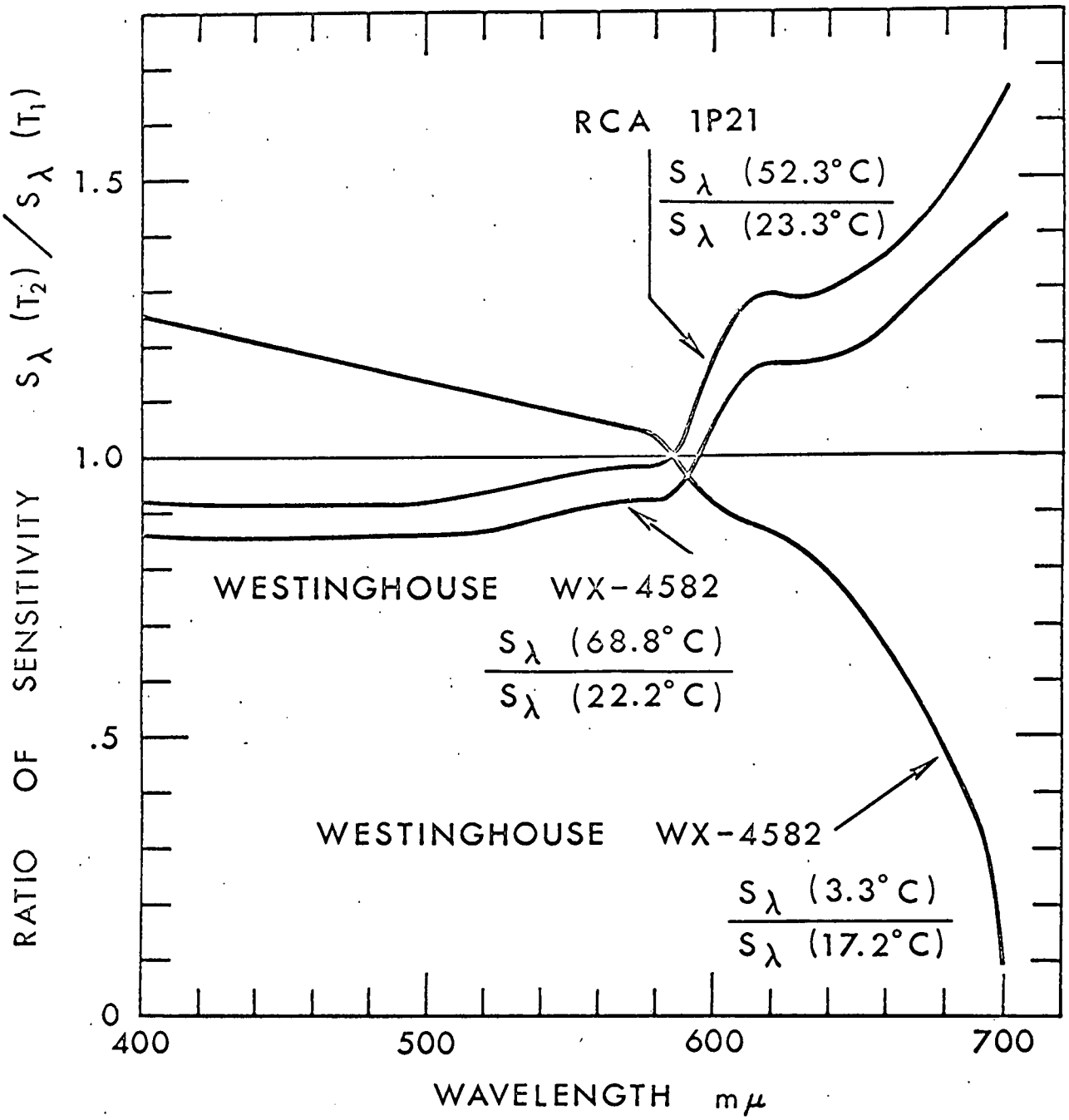

Fig. 8.1 Effect of temperature on Cs-Sb photocathode spectral response. Curves show ratio of response at elevated (or reduced) temperature to the response of the same tube at room temperature. Note that the effect changes sign as the wavelength is shifted from the blue to the red, passing through a region (585 to 595 mμ) where the sensitivity is essentially independent of temperature.

8.2 Illuminometers

The sensitivity of any illuminometer must vary as the cosine of the angle of incidence of the incoming flux. This is particularly important when the major source of flux has a large angle with respect to the surface normal and it is in this region that most illuminometers fail. Fig. 8.2 shows a unit constructed by this laboratory which is an adaption of the method of Boyd (1951) and which properly measures the illuminance within $\pm$ 2% out to 90 degrees.

Illuminometer and Shadow Intensity Meter. This instrument, shown in Fig. 8.3, is an illuminometer which measures sequentially the total illuminance on a horizontal plane from both the sky and the sun, E_{total}, and then the illuminance from the sky alone, E_{sky}. It uses two semicircular straps which rotate about a verticle axis in order to occlude the sun from the illuminometer cap. The solid angle of sky which is removed by the straps requires a small correction which can be introduced in data reduction. The expression $(E_{sky} / E_{total}) - 1$ is defined as shadow contrast.

Goniophotometer. In order to determine the luminance of objects or terrains from various viewing angles it is necessary to be able to measure them directly under the desired illuminating conditions or to compute their luminance from a knowledge of the radiance distribution surrounding the object and its directional reflectance. The direct measurement approach is simpler and preferable. The goniophotometer in Fig. 8.4 is a dual instrument capable of measuring two surfaces simultaneously under natural illumination.

3 pièce

9. OBJECT CLASSIFICATION

by J. L. Harris

In performing a visibility calculation object properties, atmosphere or water properties, and visual system properties are combined to give a prediction of the distance at which any object can be detected with a specified probability. For many important practical applications of this type of Visibility Engineering, the number of permutations of the problem parameters is extremely large. It is therefore a matter of prime importance that means be available which minimize the computational steps which must be performed. Of the various parameters which define a visibility calculation, the most variable is undoubtedly the nature of the object itself. This section is primarily concerned with methods for simplifying the specification of objects.

9.1 Object Descriptions

The vast majority of basic vision data related to detection has been obtained utilizing circular, uniform-luminance objects. This type of object is adequately described by specifying the contrast and the angular subtense. In most practical visibility problems, the objects in question are not circular. They seldom have uniform luminance. In a great many cases of interest the shadow of the object plays an important role in detection. The situation then is that, not only are the objects non-circular, and non-uniform in luminance, the size, shape, and pattern of one single object can change dramatically with the lighting geometry. While the realization that the number of possible object patterns is virtually unlimited may be comforting to

those persons concerned with unemployment, it is much less comforting to those persons who have a real and immediate need for the solution of visibility problems.

Quantization of detection range. On the basis of practical considerations it is possible to quickly devaluate the importance of the existence of an infinite variety of object patterns. An intuitive argument will serve to illustrate the concepts.

The first step is to place practical bounds on the maximum distance at which objects are likely to be detected. If, for example, for the case of ground-level observations this maximum was set at 50 miles, the detection interval from 0 to 50 miles would most certainly contain an extremely high percentage of all objects of interest. The next step is to establish the precision with which the detection range must be obtained. For the purposes of illustration assume that a precision of $\pm$ 0.5 miles was satisfactory. The overall range of 0 to 50 miles contains 50 such precision intervals. If a detection probability is specified, all objects which fall within the 50-mile interval will now be detected within one of the 50 precision intervals. In general, any one precision interval will contain many objects. These objects may be very dissimilar in size, shape, and pattern, but for purposes of classifying objects in terms of visual detection, the fact that they are all detectable at the same range makes them detectably "identical." This suggests that in terms of some sort of detection classification system these objects have identical index numbers.

Detectability as a function of range. The arguments just advanced indicate that the number of significantly different objects insofar as visual detection is concerned is not unlimited. It is suggestive that the

proper grouping or classification of objects will reduce the number of possible visibility calculations to a number which can be easily handled. Before attempting to implement this concept, however, the manner in which detectability changes with range should be considered.

Figure 9.1 is a plot which shows detection probability as a function of range for three circular visual targets having areas as indicated. The contrast of the three objects were chosen such that all three are liminally detectable (50% probability) at 4000 yards. The contrast values and the adaptation luminance are given in the Figure caption. The detection ranges are those which would occur in the absence of atmospheric attenuation. In the sense of the preceding discussion here are three objects equally detectable at 4000 yards and hence "identical." Figure 9.1 makes clear, however, that the objects are not identical if a detection probability of 0.9 is specified. It should also be clear that the three objects will not be liminally detectable at the same range if atmospheric contrast reduction is introduced.

What might appear to be a major problem is actually easily resolved. The problem is that the visual system does not detect in terms of range and object area but rather in terms of angular subtense. If detection probability is plotted as a function of angular subtense then in the absence of atmospheric attenuation all circular objects of the same contrast and angular subtense are equally detectable regardless of the various range and target area combinations which may exist. This is strongly suggestive that any classification system ought to be based on angular subtense rather than range and object area.

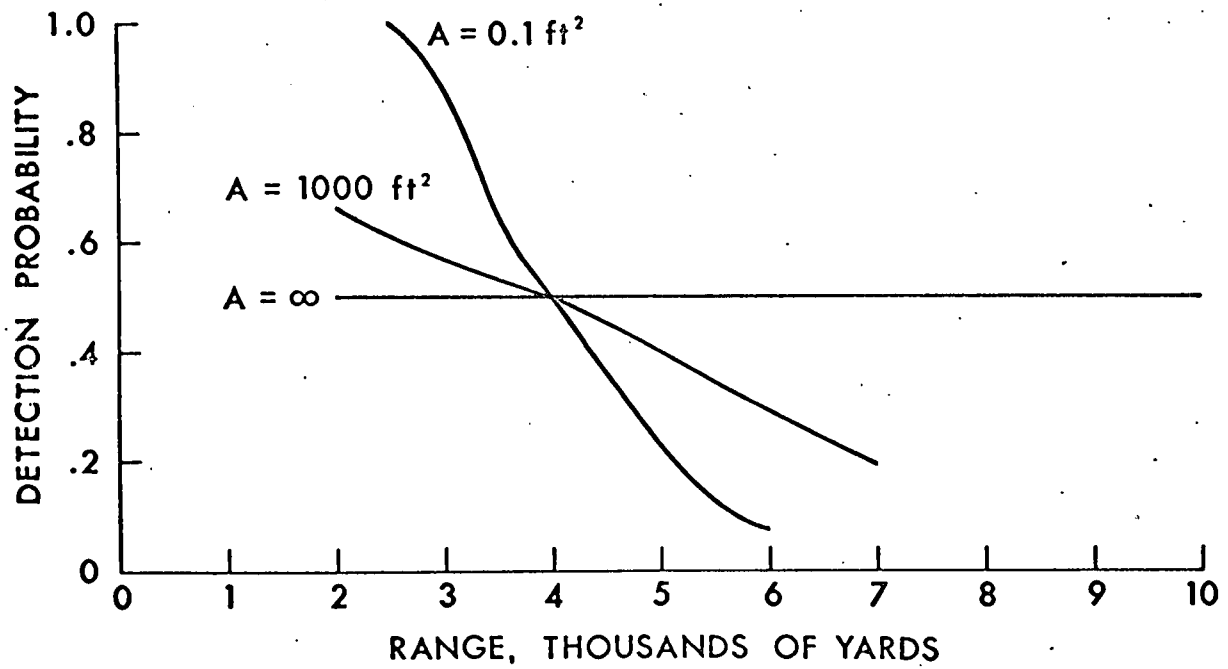

Fig. 9.1 Manner in which detection probability changes with detection range. The three objects are circular and uniform-luminance with areas as indicated. The contrast values associated with these objects were selected such that all three objects were liminally detectable (50 °/o probability) at 4000 yards. The contrast values are $C_{oo} = 0.0025$, $C_{1000} = 0.009$, and $C_{0.1} = 28$ and were taken from the long stimulus duration Tiffany smoothed data for 1000 ft-L adaptation level.

9.2 Index Number

A non-uniform luminance, non-circular object could be specified by many different arbitrary definitions. The concept of object contrast could be extended to include the concept of point contrast which varies over the object region, and it would then be possible to talk in terms of peak contrast, average contrast, root-mean-square contrast, etc. None of these arbitrary definitions will supply a numerical value which is a monotonic function of the detectability of the object. If the purpose of the classification is to aid in the prediction of detection ranges then the appropriate numerical classification should be that which is achieved by weighting the various object elements in the same manner as they are weighted by the visual system in the process of performing detection. The description which is appropriate is therefore that provided by previous studies of the visual weighting or summative function as exemplified by the element contribution theory. (See Blackwell, 1963).

Here the visual system is treated as a linear spatial filter. The output response of the visual system can then be described by convolving the object and the visual weighting function. All objects which yield the same maximum value from this convolution are equally detectable.

Quantization is again introduced when a precision of measurement is specified. The nature of the weighting function for the visual system is a function of adaptation level, stimulus duration, and position of the retinal image with reference to the fixational center. These weighting functions may be derived from experimental vision data for circular objects.

The numerical value associated with the convolution of object and weighting function does much more than show equality of detectability. It is a monotonic function of the probability of detection. If the index number is chosen such that liminal detection (50% detection probability) is chosen as unity, then higher and lower values of index number can be directly related to detection probability in the manner indicated by Taylor in an earlier section.

Experimental determination of index number. The convolution integral process previously described must be implemented in order to achieve object classification as a practical tool for visibility engineering. There are many possible mechanizations which may be accomplished. The Visibility Laboratory has implemented two of these.

The first mechanization is in the form of a photoelectric scanner in which the object, model, or photograph of the object is imaged by a zoom lens upon a film transparency the transmission of which is proportional to the appropriate visual weighting function. The flux passing through the weighting function is collected on the photocathode of a multiplier phototube. The output of the multiplier phototube is proportional to the convolution integral for one position of the weighting function relative to object space. Two pairs of counter rotating prisms achieve a scanning of object space by means of rapid horizontal and slow vertical sinusoidal displacements of the image falling on the summative function. Thus the entire convolution of object space and weighting function is obtained. A second channel of the system performs a convolution of weighting function with uniform background. The system alternately examined one channel and then the other, differencing the two to achieve the desired convolution

of the weighting function with the luminance difference map which constitutes the visual signal.

The electronics associated with the visual target classifier provide complete remote operation of the scanner including start, stop, and speed control. The convolution integral may be continuously recorded during the scanning operation. Auxiliary circuits provide a means for automatically determining and storing the peak value of the convolution integral which is obtained during a complete scan. It is this peak reading which is utilized to predict the detectability of the target.

The alternate method of performing target classification utilizes a film scanner constructed in connection with another laboratory research program. The film image is projected onto a screen in the center of which is an aperture whose size and shape may be selected. The flux passing through the aperture is collected by a field lens and deposited on the photocathode of a multiplier phototube. The output of the multiplier phototube is fed into a voltage-to-frequency converter, and the frequency is then counted by means of a decade counter. Serializing of the counter output provides a direct input to an IBM card punch with up to four significant figures recorded on an IBM card.

Scanning is accomplished by means of a discrete line scan achieved by discrete stepping of the film. Synchronous sampling circuits provide that a reading is punched at each film position.

A gray scale is scanned prior to the scanning of the object to be classified. The first operation performed by the CDC 1604 digital computer used to perform the classification is to construct the H and D curve for the film and to correct all subsequent readings for the film characteristics.

The weighting functions are also converted to computer language, and the computer then performs the convolution integrals, determines the peak value of the convolution integral and prints out the required information.

Each of the two classification mechanizations has advantages and disadvantages. The mechanical optical scanner has versatility in terms of being able to operate directly upon real objects, or models of objects, without the requirement for intermediate photographic steps. The primary advantage of the film scanner and computer convolution method is related to the fact that there is a new summative function for every adaptation level, glimpse time, and position of the image on the retina. Since with the film scanner the object information is collected in basic form, the object need be scanned only once, with convolutions being performed by the computer with any number of weighting functions. With the mechanical-optical scanner each new summative function must be photographically constructed and the object, model, or photograph of the object rescanned. The combination of the two devices offers considerable versatility in obtaining target detection information.

9.3 Experimental Verification of Threshold Predictions

A vision experiment was performed as a means of testing the prediction capability of the apparatus. Two objects were photographed under conditions of low, medium, and high sun elevations. The shadow patterns, which were the predominate optical signal, were abstracted to a black and white grid structure. The abstraction was made because the computer program for object classification utilizes a grid structure description of the object. The use of a grid type object therefore simplified the insertion of object descriptions into the computer. These six targets were then viewed by five

observers in a temporal forced choice experiment with contrast as the variable. The liminal contrast thresholds (50% probability of detection) were determined for each target and each observer.

These same five observers had previously been used to obtain thresholds on circular object as a function of the angular subtense of the object for the same adaptation level (75 foot-lamberts) and stimulus duration (1/3 second). This basic vision data, averaged over the five observers, was used to calculate an average spatial weighting function which was then used to predict the thresholds for the shadow pattern targets. The digital computer classification program was used. Figure 9.2 shows the results of both the vision experiment and the computer predicted thresholds. The thresholds for each of the observers are shown above a picture of each object. The dashed lines connect the results for each observer in order that it may clearly be seen that the variability of the observer thresholds is due largely to individual differences rather than a lack of stability of the data. The computer-predicted thresholds are connected by means of the solid lines with the results falling well within the variability due to individual differences. It should be noted that the five observers were chosen because of their availability and not because they represented any desired observer population. The predictions, which are based on weighting functions derived from averaging the vision data of these same five observers, are as good as one might reasonably expect. There is every reason to believe that prediction of performance for an individual observer based on his own weighting function could be made with much greater precision.

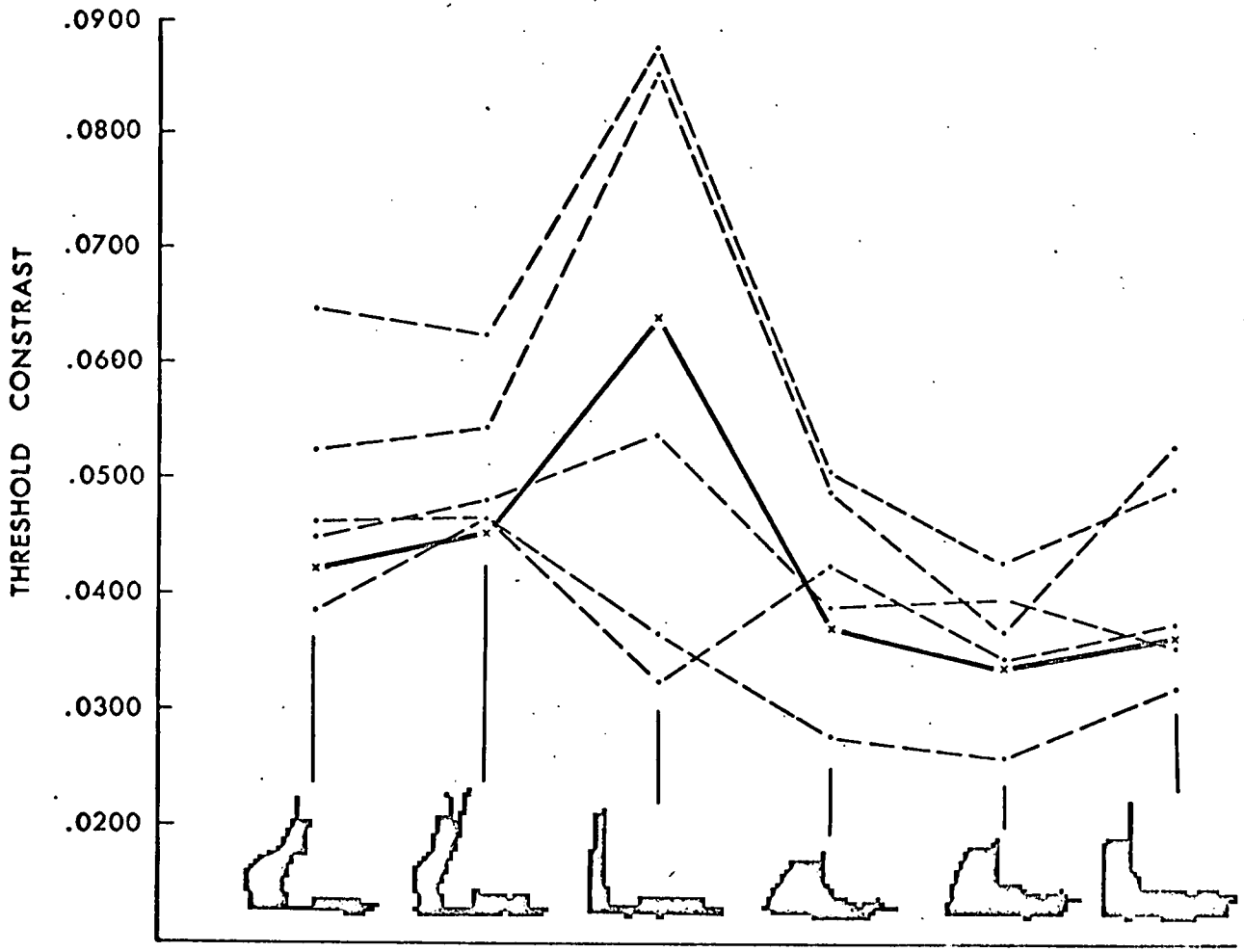

Fig. 9.2. Results of the abstracted shadow pattern detection experiment. The shapes of the shadow patterns are shown below the threshold values as experimentally determined. Each of the patterns subtended 6 min of arc in the horizontal dimension. The experiment was a temporal forced-choice presentation with stimulus durations of 1/3 sec and 75 ft-L adaptation. The dashed lines connect the data points of the individual observers. The solid line connects the computer-predicted thresholds based on a weighting function which was obtained from data averaged for the same five observers.

9.4 A Sample Object Classification

Figure 9.3 shows the appearance of a trailer van as viewed from two elevation angles of the path of sight, for two orientations of the vehicle relative to the path of sight, and for two orientations of the vehicle relative to the sun. Film transparencies for these eight viewing conditions were scanned by the apparatus previously described. The CDC 1604 digital computer was then used to perform the convolution with the weighting function in order to obtain index numbers for the various viewing conditions. The weighting functions which were used were derived from Taylor's 1/3-second, 75-ft-lambert data.

In order to perform visual search calculations it is necessary to determine the visual detection lobe. This means that the detectability of the object must be determined not only for the fixational center but also for a number of peripheral points sufficient to define the lobe structure. This requires that a weighting function be generated for each peripheral angle with the convolution operation repeated for each.

Figure 9.3 shows graphically the results of the computer classification of the van for the selected fixational points as described in the caption. The angular subtense shown is measured in terms of the maximum horizontal or vertical dimension of the object plus shadow. Classification at the various angular subtense values is accomplished by a computer program which demagnifies the object relative to the weighting function. The resulting data may be replotted as index number as a function of distance to the object by determining, from scaling of the film, the linear distance of the maximum object dimension.

Fig. 9.3. The eight outside figures show photographs of the trailer van in the various viewing conditions. The van was viewed at 30° and 60° elevation angles of the path of sight, with the sun parallel and perpendicular to the plane of the path of sight, and with the axis of the van parallel and perpendicular to the path of sight. For each of these viewing conditions the index number is plotted as a function of the angular subtense of the longest dimension of the van-shadow complex. Each of the family of seven curves is for a retinal position relative to the fixational center. From top to bottom, the angular positions are 0°, 1.25°, 2.5°, 5.0°, 7.5°, 10.0°, and 12.5°. The central curve family is a composite of the 0° curves from each of the eight viewing conditions. In order to compare the curve shapes the eight curves have been normalized to have an index number of 0.1 at an angular subtense of 1 minute of arc.

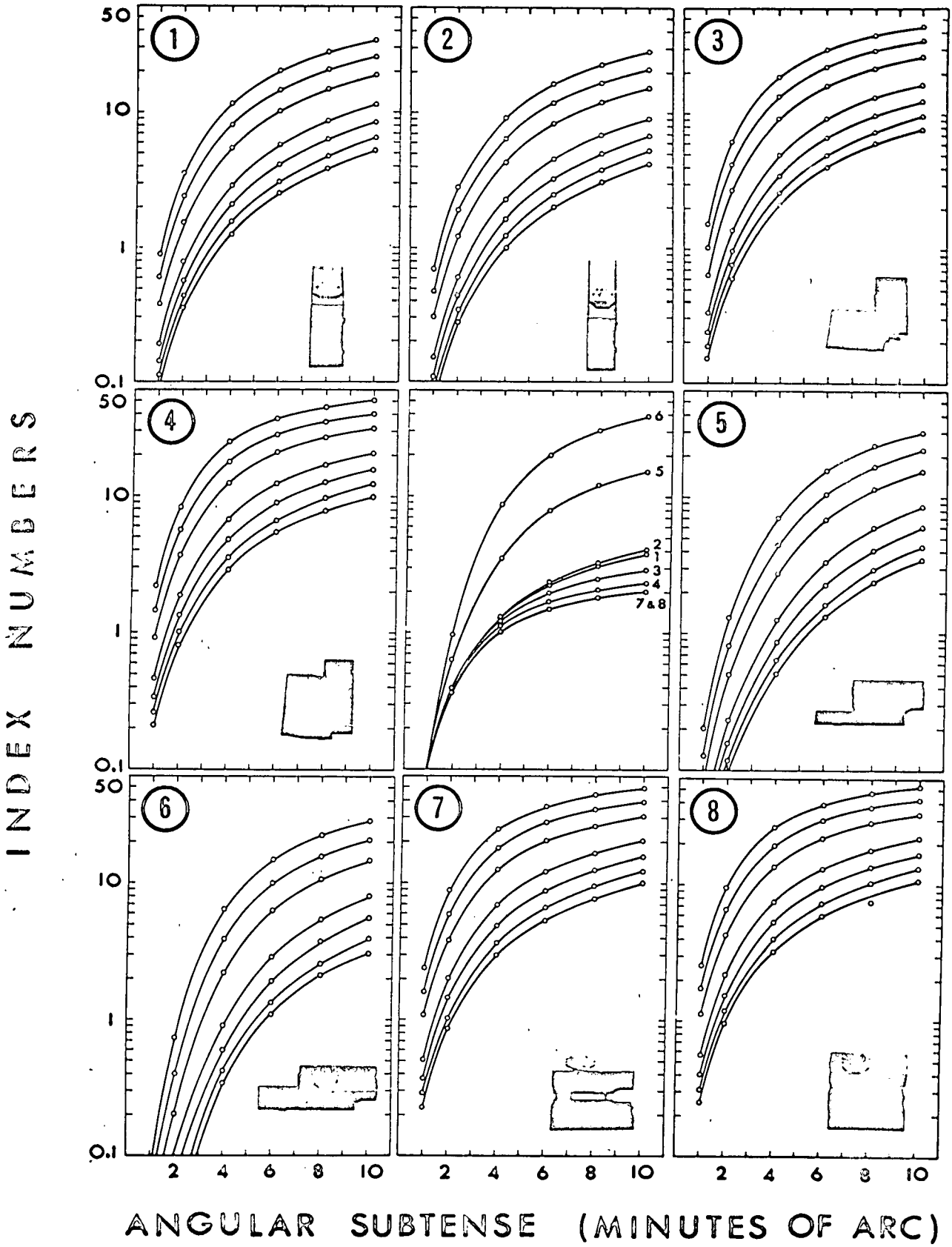
INDEX NUMBERS
50
10
1
0.1
1
2
3
4
5
6
7
8
6
5
2
1
3
4
7 & 8
2
4
6
8
10
ANGULAR SUBTENSE (MINUTES OF ARC)

Fig. 9.3

9.5 The Nature of Index Number vs Angular Subtense

The utility of the index number concept would be largely negated if every object had a significantly different functional relationship between index number and angular subtense. Once again quantization by virtue of precision can be imposed to limit the number of index number vs angular subtense curves to a finite number. Since finite numbers can get very large it is still necessary to show that the number of such curves is sufficiently small to make classification practical. This question requires further study but there is good reason to believe that perhaps as few as 10 such curves might cover the vast majority of objects of interest. The eight van pictures of Figure 9.3 show a considerable variation in pattern for the object in question. The central graph superimposes the foveal index number versus angular subtense curves for the eight viewing conditions. The curves have been normalized to have the same values at 1.0 minutes of arc in order that the same scale could be utilized. This graph illustrates the variations in the shape of the index number versus angular subtense which may be encountered in a typical practical problem.

Three values are required to fully classify an object. The first is the nature of the index number vs angular subtense curve. This might be termed the class of the object, perhaps designated by Roman numerals. The second value is the scale factor which transforms the normalized class curve into an absolute curve. This might be chosen to be the value of the index number, I, at an angular subtense of 1 minute of arc. The third value is the scale factor which translates angular subtense into distance. This might be chosen to be the distance at which the maximum

object dimension subtends 1 minute of arc. Thus a complete object description might take the form of specifying: Class III, $I_{\alpha=1} = 0.82$, $R_{\alpha=1} = 13.2$ miles.

9.6 Summary, Conclusions, and Future Trends

This section has described techniques by which the infinite number of possible object patterns can be reduced to a practical number commensurate with the overall precision requirements of the visibility calculation. The classification operation in itself makes visibility calculations become cumulative in the sense that some new object when classified may have a set of classification numbers for which many calculations have been previously made.

The ability to specify a complex object pattern by a set of numbers is a first important step toward the complete solution of visibility problems by means of high speed digital computers. When atmospheric and hydrologic transmission properties have been similarly classified into a finite number of significantly different types of situations then visibility calculations will be performed by the writing of a simple prescription from which the computer will provide rapid and inexpensive solutions.

10. VISUAL SEARCH

by J. I. Gordon

The preceding sections have discussed object and background properties, atmospheric and hydrologic properties, and visual system properties. A visibility calculation is accomplished by combining these properties to determine the distance at which an object can be detected. If the exact position of the object is known then the observer can use the most sensitive portion of the fovea for accomplishing detection and the calculation will indicate the distance at which the object can just be detected. This is sometimes termed the maximum sighting range. When the exact position of the object is unknown, the observer cannot use the most sensitive region of the fovea and the detection distance will be less than the maximum sighting range. If the angular uncertainty as to the location of the object is large compared with the angular size of the sensitive foveal region, detection can only be accomplished by making a series of fixations at different points in object space in the hope that one of these fixations will place the image of the object on a retinal position where the sensitivity is sufficient for detection to take place. By making assumptions about the probable distribution of objects in the field and with knowledge of the capabilities of the visual system, search procedures can be evolved. The optimum strategy for visual search defines the positioning of the successive fixations in such way as to maximize the probability of detection, (Harris, 1960). This section deals with the manner in which visual search calculations are performed.

10.1 Visual Detection Lobe

The concept of the visual detection lobe is essential to visual search calculations. It is a three-dimensional surface which bounds the volume within which a specified target can be detected with a stated probability. The lobe is associated with a specific observer position in space and a specific orientation of his fixational center, i.e., his most sensitive foveal region. The lobe incorporates the features of target, background, atmosphere, and visual system. Ordinarily, lobes are non-symmetric about the fixational axis and have a complex slope. This results from the manner in which the target, background, and atmospheric transmission characteristics change with viewing angle.

Fig. 10.1 is a sketch which illustrates the complex three-dimensional structure of a typical lobe. The observer is located at 20 000 feet (3.3 nautical miles) and his path of sight is inclined downward with a zenith angle of 101°. The object is a large airliner at very low altitude, as in landing or taking off. The atmospheric and lighting conditions tabulated in Sects. 3 and 6 have been assumed. Further details of the viewing conditions are found in the figure caption. The fixational axis is shown as a dashed line. The intersection of the lobe with the ground plane is indicated by the diagonal line shading. The lobe extends below the ground plane as shown by the mottled shading. This indicates that the airliner is supra-threshold for this visual fixation if it flies above the cross-hatched area of the ground plane. The large lobe radius below the ground plane is largely due to the increase in object contrast and

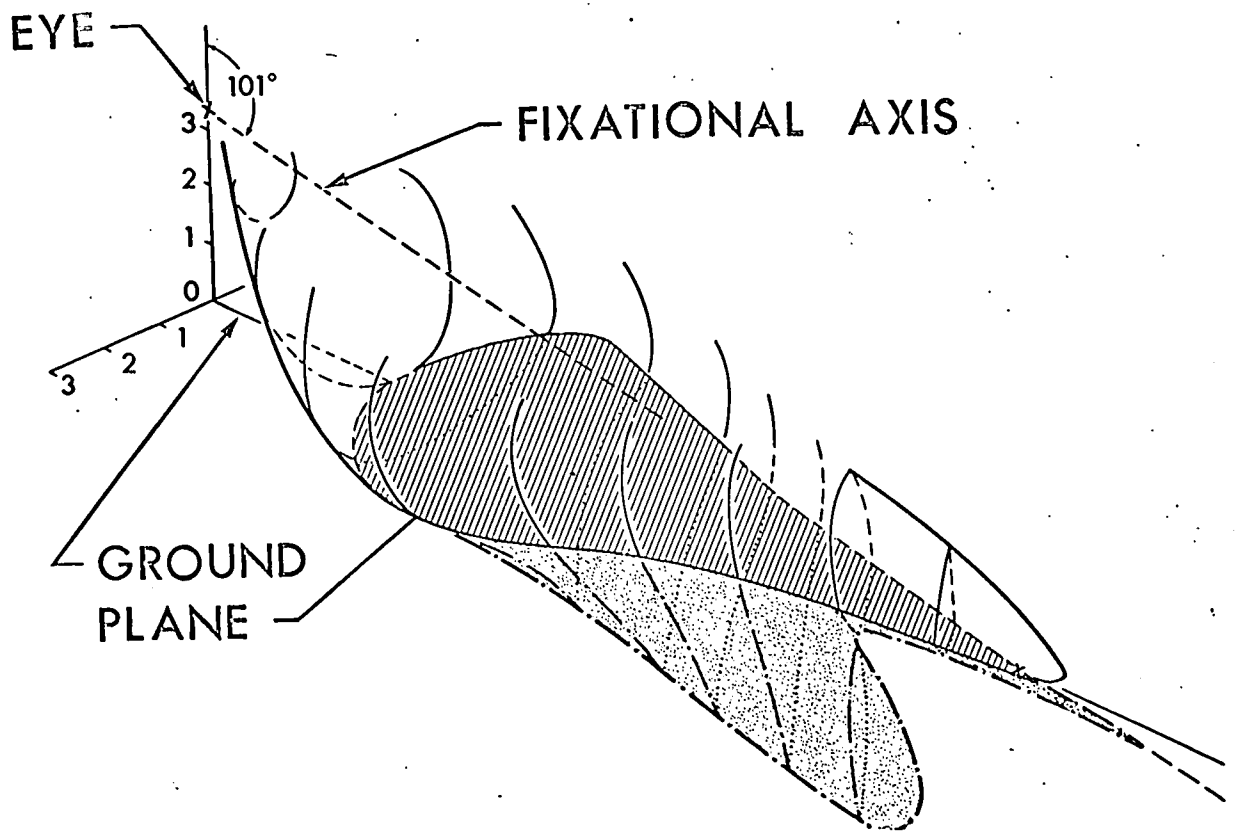

Fig. 10.1. Three-dimensional lobe. The aircraft is a large jet airliner having some surfaces painted with glossy white, some with an aluminum paint, and the remaining surfaces weathered aluminum. The plane is flying cross-sun on an approach over a mixed evergreen and deciduous forested area. The glimpse time is 1/3 sec. The X at the lower right is the intersection of the fixational axis with the ground plane.

projected area which is sufficient to override substantially the decrease in visual sensitivity.

As the observer changes his point of fixation in the process of performing visual search, the lobe structure also changes. This is illustrated in Fig. 10.2 wherein the intersection of the lobe structure with the ground plane is shown for four positions of observer fixation indicated by the small x's. At the most extended fixation point the object is just detectable foveally, i.e., the lobe is tangential to the surface of the earth and there is zero area of intersection. The next fixation point is identical with that chosen for Fig. 10.1 and the intersection area is that shown by cross-hatching in Fig. 10.1. The remaining two fixation points show the change in intersection area which takes place as the observer further depresses his line of sight. Since the single-look probability is proportional to the area of intersection, the importance of a proper search technique is apparent.

Some visual detection lobes are simpler in shape than the one discussed above. Figure 10.3 shows the vertical cross section and ground-plane intersection of a simple lobe. The object in this case is a large tractor viewed against a background of grass. The observer is at 6000-feet altitude looking down at a zenith angle of 109.3°. Figure 10.4 shows the variation in size and shape of the ground-plane intersection for various points of fixation.

Sensitivity lobes. The concept of the visual detection lobe incorporates the characteristics of the object and background, the

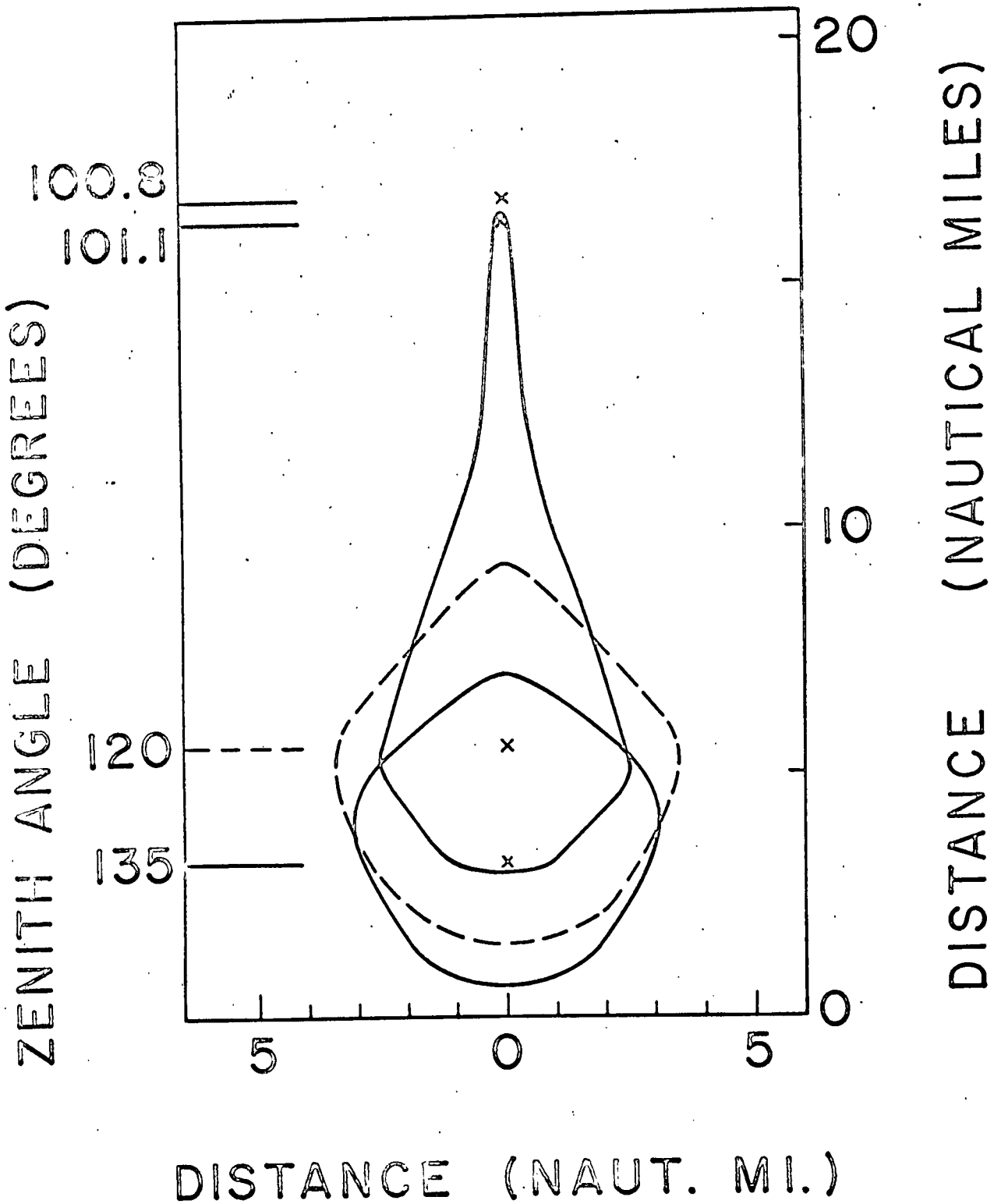

Fig. 10.2. Intersection of the visual detection lobe with the ground plane for the four points of fixation designated by the X's.

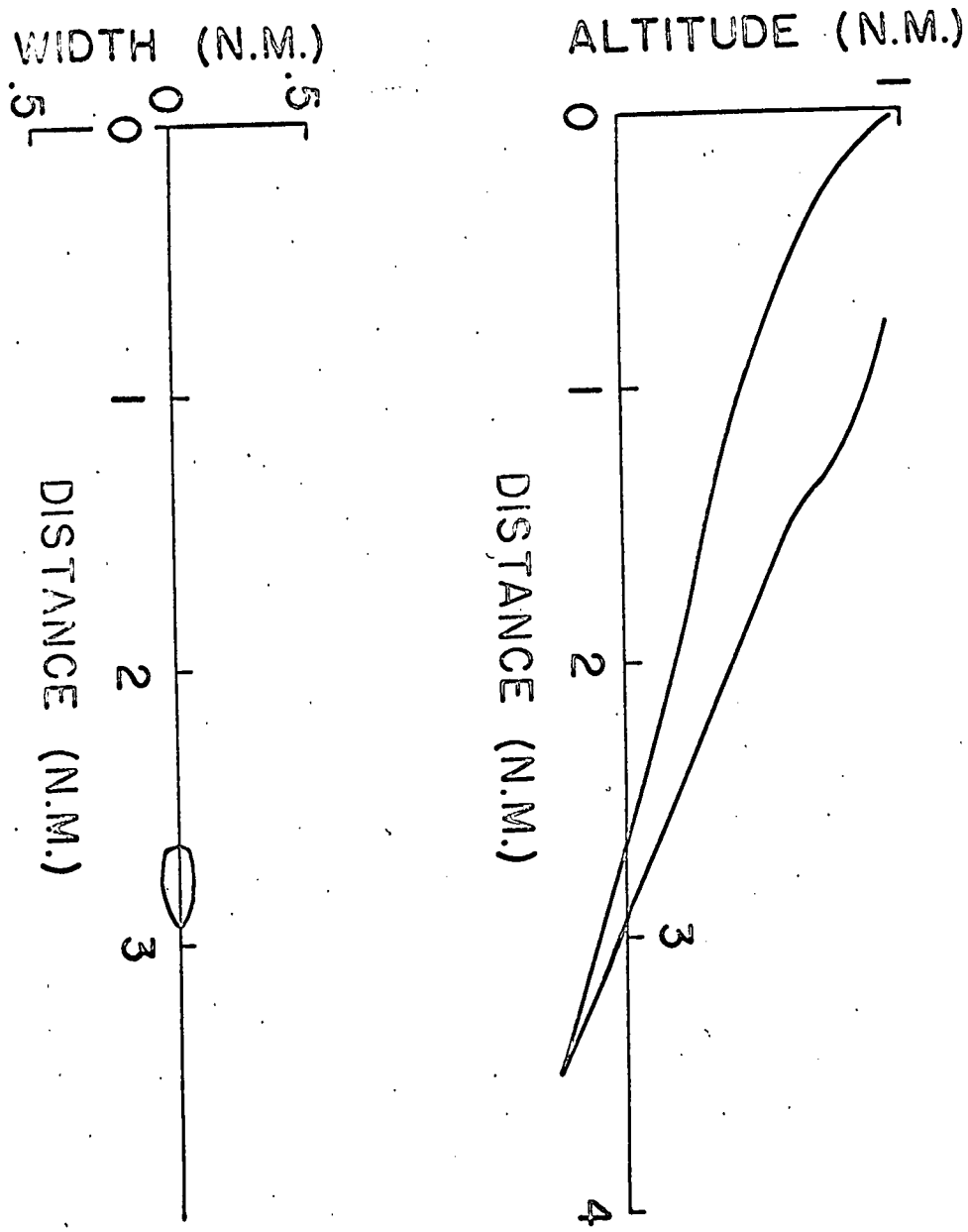

Fig. 10.3. Vertical profile and ground plane intersection of the visual detection lobe for the detection of the tractor.

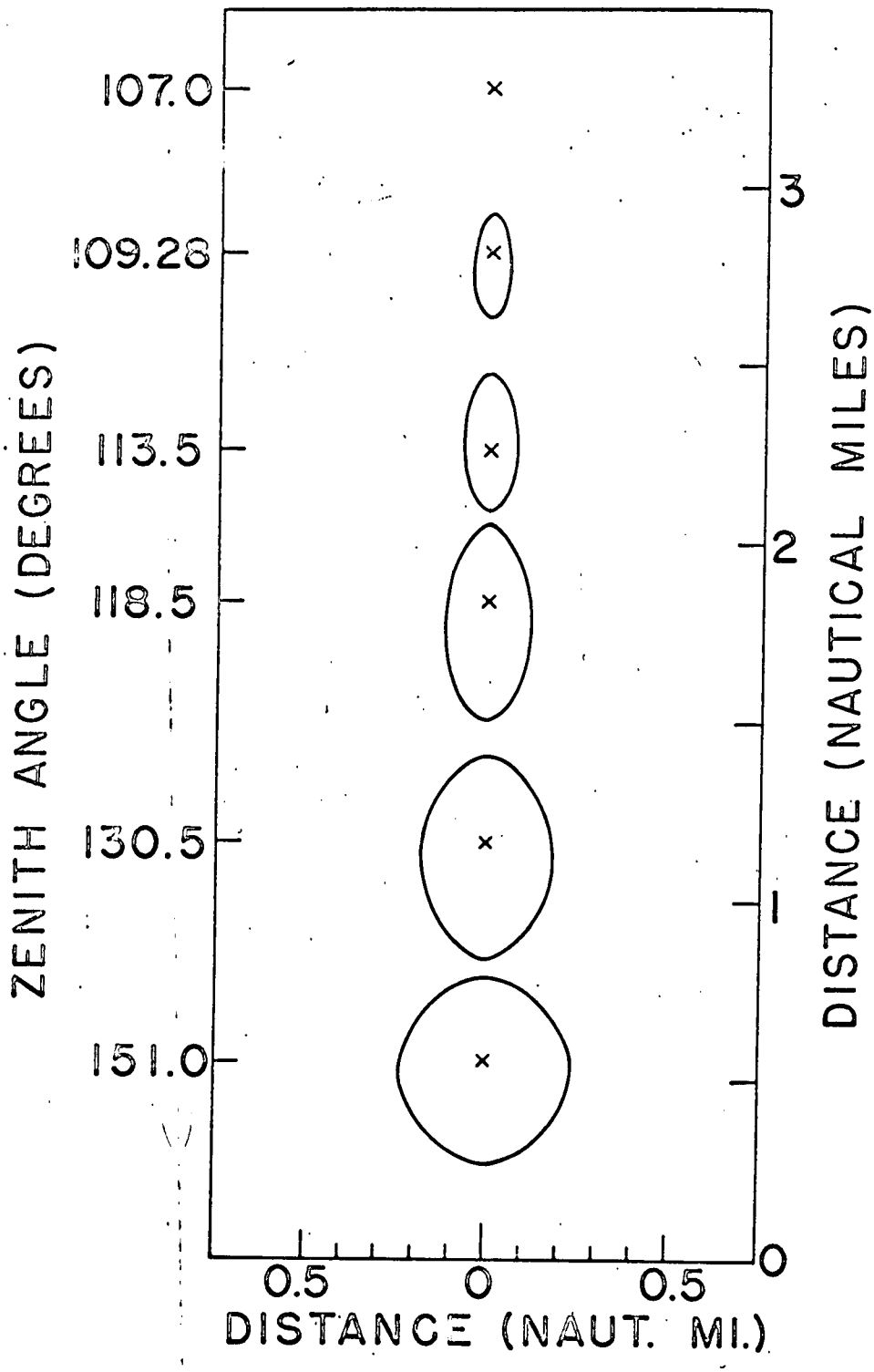

Fig. 10.4. Ground intersection of the tractor visual detection lobe for the fixation points as indicated by the X's.

atmosphere, and the visual system. It differs then from the concept of a radar lobe which conventionally shows only the angular sensitivity pattern of the receiver. To perform radar search analysis, a sensitivity lobe must ultimately be combined with the object and transmission properties. The choice of concept is primarily a matter of obtaining calculational simplicity. The primary deterrent to the use of sensitivity lobes for visibility calculations is that the sensitivity lobe for the visual system is not just a numerical factor as in the radar case but instead is a distinctly different weighting function associated with each angular deviation from the center of fixation. Thus convolution integrals are required to determine detection rather than simple products as in the radar case. However, further study of the sensitivity lobe concept should be made before this technique is discarded.

10.2 A Sample Visual Search Calculation

Every visual search calculation is unique because of the great variability in objects, backgrounds, lighting geometries, atmospheric properties, and viewing geometries. Each calculation starts with the construction of visual detection lobes corresponding to the various possible fixation points which the observer may select. Assumptions must then be made as to the search procedure which the observer will follow. The cumulative probability of detection can then be computed throughout the period of conduct of the search. A sample of a search calculation will be presented to illustrate the techniques involved, (Gordon, 1963).

Let it be assumed that the observer is flying north at an altitude of 4000 feet and following a long, straight, south-to-north dirt roadway. The object of the search is a trailer van which is known to be located somewhere on a designated portion of the roadway 26 000 feet long. Restriction of the search to a road shortens the calculation considerably, since the search is essentially one dimensional, but there is no loss in the generality of the example.

For this illustrative problem, the optical properties of the object were derived from photographs of a scale model of the trailer van. These pictures were scanned and classified by techniques described in the preceding section.

Figure 10.5 shows the computer-calculated apparent index numbers for each zenith angle of the path of sight and for selected angular positions in the visual field measured relative to the fixational center. Appropriate choice of field factors (see Sect. 4) indicated that an apparent index number of 3 (shown by the dashed line in Fig. 10.8) is required to obtain a 94 °/o probability of detection. Figure 10.5 contains the information required to construct the intersections of a 94 °/o detection probability lobe with the roadway. This has been done in Fig. 10.6, wherein the solid line shows the lobe boundaries within which detection occurs. For any chosen path of sight the forward and rear intersections of the lobe with the roadway may be found by drawing 45° lines from the zenith angle of the fixational center to the solid curve as illustrated by the dashed lines. The angular field within which detection will occur can then be read directly.

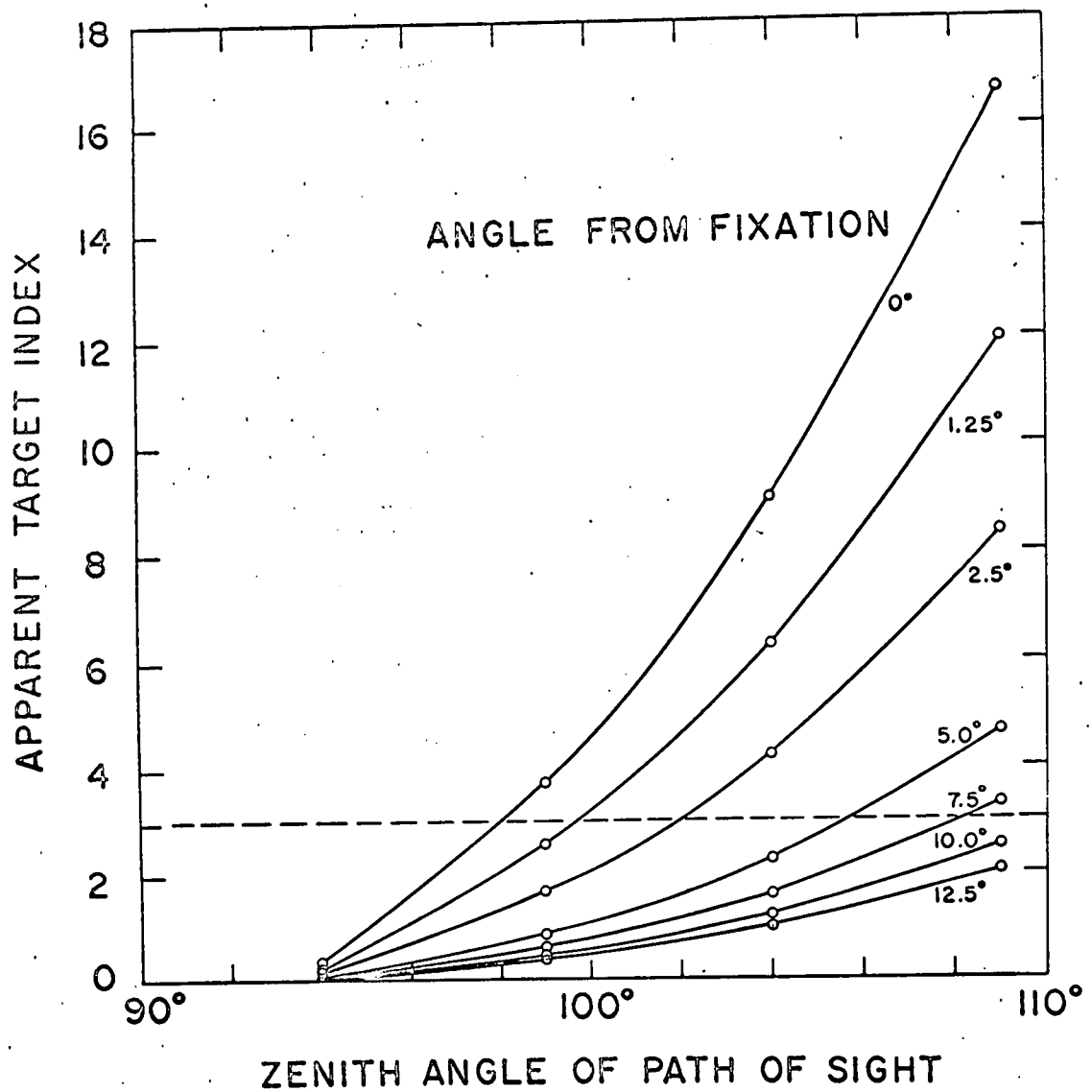

Fig. 10.5. Classification of the trailer van for various viewing angles and retinal image positions.

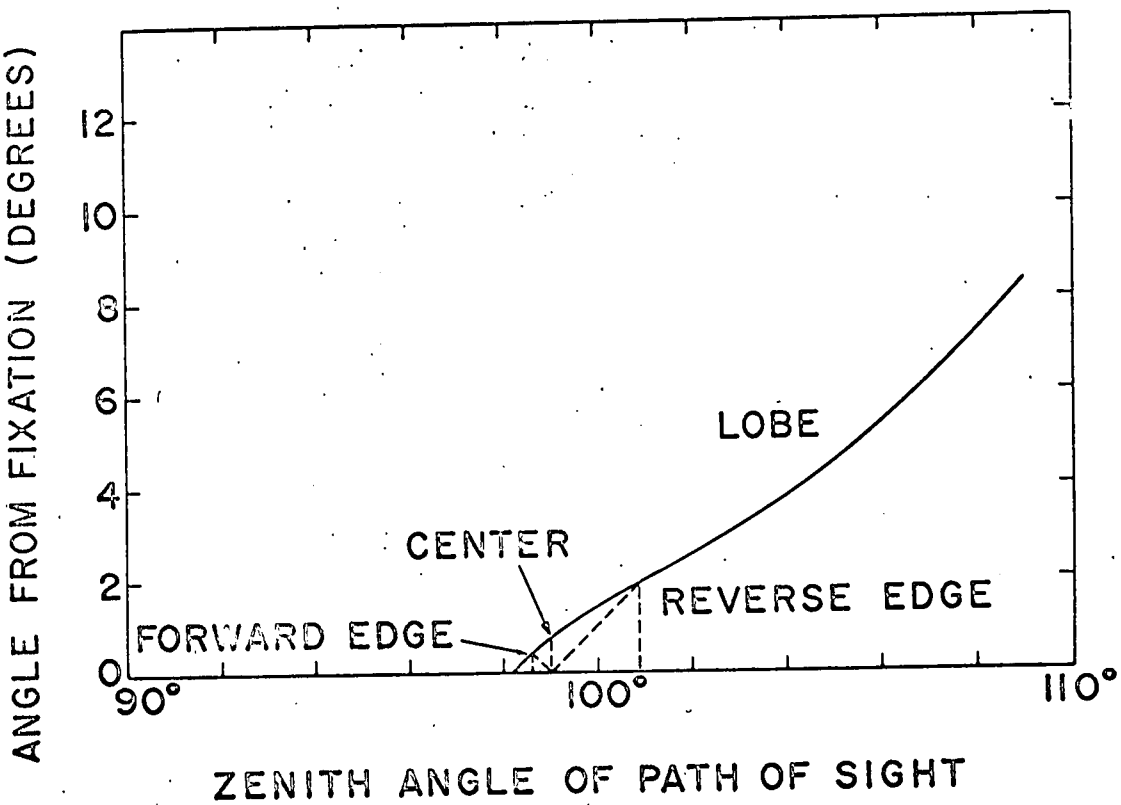

Fig. 10.6. Angular boundaries of the visual detection lobe.

The angular information from Fig. 10.6 can be translated into ground distances by the method shown in Fig. 10.7. This graph shows the distance to the forward and rear edge of the lobe for every specified distance to the point of fixation. From this graph the extent of the coverage of the roadway can be determined for every possible point of fixation.

The graph of Fig. 10.5 can be used to obtain information of more generality than that of finding the region within which the detection probability is 94 %. Since the index number can be directly related to detection probability, the probability of detection at each point on the roadway can be determined for a specified orientation of the path of sight. This is illustrated in Fig. 10.8. The point of fixation is designated by the X.

The search area is in motion relative to the observer, as is illustrated in Fig. 10.9. The visual search is assumed to be initiated 40 000 feet from the near (south) bound of the 26 000-foot region in which the object is located. From this figure the relative position of the 0 and 26 000-foot boundaries can be determined for any instant of time throughout the pass. The graph therefore defines the instantaneous bounds of the search. The dashed line marked foveal denotes the maximum distance at which the object can be detected foveally and hence time spent in looking at distances exceeding this value is wasted. In this example it was assumed that the observer would look no more than 2000 feet beyond this point as indicated by the solid line bounding systematic search. It was assumed that the observer would make fixations at random within

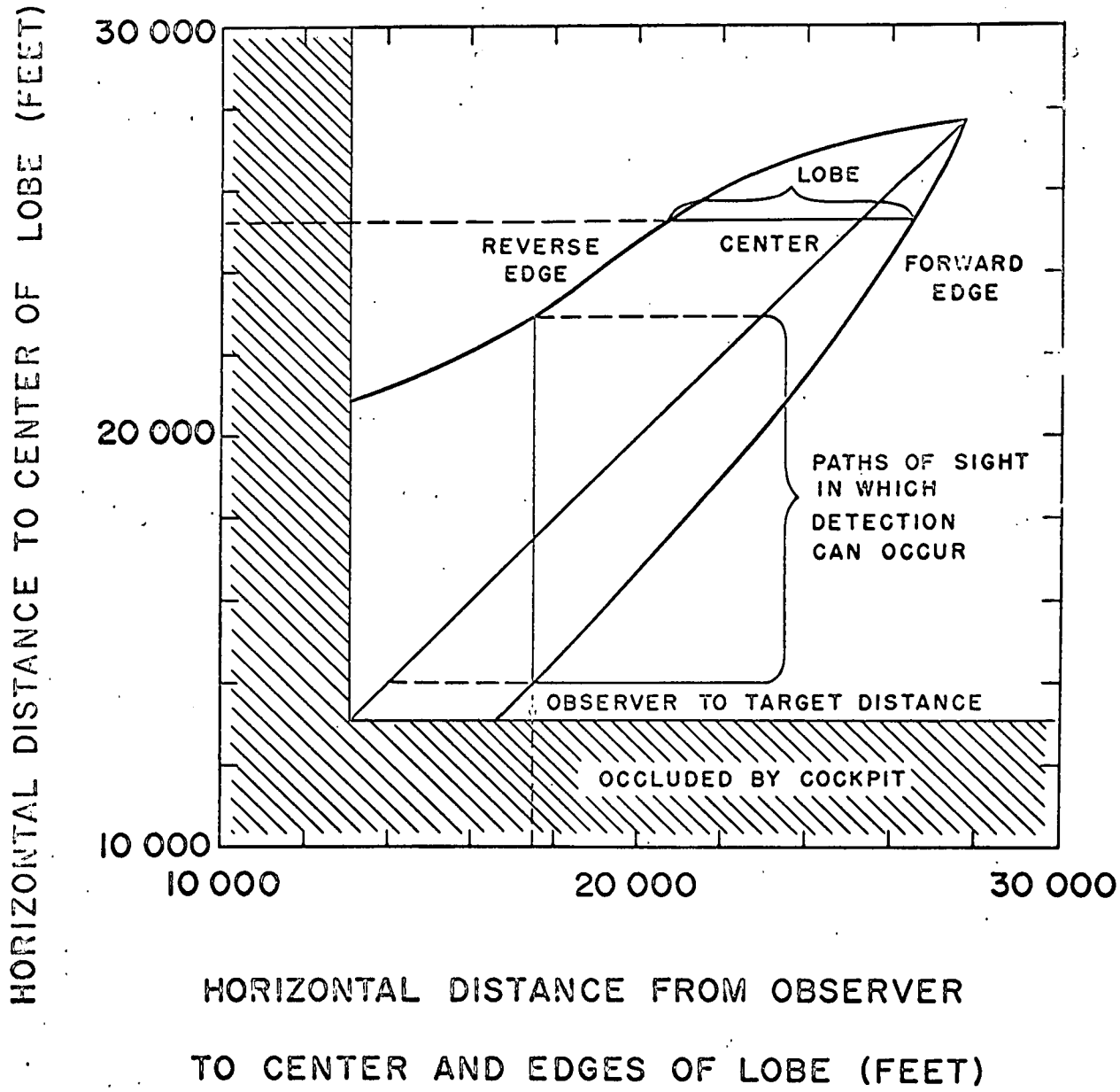

Fig. 10.7. Translation of the angular lobe description into a ground distance description.

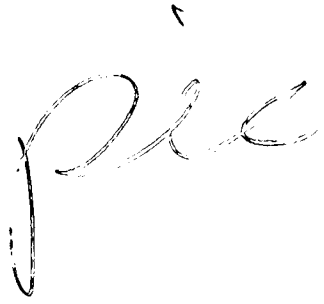

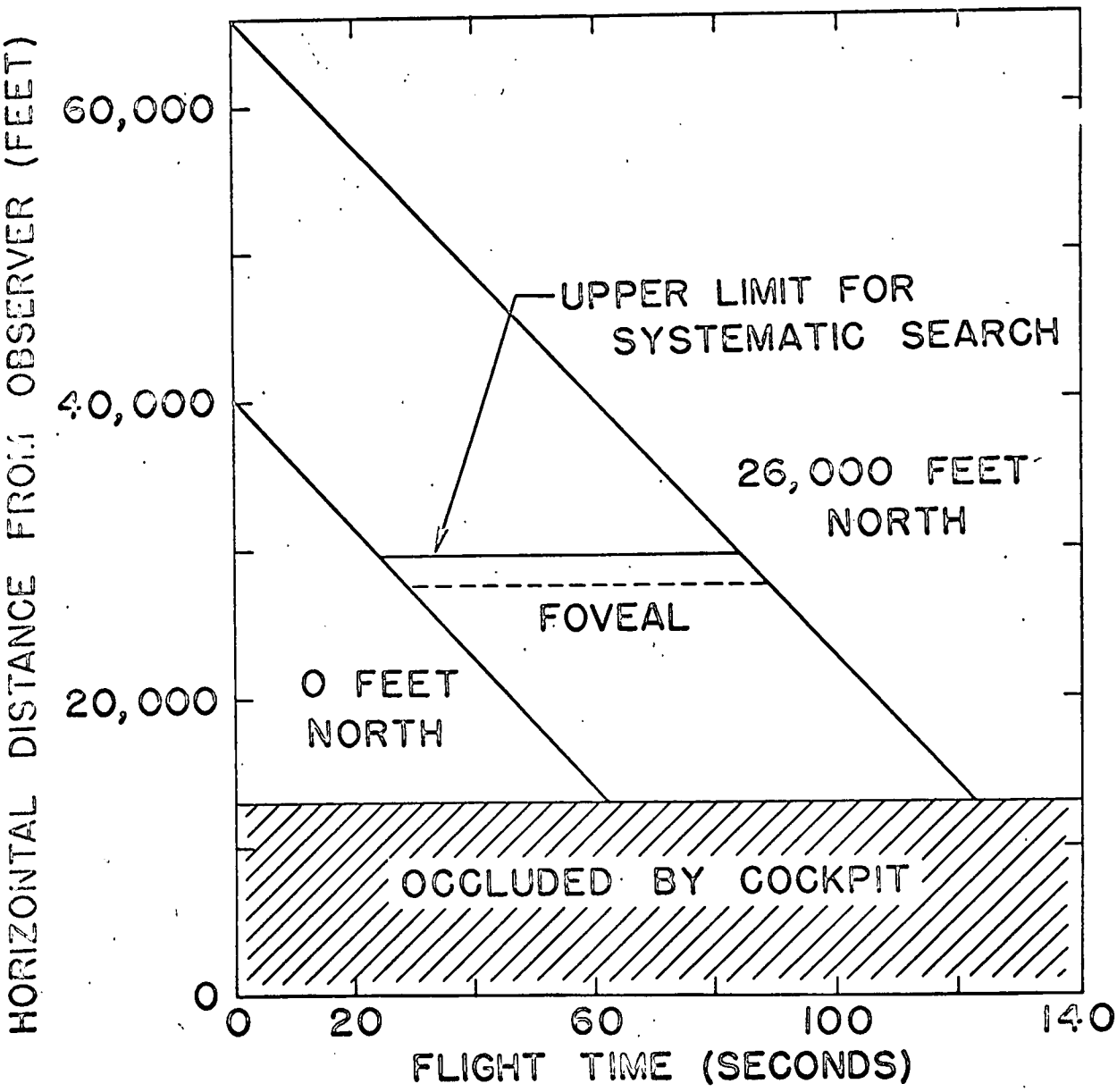

Fig. 10.9. Dynamics of the search field.

the time-varying boundaries established by Fig. 10.9. It was further assumed that the observer would not fixate at a point closer than the near boundary of the known region of object location.

The next step in the calculation is to find the detection probability associated with single fixations made at various distances from observer to object and for selected samples of possible object location measured from 0 to 26 000 feet. The results of this calculation are shown in Fig. 10.10. The falloff in probability at the shorter distances for the extreme object locations (0 and 26 000 feet) are the result of an edge effect which arises from the nature of the search doctrine. Objects at intermediate ranges may be detected by fixations made on either side of the object whereas the end points are detected from fixations made on only one side of the object. The net effect of the search doctrine is that the observer spends more time searching for targets at the midrange positions.

As the pattern of random fixations progresses, the probability of detection increases for each possible object location. Figure 10.11 shows a plot of this cumulative probability as a function of the distance from the observer to the object. As indicated in this figure, the detection probability is high for all object locations by the time the sighting range has been reduced to a ground distance of 20 000 feet.

The relationship of the median and the mean to the cumulative probability curve for a 5000-foot object position is illustrated in Fig. 10.12. The histogram shows the percentage of detections which will occur at the different range intervals. On the assumption that the

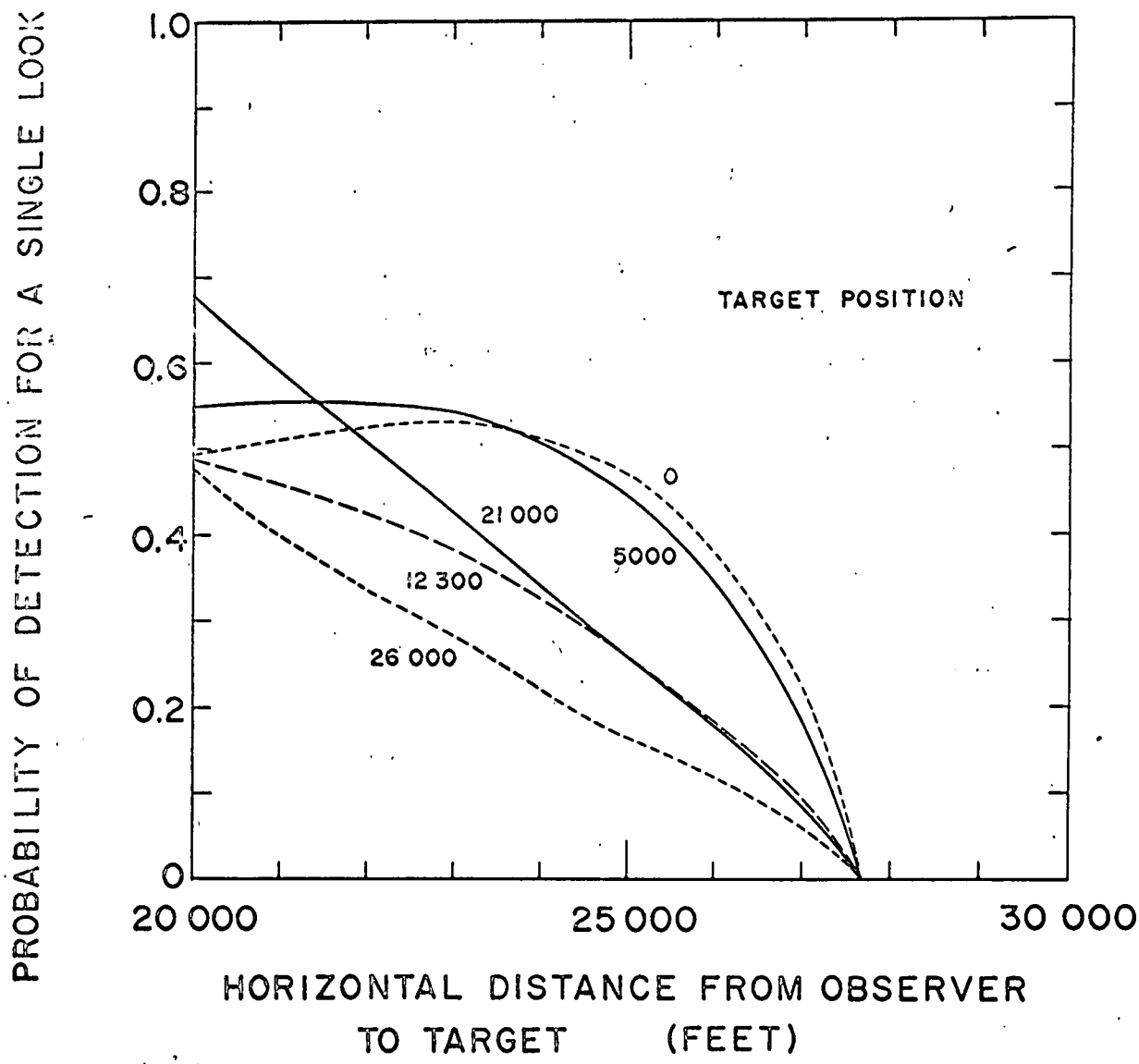

Fig. 10.10. The probability of detection for a single fixation for target positions as indicated.

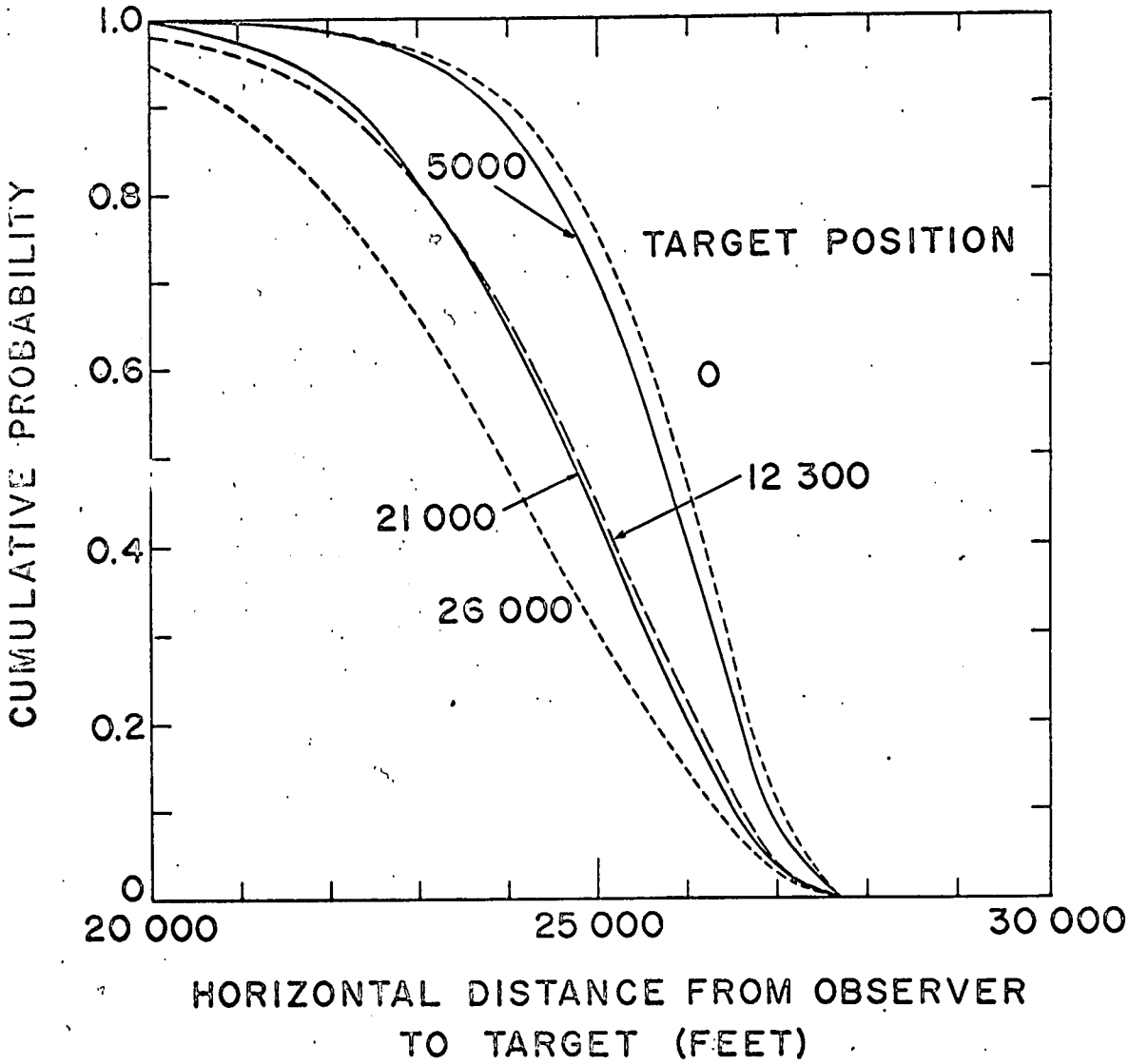

Fig. 10.11. Cumulative probability of detection for systematic search.

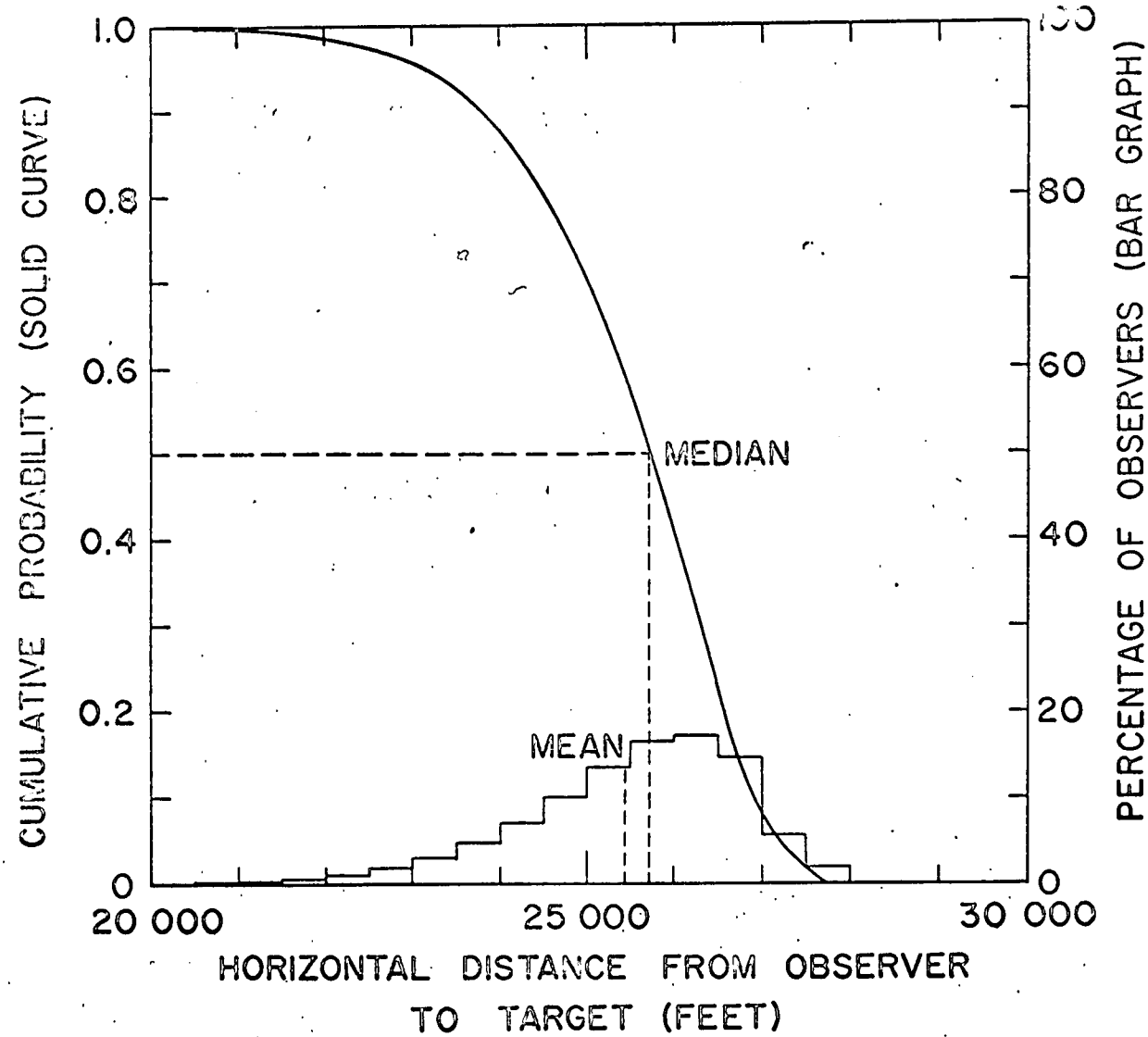

Fig. 10.12. The calculated mean and median sighting distances.

object position was random within the 26 000-foot boundary, the average sighting distance would be the average of the means for all object positions.

10.3 Summary

All visual search calculations begin with the combining of object, background, atmospheric, and visual properties to determine the detectability of the object for all object positions and viewing geometries which are defined by the search task. The visual detection lobe is a convenient means for displaying the results of these multiple inputs. By constructing visual detection lobes for a large number of fixational possibilities, various search strategies can be assumed and the cumulative detection probability calculated for each point in time throughout the period during which the search is conducted.

REFERENCES

Alpern, M. (1962), The Eye (Academic Press, New York and London, 1962) Vol. 3, p. 63.

Baker, C. H. (1958), J. Psychol. (Brit.) 49, 279 (1958).

Baker, C. H. (Ed.) (1963), Human Factors 5, June 1963: Special issue: Visual capabilities in the operation of manned space systems.

Barlow, H. B. (1958), J. Physiol. 141, 337 (1958).

Blackwell, H. R. (1946), J. Opt. Soc. Am. 36, 624, 714(A) (1946).

Blackwell, H. R. (1958), Univ. of Mich. Report No. 2455-12-F, June 1958.

Blackwell, H. R. and D. W. McCready, Jr. (1958), Univ. of Mich. Report No. 2455-13-F, June 1958.

Blackwell, H. R. and A. B. Moldauer (1958), Univ. of Mich. Report No. 2455-14-F, June 1958.

Blackwell, H. R. (1959), Illuminating Engineering LIV, 317 (1959).

Blackwell, H. R. and G. A. Bixel (1960), The Ohio State Univ., Inst. for Research in Vision, Tech. Rept. No. 890-1, April (1960).

Blackwell, H. R. (1963), J. Opt. Soc. Am. 53, 129 (1963).

Boyd, R. A. (1951), Univ. of Mich., Engr. Research Inst., Bull. No. 32, (1951).

Brown, D. R. E. (1952), Natural Illumination Charts, BuShips Proj. Ns-714-100, Rept. No. 374-1, p. 3,7 (1952).

Cathey, L. (1958), IRE Trans. on Nuclear Sci., NS-5, No. 3, 109 (1958).

Causse, J. P. (1960), IRE Trans. on Nuclear Sci., NS-7, No. 2-3, 66 (1960).

Duntley, S. Q. (1946), Visibility Studies and Some Applications in the Field of Camouflage, Summary Tech. Rept. Div. 16, NDRC, (Columbia Univ. Press, New York, 1946), Vol. 2, p. 65.

Duntley, S. Q. (1948a), J. Opt. Soc. Am. 38, 179 (1948).

Duntley, S. Q. (1948b), J. Opt. Soc. Am. 38, 237 (1948).

Duntley, S. Q. (1952), Visibility Lab., Scripps Inst. of Oceanog., Final Report of Contract N5ori-07864 MIT (1952).

Duntley, S. Q., A. R. Boileau, and R. W. Preisendorfer (1957), J. Opt. Soc. Am. 47, 499-506 (1957).

Duntley, S. Q. (1963a), J. Opt. Soc. Am. 53, 214 (1963).

Duntley, S. Q. (1963b), J. Opt. Soc. Am. 53, 351 (1963).

De Palma, J. J. and E. M. Lowry (1962), J. Opt. Soc. Am. 52, 328 (1962).

Elterman, Louis (1963), "A Model of a Clear Standard Atmosphere for Attenuation in the Visible Region and Infrared Windows," Optical Physics Lab., Air Force Cambridge Research Labs., Bedford, Mass., July (1963).

Engstrom, R. W. (1960), RCA Review 21, 184 (1960).

Enoch, J. M. (1959), J. Opt. Soc. Am. 49, 280 (1959).

Ford, A., C. T. White, and M. Lichtenstein (1959), J. Opt. Soc. Am. 49, 287 (1959).

Gerathewohl, S. J. (1952), J. Aviat. Med. 23, 597 (1952).

Gordon, J. I. (1963), Scripps Inst. of Oceanog. Ref. 63-23 (1963).

Graham, C. H., R. H. Brown and F. A. Mote (1939), J. Exptl. Psychol. 24, 555 (1939).

Hamilton, C. E. and H. R. Blackwell (1957), Univ. of Mich. Rept. No. 2455-8-F, April (1957).

Harris, J. L. (1959), Scripps Inst. of Oceanog. Ref. 59-65 (1959).

Harris, James L. (1960), Proc. of Symp. Armed Forces-NRC Com. on Vision, Publ. 712, Natl. Acad. Sci.--NRC Council, Washington, D.C., p. 69 (1960).

Hecht, S. and E. U. Mintz (1939), J. Gen. Physiol. 22, 593 (1939).

Hufnagel, R. E. and N. R. Stanley (1964), J. Opt. Soc. Am. 54, 52 (1964).

Hulbert, E. O. (1957), Naval Res. Lab. Rept. No. 4870 (1957).

Ingrao, Hector C. and Jay M. Pasachoff (1961), Rev. Sci. Instr., 32, No. 7, pp. 866-867 (1961).

Jayle, G. E. and A. G. Ourgaud (1950), La Vision Nocturne Et Ses Troubles, (Masson et C^{ie} Editeurs, Libraires de L'academie de medecine, 120 Boulevard Saint-germain, Parie VI^{e} (1950).

Jerison, H. J. and R. M. Pickett, Human Factors 5, 211 (1963).

Judd, D. B. (1952), Color in Business, Science, and Industry (John Wiley and Son's, Inc., New York, 1952).

Krinov, E. L. (1947), "Spectral Reflectance Properties of Natural Formations," Aero Methods Laboratory, Acad. of Sci. USSR, Izdaltel'stvo Akademii Nauk USSR (1947) translated by G. Belkov, Natl. Res. Council of Canada, Tech. Trans. TT-439 (1953).

Lamar, E. S. (1946), Chap. 4, Search and Screening (Columbia Univ. Press, New York, 1946).

MacAdam, D. L. (1946), Summary Tech. Rept. of Div. 16, NDRC, (Columbia Univ. Press, New York, 1946), p. 59.

Marshall, F. and J. W. Coltman and L. P. Hunter (1947), Rev. Sci. Instr. 18, 504 (1947).

Mees, C. E. K. (1944), The Theory of the Photographic Process, (MacMillan, New York, 1944).

Middleton, W. E. K. (1942), J. Opt. Soc. Am. 32, 139 (1942).

Middleton, W. E. K. (1952), Vision through the Atmosphere (Univ. of Toronto Press, Toronto, 1952).

Middleton, W. E. K. and A. G. Mungall (1952), J. Opt. Soc. Am. 42, 572 (1952).

Miller, James W. (Ed.) (1962), Visual Problems of Space Travel, Armed Forces-NRC Committee on Vision, April (1962).

Minzner, R. A., Champion, K. S. W., Pond, H. L. (1959), "The ARDC Model Atmosphere, 1959," Report No. 115, Geophysics Research Directorate, Air Force Cambridge Research Center, August (1959).

Moon, P. and J. Lawrence (1941), J. Opt. Soc. Am. 31, 130 (1941).

Moon, P. and D. E. Spencer (1942), Illuminating Engineering 37, pp. 707-726 (1942).

Murray, R. B. and J. J. Manning (1960), IRE Trans. on Nuclear Sci., NS-7, No. 2-3, 80 (1960).

Neeland, G. K., M. K. Laufer and W. R. Schaub (1938), J. Opt. Soc. Am. 28, 280 (1938).

Optical Society of America (1953), The Science of Color (Thomas Y. Crowell Company, 1953), p. 178.

Proc. of Sixth Scintillation Counter Symposium (1958), IRE Trans. on Nuclear Sci., NS-5, No. 3, pp. 98-126 (1958).

Proc. of Seventh Scintillation Counter Symposium (1960), IRE Trans. on Nuclear Sci., NS-7, No. 2-3, pp. 44-86 (1960).

Proc. of Eighth Scintillation Counter Symposium (1962), IRE Trans. on Nuclear Sci., NS-9, No. 3, pp. 54-96 (1962).

Rittner, E. S. (1947), Rev. Sci. Instr. 18, 36 (1947).

Stevens, S. S. (Ed.) (1951), Handbook of Experimental Psychology (John Wiley and Sons, Inc. - New York; Chapman and Hall Ltd., London (1951), Chaps. 22, 23, and 24.

Sweet, M. H. (1950), J. Soc. Motion Picture and Tel. Engrs. 54, 35 (1950).

Symposium on Physiological Optics (1962), Reprinted from J. Opt. Soc. Am. 53, No. 1.

Taylor, J. H. (1960), Scripps Inst. of Oceanog. Ref. 60-25, June (1960).

Taylor, J. H. (1960), Scripps Inst. of Oceanog. Ref. 60-31, June (1960).

Taylor, J. H. (1961), Scripps Inst. of Oceanog. Ref. 61-10, March (1961).

Taylor, J. H. and J. J. Rennilson (1962), J. Appl. Meteor. 1, 184 (1962).

Taylor, J. H. (1964), Nature, 201, pp. 691-692 (1964).

Volkmann, F. C. (1962), J. Opt. Soc. Am. 52, 571 (1962).

Walsh, J. W. T. (1958), Photometry (Constable, London, 1958).

White, C. T. and A. Ford (1960), J. Opt. Soc. Am. 50, 909 (1960).

Wood, L. A. (1936), Rev. Sci. Instr. 7, 157 (1936).

Wulfeck, J. W. and J. H. Taylor (Eds.) (1957), Form Discrimination as Related to Military Problems, Proc. of Symposium of Armed Forces--NRC Committee on Vision at Tufts Univ. April (1957).'

Wulfeck, J. W. (Ed.) (1958), Vision in Military Aviation, WADC Tech. Rept. 58-399, November (1958).

Young, A. T. (1963), Applied Optics 2, 51 (1963).

Zworykin, V. K. and E. G. Ramberg (1959), Photoelectricity and its Application (John Wiley and Sons, New York, 1949).